



UNIVERSIDADE
ESTADUAL DE LONDRINA

EDWIN JOSÉ TORRES DE OLIVEIRA

**“NOVO COMPLEXO Bis(((Z)-4-((4-clorofenil)amino)-4-oxobut-
2-enoil)oxi)cobre:
CITOTOXICIDADE EM CÉLULAS 4T1 E POTENCIAL
TOXICOGENÉTICO EM CAMUNDONGOS *Swiss*”**

Londrina
2019

EDWIN JOSÉ TORRES DE OLIVEIRA

**“NOVO COMPLEXO Bis(((Z)-4-((4-clorofenil)amino)-4-oxobut-
2-enoil)oxi)cobre:
CITOTOXICIDADE EM CÉLULAS 4T1 E POTENCIAL
TOXICOGENÉTICO EM CAMUNDONGOS *Swiss*”**

Dissertação apresenta ao Programa de Pós-Graduação em Genética e Biologia Molecular, da Universidade Estadual de Londrina, como requisito para obtenção do título de Mestre.
Linha de pesquisa: Genética Toxicológica e Câncer

Orientador: Prof. Dr. Rodrigo Juliano Oliveira

Londrina
2019

Ficha de identificação da obra elaborada pelo autor, através do Programa de
Geração Automática do Sistema de Bibliotecas da UEL

Oliveira , Edwin José Torres de Oliveira.

Novo complexo Bis(((Z)-4-((4-clorofenil)amino)-4-2-enoil)oxi)cobre:
citotoxicidade em células 4T1 e potencial toxicogenético em camundongos Swiss /
Edwin José Torres de Oliveira Oliveira . - Londrina, 2019.
56 f. : il.

Orientador: Rodrigo Juliano Oliveira Oliveira.

Dissertação (Mestrado em Genética e Biologia Molecular) - Universidade Estadual de
Londrina, Centro de Ciências Biológicas, Programa de Pós-Graduação em Genética e
Biologia Molecular, 2019.

Inclui bibliografia.

1. Câncer - Tese. 2. Danos no DNA - Tese. 3. Apoptose - Tese. 4. Atividade antitumoral
- Tese. I. Oliveira , Rodrigo Juliano Oliveira . II. Universidade Estadual de Londrina. Centro
de Ciências Biológicas. Programa de Pós-Graduação em Genética e Biologia Molecular. III.
Título.

EDWIN JOSÉ TORRES DE OLIVEIRA

**“NOVO COMPLEXO Bis(((Z)-4-((4-clorofenil)amino)-4-oxobut-
2-enoil)oxi)cobre:**

**CITOTOXICIDADE EM CÉLULAS 4T1 E POTENCIAL
TOXICOGENÉTICO EM CAMUNDONGOS *Swiss*”**

Dissertação apresentada ao Programa de Pós-Graduação em Genética e Biologia Molecular, da Universidade Estadual de Londrina, como requisito para obtenção do título de Mestre.

BANCA EXAMINADORA

Orientador: Prof. Dr. Rodrigo Juliano Oliveira
Universidade Estadual de Londrina – UEL

Profa. Dra. Sandra Regina Lepri
Universidade Estadual de Londrina – UEL

Prof. Dra. Fernanda Simões de Almeida
Universidade Estadual de Londrina – UEL

Londrina, 13 de março de 2019

Dedicatória

Aos meus pais **Maria Lucia Torres e Edgar Ferreira de Oliveira**

Mãe, Pai, se hoje eu dou mais um passo na minha carreira, a caminho do título de Mestre em Genética e Biologia Molecular, é porque em todos os momentos eu encontrei apoio em vocês. Foram momentos alegres e outros de dificuldades, mas em ambos os filhos sempre foram prioridade em suas vidas, sempre colocaram meus problemas e de meus irmãos, bem como nossos sonhos, ante os seus, nos orientando e nos ajudando nas escolhas da vida.

O título que eu receberei em breve é fruto de dois anos de esforço, mas também é fruto de uma vida de dedicação, a qual vocês possibilitaram minha educação e criação com apoio incondicional.

Mãe a senhora sempre foi e será meu anjo da guarda, agradeço à Deus por você existir em minha vida.

Pai, o senhor é meu melhor amigo. Minha referência!

“Esta família é muito unida e também muito ouriçada.

Brigam por qualquer razão, mas acabam pedindo perdão!”

Amo muito vocês!

À minha esposa **Raissa Ishikawa** e meu filho **João Pedro**

Vocês são minha razão de viver. Embora o título de mestre esteja em meu nome, ele é tão de vocês quanto meu. Não há palavras que possam explicar o quanto sou grato pelo amor de vocês.

Raíssa, me orgulho da profissional que você é. Sou muito feliz com você ao meu lado. Sei que me dedico mais ao laboratório do que a nossa casa, sei também que passei muitos dias ao computador, fazendo trabalhos, artigos ou preparando aulas, e que não pude, nesse tempo, ser o marido e amigo que você precisava. Prometo buscar um futuro diferente. Um em que seremos plenamente felizes. Os problemas existirão, mas não serão suficientes para abalar nossa paz. Te amo, hoje e sempre!

Filho se hoje abduco do nosso tempo em família para estudar é com o intuito de um dia proporcionar a você toda a base para que você tenha condições de vencer na vida, com dignidade, caráter e humildade. Te amo, sei que hoje você não entende, mas espero que um dia tenha orgulho de seu pai.

Agradecimentos

Ao meu orientador, Professor Dr. Rodrigo Juliano Oliveira.

Rodrigo, quando vários me disseram não, você me deu a chance do sim. Só tenho a agradecer por toda dedicação que você teve nesses dois anos. Percebo em você o pesquisador que espero um dia ser. Agradeço pela oportunidade ao abrir as portas do CeTroGen para que eu pudesse aprender e crescer profissionalmente. Espero que do mestrado continuemos a parceria no doutorado, e que um dia, quando eu conseguir a tão almejada vaga em um concurso para docente, possamos ser parceiros, colegas pesquisadores. Até lá, conto com sua paciência em meu processo de formação.

Ao Professor Dr. Roberto da Silva Gomes

Pelo apoio na execução do meu projeto de mestrado e por estar sempre à disposição para elucidação das diversas dúvidas que surgiram, principalmente relacionadas ao composto RC1. Obrigado pela parceria e amizade nesses dois anos.

À Dra. Professora Silvia, e toda equipe do Programa de Pós-Graduação em Genética e Biologia Molecular.

Pela compreensão nas horas de dificuldade e por todo apoio na questão acadêmica.

Ao Professor Dr. Mário Sérgio Mantovani.

Professor muito obrigado pelo apoio e por me receber tantas vezes em seu laboratório.

Ao Me. Lucas Roberto Pessatto e Me. Bruno Ivo Pelizaro

Pela ajuda em todas as fases de execução do meu projeto, pela parceria em passar as madrugadas no laboratório rodando experimentos. Pela amizade quando mais precisei. Algumas pessoas chegam em nossas vidas e nunca mais saem. A amizade de vocês é para sempre. Grande abraço!

À Ma. Ana Paula Maluf Rabacow

Pela amizade e momentos de descontração. Obrigado por me aceitar na entrevista de estágio em 2010, a experiência adquirida no Instituto de Perícias Científicas abriu-me muitas portas, dentre elas o mestrado. Muito obrigado também, por toda ajuda inerente à tradução do meu manuscrito e dos demais trabalhos científicos.

Ao Dr. João Renato Pesarini

Pelos momentos de diversão e pelos ensinamentos referentes às publicações, muito obrigado.

Aos amigos do CeTroGen

Por toda ajuda. Cheguei perdido, vocês me acolheram e me ensinaram. Me deram condições de realizar meus experimentos, contribuindo, hora com conhecimento, outrora com diversão. Lucas, Bruno, Raíssa, Ana Paula, João, Joyner, Juliana, Sílvia, Giovana, Yasmin, Bruna, Luana, Luane, Andreza, Laynna, Viviane, Thaís e Verônica, a vocês meu muito obrigado!

À CAPES

Pela bolsa de Mestrado.

"A ignorância mais frequentemente gera confiança do que o conhecimento. São os que sabem pouco, e não aqueles que sabem muito, que afirmam de uma forma tão categórica que este ou aquele problema nunca será resolvido pela ciência."

Charles Darwin

RESUMO

OLIVEIRA, Edwin José Torres: Novo complexo Bis(((Z)-4-((4-clorofenil)amino)-4-oxobut-2-enil)oxi)cobre: citotoxicidade em células 4T1 e potencial toxicogenético em camundongos *Swiss*. 2018. 48 f.(Dissertação de mestrado) Londrina – PR: Programa de Pós-Graduação em Genética e Biologia Molecular – Universidade Estadual de Londrina. 2019.

Complexos de cobre (II) são promissores candidatos para o desenvolvimento de novos tratamentos para diversos tipos de câncer, incluindo o câncer de mama. O presente trabalho avaliou a atividade antitumoral *in vitro* e os efeitos toxicogenéticos *in vivo* de um novo complexo de cobre (II). O composto Bis(((Z)-4-((4-chlorophenil)amino)-4-oxobut-2-enil)oxi)cobre (RC1) foi sintetizado e posteriormente utilizado nos ensaios biológicos. Um total de $2,5 \times 10^4$ células 4T1 foram plaqueadas e submetidas à tratamento com as concentrações de 3,125; 6,25; 12,5; 25; 50; 100; 250; 500 e 1000 $\mu\text{g/mL}$ do composto RC1, durante 24, 48 e 72 horas. A partir dos resultados de citotoxicidade a IC₅₀ do composto RC1 foi calculada e utilizada nos demais ensaios *in vitro*. Para análise da genotoxicidade utilizou-se o ensaio do cometa e para análise do tipo de morte celular a análise morfológica com coloração diferencial de brometo de etídio e acridina, e a marcação em citometro de fluxo com kit de detecção de apoptose PE Anexina V. Ainda por citometria foi analisada a integridade da membrana das células 4T1, bem como o ciclo celular, após 24 horas de tratamento com o composto RC1. O ensaio de expressão gênica foi realizado por qPCR e genes relacionados à danos, reparo do DNA e apoptose foram estudados. *In vivo* o potencial toxicogenético foi avaliado em camundongos *Swiss* com as concentrações de 3, 6 e 12mg/kg do composto RC1 por meio dos ensaios de cometa, micronúcleo e fagocitose. Os resultados demonstraram que o composto RC1 induziu citotoxicidade nas células 4T1, possivelmente, via danos no DNA que levara ao aumento da expressão de ATM e p21, induzindo parada de ciclo celular em G1. O mecanismo de morte celular do RC1 em células 4T1 foi a apoptose desencadeado pelo aumento na expressão de BAX e CASP- 7, sem alterar a integridade de membrana das células 4T1. *In vivo*, o composto foi genotóxico em camundongos e causou aumento da frequência de danos genômicos (cometa), mas não cromossômicos (micronúcleo), no DNA e quando comparado ao quimioterápico de referência, cisplatina, foi menos genotóxico. O RC1 também foi capaz de aumentar a frequência de fagocitose esplênica. Esses resultados indicam que o novo complexo de cobre (II), descrito pioneiramente neste trabalho, apresenta potencial terapêutico no tratamento do câncer de mama.

Palavras-chave: Complexos de Cobre (II); danos no DNA; Apoptose; atividade antitumoral; câncer de mama.

ABSTRACT

OLIVEIRA, Edwin José Torres. New Bis complex ((Z)-4-((4-chlorophenyl)amino)- 4-oxobut-2-enoyl)oxy) copper: cytotoxicity in 4T1 cells and toxicogenic potential in *Swiss* mice. 2018. 48 p. (Work Master's Dissertation) Londrina – PR: Programa de Pós- Graduação em Genética e Biologia Molecular – Universidade Estadual de Londrina. 2019.

Copper (II) complexes are promising candidates for the development of new treatments for various types of cancer, including breast cancer. The present paper reported on the evaluation of the *in vitro* antitumor activity and toxicogenic effects *in vivo* of a new copper (II) complex. The Bis(((Z)-4-((4-chlorophenyl)amino)-4-oxobut-2-enoyl)oxy)copper (RC1) compound was synthesized and subsequently used in the biological assays. A total of 2.5×10^4 of 4T1 cells were plated and treated with the RC1 compound at concentrations of 3.125; 6.25; 12.5; 25; 50; 100; 250; 500 and 1000 $\mu\text{g/mL}$ for 24, 48 and 72 hours. The IC₅₀ of RC1 compound was calculated from the cytotoxicity results and used in the others *in vitro* assays. The comet assay was the method employed for analysis of the genotoxicity, as for the identification of the type of cell death, the method was the morphological analysis with differential staining of bromide and acridine, and the marking in flow cytometry with apoptosis detection kit PE Annexin V. 4T1 cells membrane integrity and the cell cycle, was analyzed after 24 hours of treatment with compound RC1 by flow cytometry. The gene expression assay was performed by qPCR and genes related to DNA-damage, DNA repair and apoptosis were studied. The *in vivo* toxicogenic potential was evaluated in *Swiss* mice with the concentrations of 3, 6 and 12mg/kg of RC1 compound RC1 by the comet, micronucleus and phagocytosis assays. The results demonstrated that RC1 compound induced cytotoxicity in 4T1 cells, which appears to occur because of DNA damage, which increased ATM and p21 expression, inducing cell cycle arrest in G1. The mechanism of cellular death of RC1 in 4T1 cells was apoptosis, that occurred by the increase in expression of BAX and CASP-7, without altering the membrane integrity of 4T1 cells. In *in vivo*, the compound was genotoxic in mice and caused an increase in the frequency of genomic damage (comet), but not chromosome (micronucleus), and when compared to the reference chemotherapy, cisplatin, it was less genotoxic. RC1 was also able to increase the frequency of splenic phagocytosis. These results indicate that the new copper (II) complex, firstly described in this work, presents therapeutic potential in the treatment of breast cancer.

Keywords: Copper (II) complexes; DNA damage; apoptosis; antitumor activity; breast cancer.

LISTA DE TABELAS

Tabela 1 – Sequência dos oligonucleotídeos utilizados no ensaio de expressão gênica.

Tabela 2 – Frequências (ν , cm^{-1}) das bandas vibratórias selecionadas no espectro IR do RC1.

Tabela 3 – Comparação dos Parâmetros Biométricos entre os grupos experimentais.

Parâmetros biométricos de camundongos tratados com solução salina (DMSO 1%), cisplatina (6mg/kg), diferentes doses do composto RC1 (D1, D2 e D3) e diferentes doses do composto RC1 associado com cisplatina (6mg/kg). Os resultados estão apresentados em Média \pm EPM e letras diferentes indicam diferenças estatisticamente significativas ($p \leq 0,05$; ANOVA seguido de teste de Tukey Kramer).

Tabela 4 – Média \pm Erro Padrão, frequência de células danificadas, distribuição entre classes de danos e *Score* relacionado ao ensaio do cometa.

Frequência de células com danos genômicos, distribuição entre as classes e *score* do ensaio do cometa realizado com sangue periférico de camundongos tratados com solução salina (DMSO 1%), cisplatina (6mg/kg) diferentes doses do composto RC1 (D1, D2 e D3) e diferentes doses do composto RC1 associado com cisplatina (6mg/kg). ¹Os resultados estão apresentados em Média \pm EPM e letras diferentes indicam diferenças estatisticamente significativas ($p \leq 0,05$; ANOVA seguido de teste de Tukey Kramer).

Tabela 5 – Frequência de micronúcleos no sangue periférico de camundongos tratados com o composto RC1.

Frequência de micronúcleos em sangue periférico de camundongos tratados com solução salina (DMSO 1%), cisplatina (6mg/kg), diferentes doses do composto RC1 (D1, D2 e D3) e diferentes doses do composto RC1 associado com cisplatina (6mg/kg). Os resultados estão apresentados em Média \pm EPM e letras diferentes indicam diferenças estatisticamente significativas ($p \leq 0,05$; ANOVA seguido de teste de Tukey Kramer).

LISTA DE FIGURAS

- Figura 1 – Tipos mais comuns de cânceres conforme o sexo
Figura 2 – Fases da carcinogênese
Figura 3 – Representação do ciclo celular
Figura 4 – Representação do ciclo celular com os principais pontos de chacagem
Figura 5 – Estrutura da cisplatina

Manuscrito

- Figura 1 – ^1H -NMR espectro do RC1 em DMSO-*d*₆ a 300 MHz.
Figura 2 – ^{13}C -NMR espectro do RC1 em DMSO-*d*₆ a 75 MHz.
Figura 3 – Citotoxicidade do composto RC1 em células de adenocarcinoma mamário murino 4T1.

(A) comparação das concentrações em três diferentes tempos, 24, 48 e 72 horas, onde * indicam diferenças estatisticamente significativas ($p < 0,05$; ANOVA/Bonferroni); (B) curva de regressão não linear construída a partir dos valores de viabilidade celular obtidos no ensaio do MTT após 24 horas de tratamento com o composto RC1; (C) comparação dos efeitos citotóxicos das diferentes concentrações do composto RC1 em cada período de tratamento. Diferentes letras indicam diferenças estatisticamente significativas ($p < 0,05$; ANOVA/Bonferroni). Os gráficos foram construídos por meio do *Software* GraphPad Prism 6.

- Figura 4 – Análise dos danos genômicos induzidos pelo composto RC1 em células de adenocarcinoma mamário murino 4T1.

(A) critério de classificação dos danos genômicos por meio do ensaio do cometa, onde 0 representa nucleóide com ausência de danos e 1, 2 e 3, as respectivas classes de danos; (B) nucleóides com danos genômicos induzidos pelo composto RC1 após 4 horas de tratamento; (C) porcentagem de células com danos no DNA observadas por meio do ensaio do cometa; (D) Score do dano genômico em células 4T1 tratadas a IC₅₀ do composto RC1; (E) Gráficos da análise do ciclo celular das células 4T1 tratadas com controle negativo, cisplatina e com a IC₅₀ do composto RC1; (F) Porcentagem de células em cada fase do ciclo celular após os tratamentos com controle negativo, cisplatina e com a IC₅₀ do composto RC1, sendo que letras diferentes indicam diferenças estatisticamente significativas ($p < 0,05$; ANOVA/Bonferroni); (G) Expressão de genes relacionados à dano e reparo do DNA de células 4T1 tratadas com a IC₅₀ do composto RC1, como normalizador foi utilizado o gene ACTB e * indicam diferenças estatisticamente significativas ($p < 0,05$, REST).

- Figura 5 – Apoptose em células 4T1 induzida pelo composto RC1.

(A) Células em apoptose após tratamento com a IC₅₀ do composto RC1; (B) porcentagem de células em apoptose após tratamento com DMSO (controle negativo), cisplatina e com a IC₅₀ do composto RC1, sendo que letras diferentes indicam diferenças estatisticamente significativas ($p < 0,05$; ANOVA/Bonferroni); (C) porcentagem de células viáveis, em apoptose inicial, apoptose tardia e em necrose,

após os tratamentos com 1% de DMSO, cisplatina e com a IC50 do RC1; **(D)** análise da integridade da membrana das células 4T1 realizada em citometro de fluxo com iodeto de propídeo após os tratamentos; **(E)** expressão de genes relacionados à apoptose em células 4T1 após tratamento com a IC50 do composto RC1.

Figura 6 – Análise da fagocitose esplênica em camundongos *Swiss* tratados com o composto RC1.

Porcentagem de células com características fagocíticas nos tratamentos com DMSO, cisplatina (controle positivo) o composto RC1 em três diferentes doses (D1, D2 e D3) e das três doses do composto RC1 associado a dose de cisplatina. Letras diferentes indicam diferenças estatisticamente significativas ($p \leq 0,05$; ANOVA/Tukey Kramer).

LISTA DE ABREVIATURAS E SIGLAS

¹³C	Núcleo de Carbono
¹H	Núcleo de Hidrogênio
ATCC	<i>American Type Culture Collection</i>
ATM	Ataxia-telangiectasia mutada quinase
ATPase	Adenosinatrifosfatases
ATR	Ataxia telangiectasia
BAK	Proteína antagonista de BCL-2
BAX	BCL-2-associado a proteína X
BCL2	<i>B-cell lymphoma 2</i>
CASP3	Caspase 3
CASP7	Caspase 7
CASP9	Caspase 9
Cdk2	Ciclina dependente de quinase 2
cDNA	DNA complementar
CO₂	Dióxido de Carbono
DMSO	Dimetilsulfóxido
DNA	Ácido Desoxirribonucleico
DNase	Desoxirribonuclease
DNTPs	Deoxinucleotídeo trifosfato
EDTA	Ácido Etilenodiaminotetracético
G1	<i>Gap 1 phase</i>
G2/M	<i>Gap 2 phase/Mitosis</i>
GADD45	Proteína induzida ao dano ao DNA e parada do ciclo
IC50	Concentração do composto que reduz a viabilidade celular em 50%
IV	Infravermelho
LMP	<i>Low Melting Point</i>
MgCl₂	Cloreto de Magnésio
p53	Proteína tumoral de 53kDa
PA	Pureza Analítica
PBS	<i>Phosphate Buffered Saline</i>
q.s.p.	Quantidade suficiente para

qPCR	Reação em Cadeia da Polimerase quantitativo
RC1	Bis(((Z)-4-((4-chlorophenil)amino)-4-oxobut-2-enoil)oxi)cobre
REST	<i>Relative Expression Software Tool</i>
RMN	Ressonância Magnética Nuclear
RNA	Ácido Ribonucleico
RNAse	Ribonuclease
S	<i>Synthesis phase</i>
TE	Tris EDTA
Tris	Hidroximetil-aminometano
WHO	<i>World Health Organization</i>

SUMÁRIO

1	INTRODUÇÃO	19
2	REVISÃO BIBLIOGRÁFICA	21
2.1	CÂNCER	21
2.2	CARCIONOGÊNSE	22
2.3	ABORDAGEM TERAPÊUTICA	26
3	OBJETIVOS	29
3.1	OBJETIVO GERAL.....	30
3.2	OBJETIVOS ESPECÍFICOS	30
4	METODOLOGIA	31
4.1	SÍNTESE QUÍMICA	31
4.2	EXPERIMENTOS IN VITRO	31
4.3	EXPERIMENTOS IN VIVO	35
4.4	ANÁLISE ESTATÍSTICA	37
5	MANUSCRITO: New Bis copper complex ((Z)-4-((4-chlorophenyl)amino)-4-oxobut-2-enoyl)oxy): cytotoxicity in 4T1 cells and their toxicogenic potential in Swiss mice.	38
6	REFERÊNCIAS DA DISSERTAÇÃO	51
7	ANEXO 1: Certificado da Comissão de Ética no Uso de Animais – CEUA	56

1. INTRODUÇÃO

De acordo com a GLOBOCAN (2012), são estimados mais de 17 milhões de novos casos de câncer para o ano de 2020, sendo que destes, quase dois milhões serão de câncer de mama. Em 2012, foram 521.907 óbitos em decorrência desse tipo de câncer e são estimados para o ano de 2020 aproximadamente 622 mil óbitos. A alta incidência e mortalidade tornam o câncer de mama um problema de saúde pública de ordem mundial.

O câncer pode ser definido, ainda que sem consenso, como um grupo de doenças que devido às mutações no DNA iniciam o processo de carcinogênese, culminando com proliferação celular desordenada e metástase (HUANG et al., 2016). No Brasil houve melhora na sobrevida dos pacientes com câncer de mama e de próstata, dois dos mais incidentes no mundo (ALLEMANI et al., 2015). Isso se deve ao aumento dos programas que buscam a prevenção, utilizando para esse fim os atuais meios de divulgação, que somado aos avanços científicos em cirurgia, radioterapia e quimioterapia, possibilitam o diagnóstico precoce, viabilizando o tratamento ainda nos estágios iniciais da doença.

A quimioterapia utiliza drogas citotóxicas (quimioterápicos) para eliminar as células cancerígenas. A heterogeneidade é uma importante característica das células neoplásicas, podendo implicar na sensibilidade aos quimioterápicos. Ao empregar a quimioterapia no combate a essas células (neoplásicas) aquelas que possuem resistência ao tratamento continuarão se multiplicando, e caso não seja revisto o esquema de tratamento, a quimioterapia pode falhar (WAGNER-SOUZA et al., 2003). Nesse contexto, pesquisas que busquem novas substâncias com capacidade antitumoral, são importantes ferramentas no combate e/ou prevenção do câncer.

A quimioterapia tem por objetivo eliminar as células neoplásicas por meio de tratamento farmacológico utilizando drogas com diferentes ações. Logo, os quimioterápicos podem ser divididos, quanto a sua estrutura química, em agentes alquilantes, antibióticos com ação sobre ácidos nucleicos, antimetabólitos, compostos hormonais, compostos platinados, inibidores mitóticos e modificadores da resposta biológica (LAMSON; BRIGNALL, 1999).

A cisplatina (cis-diaminadichloroplatina), um quimioterápico da classe dos alquilantes, é largamente utilizado contra diversos tipos de tumores sólidos. Sua atividade antineoplásica está relacionada com o processo de alquilação do DNA e

produção de espécies reativas ao oxigênio (EROs) que causam danos no DNA sendo que ambos os processos inibem a replicação e induzem a célula à apoptose (OLIVEIRA et al., 2013). Embora seja eficiente no tratamento de diversos tumores, efeitos colaterais são associados ao uso da cisplatina tais como a diminuição do reflexo vestibulo-ocular e a nefrotoxicidade (TAKIMOTO et al., 2016).

Diversos grupos de pesquisas buscam, por meio de novos compostos, provenientes de fontes naturais ou sintéticas, resolver os desafios inerentes à resistência das células tumorais, e inespecificidade e efeitos colaterais dos quimioterápicos. Nesse contexto, compostos complexados com cobre (II) mostram-se promissores na atividade citotóxica frente células cancerígenas (GAO et al., 2011; PIVETTA et al., 2012; THALAMUTHU et al., 2013a).

Variadas séries de substâncias que contêm o grupo 1,4-dioxo-2-butenil foram sintetizadas como candidatas a citotoxinas, incluindo N-metil aril-maleamatos, N-metil aril-fumaramatos e N-aril-maleimidias. Estas substâncias foram avaliadas em células humanas das linhagens CEM e Molt 4/C8 e em linfócitos-T (JHA et al., 2010). Estudos também foram realizados na linhagem de células L1210 de murinos (JHA et al., 2010). Os resultados demonstram que os N-aril-fumaramatos de metila apresentaram os maiores potenciais citotóxicos e, em particular, o N-(3,4-diclorofenil) fumarato de metila mostrou-se seis vezes mais potente do que o Melphalan® (padrão utilizado no tratamento paliativo de mieloma múltiplo e carcinoma ovariano epitelial não-ressecável) quando avaliado na linhagem celular L1210 (JHA et al., 2010). Já na linhagem Molt 4/C8 demonstrou uma potência equivalente com a droga de referência (JHA et al., 2010). Esses achados corroboram para a importância em se explorar novas substâncias no combate às células cancerígenas, sendo que, nesse contexto, complexos de Cobre (II) são potenciais candidatos no combate ao câncer, por apresentar atividade citotóxica em linhagens tumorais (GAO et al., 2011; PIVETTA et al., 2012; THALAMUTHU et al., 2013b) incluindo o câncer de mama (FAN et al., 2017; GOUDA et al., 2018; MANIKANDAMATHAVAN et al., 2017; SANGEETHA; MURALI, 2017).

2. REVISÃO BIBLIOGRÁFICA

2.1 Câncer

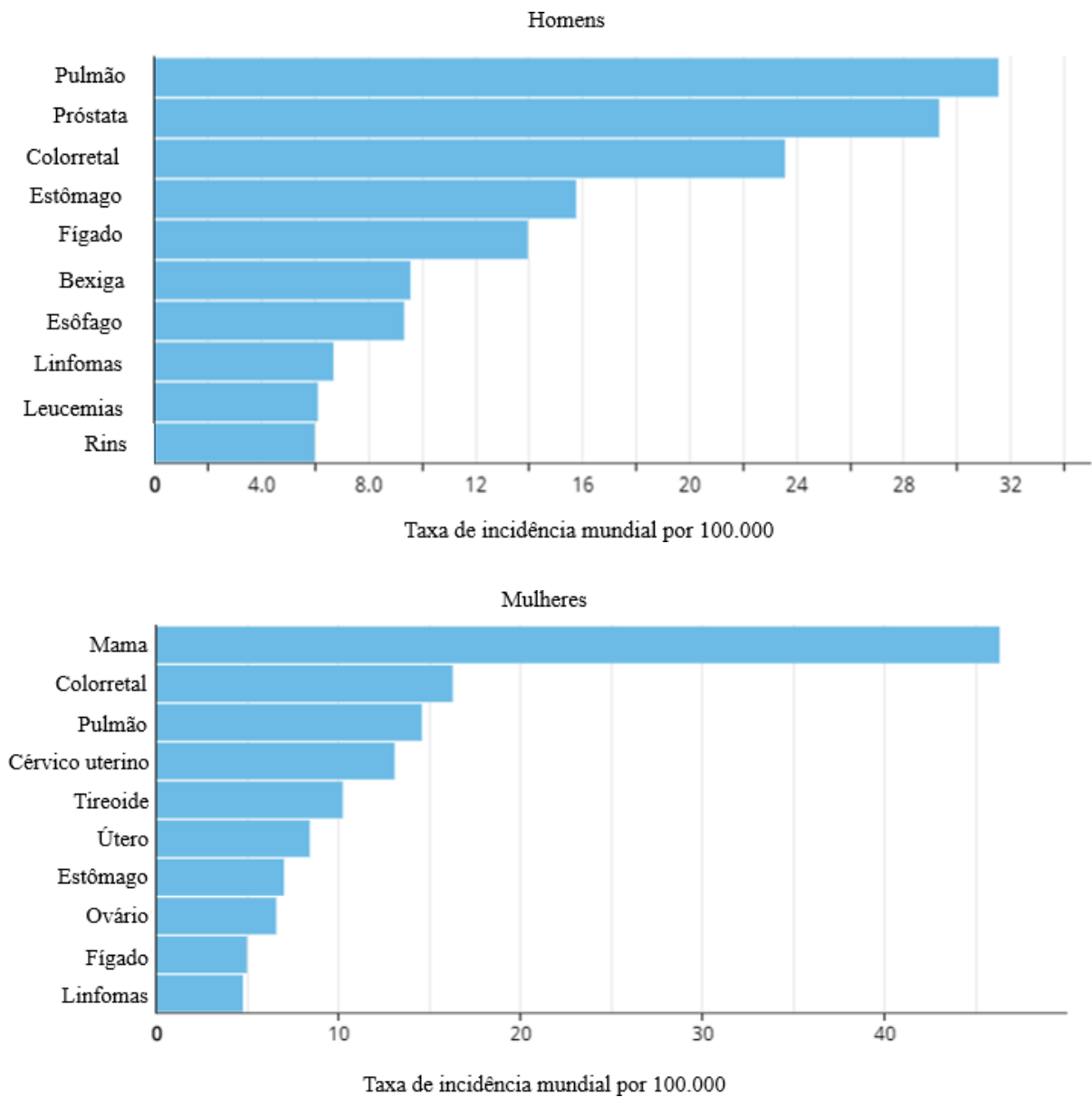
Anualmente, o câncer é responsável pela morte de milhares de pessoas, ocupando o segundo lugar como principal causa de mortalidade (OPAS, 2019). No ano de 2012 foram diagnosticados 14,71 milhões de novos casos de câncer e são estimados 27 milhões de novos casos para o ano de 2035, o que resultará em mais de 24 milhões de mortes pela doença (WCRF, 2019). Todos os países são acometidos por essa doença, mas os países subdesenvolvidos e aqueles em desenvolvimentos são os mais afetados, pois, embora a incidência nesses países seja menor que nos países desenvolvidos, a mortalidade representa quase 80% dos óbitos de câncer no mundo, devido ao difícil acesso à tratamentos adequados (FERLAY et al., 2013).

Os tipos de câncer mais incidentes à nível mundial, são o de pulmão (1,8 milhão), mama (1,7 milhão), intestino (1,4 milhão) e próstata (1,1 milhão). Quanto ao sexo (figura 1), os mais frequentes em homens são de pulmão (16,7%), próstata (15,0%), intestino (10,0%), estômago (8,5%) e fígado (7,5%), enquanto que, em mulheres as maiores frequências são de mama (25,2%), intestino (9,2%), pulmão (8,7%), colo do útero (7,9%) e estômago (4,8%) (FERLAY et al., 2013).

No Brasil, para o biênio 2018-2019, são estimados mais de um milhão de casos novos de câncer. Excetuando-se o câncer de pele não melanoma (cerca de 170 mil casos novos), ocorrerão 420 mil casos novos de câncer. Os cânceres de próstata (68 mil) em homens e mama (60 mil) em mulheres serão os mais frequentes (INCA, 2018).

Estima-se que no ano de 2018 a incidência mundial de casos de câncer de mama tenha ultrapassado 2 milhões e que mais de 600.000 óbitos foram decorrentes dessa doença (WHO, 2018). A mortalidade do câncer está relacionada ao tipo de tumor, tempo de diagnóstico e tratamento adequado.

Figura 1. Tipos mais comuns de cânceres conforme o sexo.



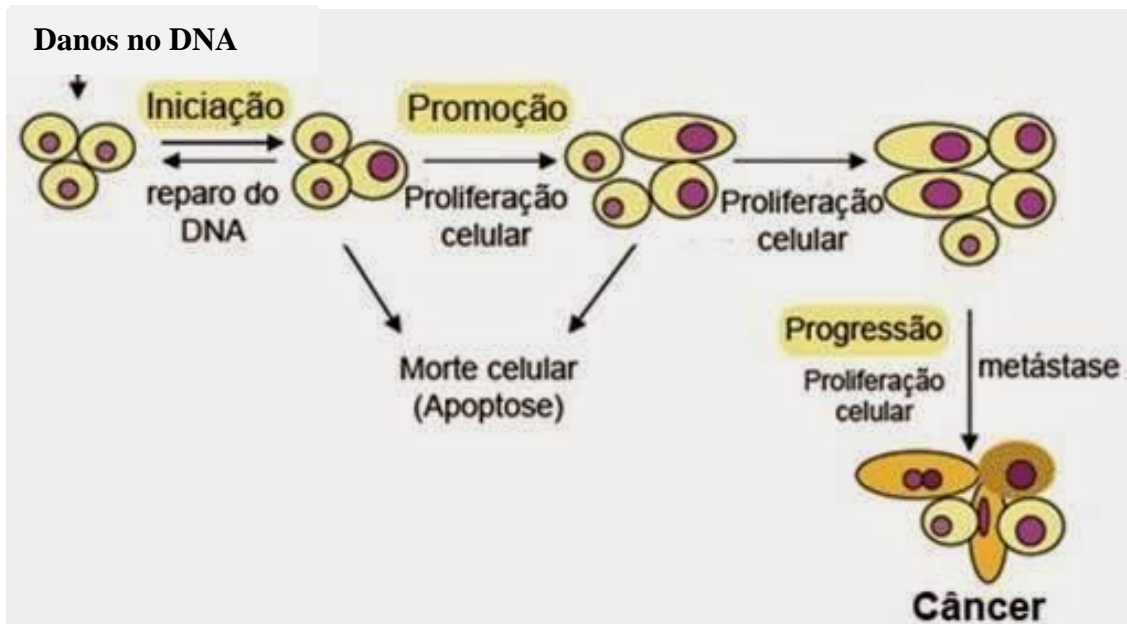
Fonte: Adaptado de lobal Cancer Observatory, disponível em <http://gco.iarc.fr/>.

2.2 Carcinogênese

O surgimento do câncer, geralmente, é um processo lento e pode ser dividido em três etapas (figura 2), denominadas iniciação, promoção e progressão (PITOT, 2011; INCA, 2012). A primeira etapa, a iniciação, tem como característica a ocorrência de danos no DNA. É uma etapa rápida e irreversível, diferente da promoção. Na fase de promoção as células já estão alteradas, ou seja, já acumularam alterações em seu DNA. Esse processo é lento e pode ser reversível, mas caso os danos no DNA não sejam reparados, as células sofrerão transformações, se tornarão células malignas e poderão

invadir outros tecidos. O estágio de invasão a outros tecidos constitui a terceira fase, a progressão, que também é considerada um estágio irreversível e resulta em multiplicação descontrolada das células, com o aumento da massa celular primária que apresenta alto potencial invasivo e metastático (PITOT, 2011).

Figura 2. Fases da carcinogênese.



Fonte: <https://www.google.com.br/imghp>

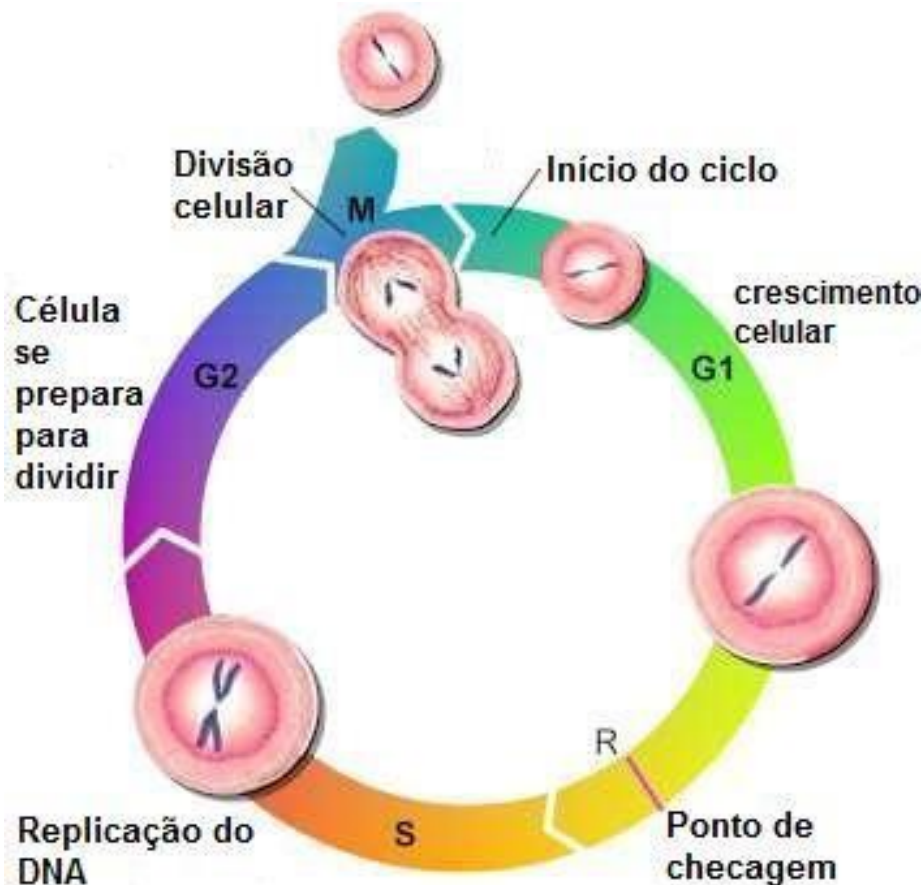
O processo de carcinogênese depende do acúmulo sequencial de mutações dentro de células, as quais não foram eficientes em reparar os danos no DNA, comprometendo a estabilidade genômica. Esse comprometimento é devido às alterações moleculares em vias de sinalização oncogênica ou em vias de sinalização de genes supressores de tumor (HAHN; WEINBERG, 2002). As modificações moleculares que ocorrem nesse processo podem conferir maior potencial proliferativo; replicação descontrolada; insensibilidade a sinais supressores de crescimento; indução da angiogênese; instabilidade genômica e mutabilidade; fuga à destruição imunológica; evasão à apoptose; capacidade de invadir tecidos adjacentes e promover metástases (VIDEIRA; REIS; BRITO, 2014). Para evitar que essas instabilidades ocorram as células possuem mecanismos de defesas.

O ciclo celular possui ferramentas para evitar que danos no DNA fixem nas células. A progressão desregulada do ciclo celular induz o processo tumoral e, por isso,

tem sido foco de pesquisadores, que têm por objetivo o desenvolvimento de fármacos antineoplásicos que atuam diretamente sobre o ciclo celular (DE ALMEIDA et al., 2005).

A divisão celular é altamente coordenada com a progressão de uma fase para outra por meio de uma maquinaria bioquímica ligada a sinais extracelulares de controle de crescimento e proliferação. A maior parte dos mecanismos envolvidos na evolução de uma célula normal para potencialmente maligna está relacionada a interferência no ciclo celular (HAHN; WEINBERG, 2002). O ciclo celular é dividido em cinco fases: fase G1 (gap 1); a fase S (síntese de DNA); G2 (gap 1); a fase M (mitose); e G0 (repouso) representado na figura 3 (BARR; GRUNEBERG, 2007).

Figura 3. Fases do ciclo celular.



Fonte: <https://www.google.com.br/imghp>

A passagem de uma fase para outra, ocorre apenas após ativação dos “checkpoints” (Figura 4), que são pontos de checagem regulados por proteínas que conduzem a célula a apoptose quando não há condição favorável de replicação. A falha ou mutação de alguma dessas proteínas pode levar ao surgimento de tumores

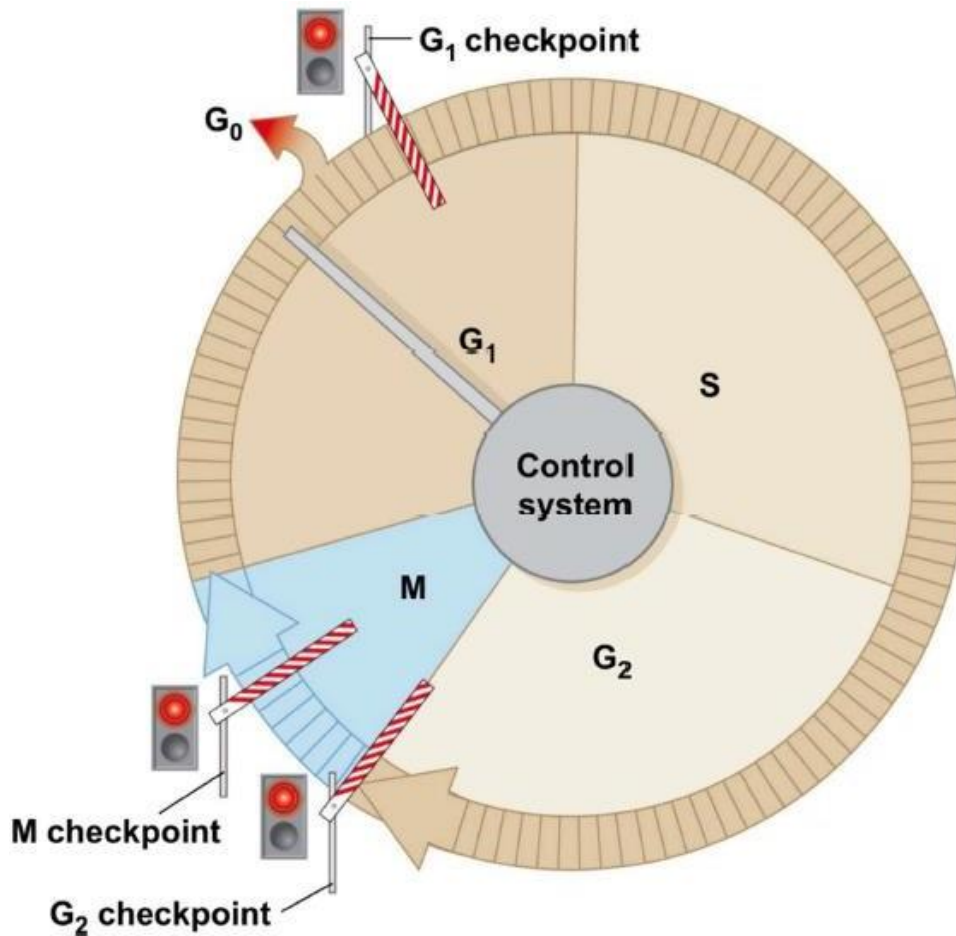
(GALLORINI; CATALDI; DI GIACOMO, 2012). Os pontos de checagem ocorrem em G1, na transição de G1 para S; em G2 na transição de G2 para M (MALUMBRES; BARBACID, 2005).

A regulação nesses pontos de checagem é exercida por diversas moléculas, dentre as quais se destacam as ciclinas e as proteínas quinase dependentes de ciclinas (CDK) e os inibidores das quinase-ciclina CDKI. As atividades das CDK são contrabalanceadas pelas CKIs, que incluem os inibidores universais como o P21, P27, e P57 que atuam em vários períodos do ciclo celular (SCHWARTZ; SHAH, 2005).

Outro componente envolvido no ponto de checagem e no reparo de erros no DNA é o fator de transcrição p53. Quando ocorrem danos irreparáveis à molécula de DNA o p53 pode ativar a transcrição de vários genes envolvidos no controle celular como o p21, Gadd45, BAX, APAF-1, PTEN, PUMA e dentre outros (KLEIN, 2004; RESNICK; INGA, 2003).

Modificações nos componentes do ciclo celular e nas vias de sinalização de checkpoint incidem na maioria dos tumores, resultantes da alteração de oncogenes e genes supressores tumorais, os quais têm fundamentais implicações na otimização de regimes terapêuticos e na seleção de novos alvos que atuam no ciclo celular (STEWART; WESTFALL; PIETENPOL, 2003).

Figura 4. Representação do ciclo celular e principais checkpoints.



Fonte: adaptado de <https://pin.it/vni2bkojy3eowv>.

2.3 Abordagem terapêutica

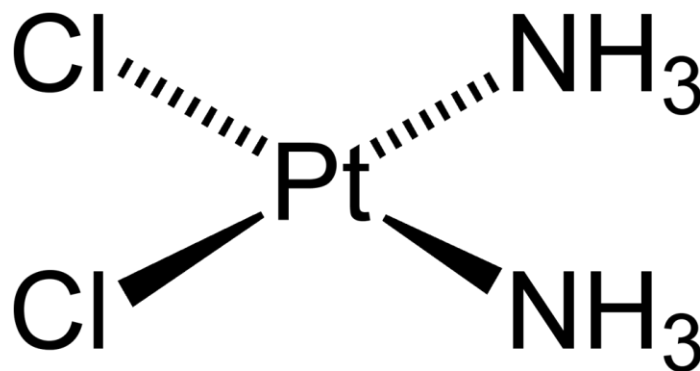
A radioterapia, a cirurgia e a quimioterapia são os três principais tipos de tratamento do câncer. No entanto, a quimioterapia é o foco das pesquisas nas últimas quatro décadas (STEWART; WILD, 2014) e uma das principais barreiras para o sucesso do tratamento é a resistência às múltiplas drogas e a necessidade de drogas seletivas, ou seja, que atuem nas células tumorais sem causar danos às suas equivalentes normais (REIS, 2006; REICHEL ET AL., 2011). Assim, busca-se, em especial, por compostos que sejam capazes de causar apoptose nas células tumorais sem aumentar a frequência de danos no DNA em células não tumorais (NAVARRO ET AL., 2018; OLIVEIRA ET AL., 2018A; OLIVEIRA ET AL., 2018B, RABACOW ET AL., 2018)

Apesar de não seletivo, um dos agentes quimioterápicos mais utilizados para o tratamento de diversos tipos de tumores é a Cisplatina (figura 4) (cis-

diaminodichloroplatina; CDDP). Sua ação biológica relaciona-se diretamente à sua interação com o DNA, capacidade de inibir a replicação do mesmo e assim desencadear a morte celular (FONSECA ET AL., 2016; TAKIMOTO ET AL., 2016).

Já existem comercialmente alguns medicamentos análogos à cisplatina tais como a carboplatina, oxaliplatina, nedaplatina, lobaplatina e heptaplatina (NEVES; VARGAS, 2011). Inspirado nesses fármacos, há um constante interesse no desenvolvimento de novos complexos de platina com a mesma efetividade. Porém, com menor toxicidade (SHAHSAVANI ET AL., 2016; SHARMA; AMETA; SINGH, 2016; ANASAMY ET AL., 2016; WANG ET AL., 2016). Entretanto, estudos recentes apontam um grande potencial no desenvolvimento de novos complexos com um perfil de ação terapêutico diferente da cisplatina com a variação do metal e consequente alteração das suas propriedades químicas (MATOS, 2002). Dentre os metais que podem ser variados, atualmente, a literatura relata o uso do cobre com propriedades anticâncer (PIVETTA ET AL., 2012; BANTI; HADJIKAKOU, 2013; IQBAL ET AL., 2015).

Figura 5. Estrutura da cisplatina.



Fonte: <https://www.google.com.br/imghp>

A coordenação de metais a fármacos apresenta-se como uma possibilidade de aumentar o arsenal de medicamentos disponíveis para tratamento de uma série de doenças e dentre elas o câncer (ROCHA ET AL., 2011). A 4-Aminoantipirina (4-AA) é resultado da metabolização da dipirona no fígado. Este metabólito já é conhecido na literatura por suas várias atividades biológicas, tais como analgésica, antipirética e propriedades anti-inflamatórias e até por sua possível capacidade de reduzir a eficiência de tratamentos quimioterápicos se usado como analgésico durante os ciclos de quimioterapia (BERNO et al., 2016).

Destaca-se ainda que diversas substâncias, as quais contêm o grupo 1,4-dioxo-2-butenil, foram sintetizadas como candidatas a citotoxinas e os resultados sugerem que os N-aril-fumaramatos de metila (4a-i) apresentaram os maiores potenciais, demonstrando uma potência maior ou equivalente com a droga de referência (JHA ET AL., 2010).

Assim, idealizar novos compostos que considerem os complexos de metais de custo relativamente baixo, como o cobre e a prata, com substâncias que possuem ação citotóxicas e/ou anticâncer já descritas e confirmadas na literatura, permitem a prospecção de novos candidatos à quimioterápicos e/ou quimioprotetores.

3. OBJETIVOS

3.1 Objetivo Geral

Analisar, em células de adenocarcinoma mamário murino 4T1, os efeitos citotóxicos do novo complexo Bis(((Z)-4-((4-clorofenil)amino)-4-oxobut-2-enil)oxi)cobre e, em camundongos *Swiss* o seu potencial toxicogenético.

3.2 Objetivos específicos

Avaliar, *in vitro*, a atividade citotóxica do composto Bis(((Z)-4-((4-clorofenil)amino)-4-oxobut-2-enil)oxi)cobre (RC1) na linhagem de adenocarcinoma mamário murino 4T1;

Determinar o valor da IC₅₀ do composto RC1 em células 4T1;

Avaliar a atividade genotóxica do composto RC1 na linhagem tumoral 4T1;

Analisar a influência do composto RC1 no ciclo celular das células 4T1;

Avaliar o tipo de morte celular decorrente da administração do composto RC1 em células tumorais 4T1;

Avaliar a expressão de genes de dano e reparo do DNA, e apoptose nas células 4T1 submetidas ao tratamento com o composto RC1;

Avaliar a influência do composto RC1 nos parâmetros biométricos de camundongos *Swiss*;

Analisar *in vivo* a atividade genotóxica do composto RC1;

Avaliar a influência do composto RC1 na fagocitose esplênica de camundongos *Swiss*.

4. METODOLOGIA

4.1 Síntese Química

Para a obtenção do composto foram reagidos 2,5 mmol de anidrido maleíco com 2,5 mmol de p-cloro-anilina em éter à temperatura ambiente, por aproximadamente 3 horas. O precipitado foi filtrado, lavado com água gelada e seco à temperatura ambiente. Após, foram reagidos 0,5 mmol do produto com 0,5 mmol de hidróxido de sódio (NaOH), em etanol, à temperatura ambiente por aproximadamente 1 hora e logo depois, foram adicionados 0,25 mmol de sulfato de cobre (II) penta-hidratado (CuSO₄.5H₂O) e deixou reagir por aproximadamente 2 horas. O precipitado azul obtido foi filtrado e seco à temperatura ambiente.

4.2 Ensaios *in vitro*

Condições de Cultivo Celular

As células de adenocarcinoma mamário murino 4T1 (ATCC number CRL-2539) foram cultivadas em frasco de cultura de 75cm² em Dulbecco's Modified Eagle Medium (DMEM) (Gibco®, Life Technologies, Grand Island, NY) suplementado com 10% de soro bovino fetal (Gibco®), em estufa de CO₂ (5%) com ambiente umidificado e a 37°C. Ao atingir a confluência de 80%, as células foram coletadas, por dissociação enzimática (tripsina 0,025% à 37°C), e distribuídas em placas em contagens variáveis, conforme a necessidade de cada experimento.

Agentes químicos

A cisplatina (Fauldcispla®, Libbs) foi utilizada como controle positivo na concentração de 50 µg/mL (Lee et al., 2009). Como substância teste utilizou-se o composto RC1 diluído em 1% de dimetilsulfóxido (Synth®) e como controle negativo meio DMEM com 1% de DMSO.

Ensaio de citotoxicidade (MTT- Thiazolyl Blue Tetrazolium Bromide)

A avaliação da citotoxicidade foi realizada pelo ensaio colorimétrico com (3-(4,5-dimethylthiazol-2-yl)-2,5-diphenyltetrazolium bromide) (MTT) conforme descrito por Schweich et al. (2017), com modificações. Foram semeadas 2,5 x 10⁴ células/poço em placas de 96 poços, mantidas por 24 horas para estabilização em incubadora (5% de CO₂ e 37°C). Em seguida, procederam-se os tratamentos com cisplatina na concentração de 50 µg/mL, nove concentrações do composto RC1 (3,125, 6,25, 12,5, 25, 50, 100, 250, 500 e 1000µg/mL) e como controle negativo as células receberam 1% de DMSO. A citotoxicidade foi avaliada em 24, 48 e 72 horas. A IC₅₀ foi calculada conforme Pesarini et al. (2017) e utilizada nos demais experimentos *in vitro*.

Ensaio do cometa

O ensaio do cometa foi realizado segundo Oliveira et al. (2014). Para a realização do teste do cometa, as células 4T1 foram cultivadas em placas de 6 poços (1,5x10⁵ células/poço) por um ciclo completo (24h) antes dos tratamentos. Os tratamentos, controle negativo (1% DMSO), controle positivo (50 µg/mL de cisplatina) e a IC50 do RC1, foram realizados em triplicatas independentes. Após o tratamento de 4 horas, as células foram coletadas por dissociação enzimática (tripsina 0,025% à 37°C), centrifugadas a 1200 rpm por 5 minutos e o sobrenadante descartado. As células foram ressuspensas em 500 µL de DMEM e uma alíquota de 20 µL acrescida de 120 µL de agarose de baixo ponto de fusão (1,5%) foi depositada em lâmina pré-revestida com agarose normal (5%). Após lise (Oliveira et al., 2007) e eletroforese (Navarro et al., 2014) as lâminas foram neutralizadas, secas e posteriormente fixadas com etanol absoluto.

A análise ocorreu em microscópio de fluorescência (Bioval® Modelo G2000 A, Brasil) utilizando 100 µL de brometo de etídio (20 x 10⁻³ mg/mL). Foram analisados 100 cometas/tratamento/repetição (aumento de 40x, filtro de excitação de 420-490 nm e de barreira de 520 nm), os quais foram classificados em classe 0 - nucleóides sem cauda do cometa; classe 1 - cauda do cometa menor ou igual ao diâmetro do nucleóide; classe 2 - cauda do cometa maior ou até duas vezes o diâmetro do nucleóide; e classe 3 - cauda do cometa maior que duas vezes o diâmetro do nucleóide (Kobayashi et al., 1995). O Score de dano genômico foi determinado multiplicando o número de células com danos em cada classe, pelo número da classe de danos (Oliveira et al. 2007; Hoff Brait et al., 2015).

Avaliação qualitativa de morte celular

Para análise qualitativa e morfológica da influência do RC1 nas células 4T1, 2 x 10⁵ células foram plaqueadas em placas de 6 poços contendo uma lamínula em sua base e mantidas em incubadora com 5% CO₂ a 37°C, por 24 horas para estabilização. Após aderência procedeu-se os tratamentos com cisplatina 50 µg/mL (controle positivo), 1% DMSO (controle negativo) e com a IC50 do composto RC1. Após 24 horas de tratamento, as lamínulas foram coletadas e processadas de acordo com o protocolo descrito por Schweich et al. (2017). Após três lavagens com PBS, as lamínulas foram retiradas das placas de cultivo e fixadas em Carnoy por 5 minutos. A lamínula foi mergulhada rapidamente em cada uma das placas contendo concentrações decrescentes de etanol (95% a 25%), seguida de lavagem com Tampão McIlvaine por 5 minutos, coloração com alaranjado de acridina (0,01%, 5 minutos) e nova lavagem com o

tampão. A análise foi realizada em microscópio de fluorescência com filtro de excitação 420-490nm e filtro de barreira 520nm.

Avaliação diferencial e quantitativa de morte celular

Para análise qualitativa e morfológica da influência do RC1 nas células 4T1, 2 x 10⁵ células foram plaqueadas em placas de 6 poços e mantidas em incubadora com 5% CO₂ a 37°C, por 24 horas. Após procedeu-se os tratamentos com cisplatina 50 µg/mL (controle positivo), 1% DMSO (controle negativo) e com a IC₅₀ do composto RC1. Após 24 horas de tratamento, as células foram coletadas por dissociação enzimática (tripsina 0,025% à 37°C), centrifugadas a 1200rpm por 5 minutos e o sobrenadante descartado. Em seguida, 50 µL da solução foi homogeneizada com 2µL de corante (100,0µg/mL de Laranja de Acridina e 100,0µg/mL de Brometo de Etídeo, ambos diluídos em PBS). Em seguida, essa suspensão celular foi disposta em lâmina de vidro recoberta por lamínula e analisada em microscópio de fluorescência com filtro de excitação 420-490nm e filtro de barreira 520nm.

A classificação das células foi realizada segundo a descrição: (I) células vivas com membrana funcional possuem coloração verde uniforme em seu núcleo; (II) células em apoptose inicial com membrana funcional, mas com fragmentação de DNA, demonstram uma coloração verde no núcleo e citoplasma, sendo visível uma marginalização do seu conteúdo nuclear; (III) células em apoptose final apresentam áreas coradas em alaranjado, tanto no citoplasma como nos locais onde a cromatina está condensada no núcleo, o que as distingue de células necróticas; (IV) células necróticas têm coloração alaranjada uniforme no núcleo (Oliveira et al., 2007). Foram contadas 100 células/tratamento. Os experimentos foram realizados em triplicata independentes.

Ensaio de citometria de fluxo

Os experimentos de ciclo celular, apoptose e integridade de membrana foram realizados por meio de citometria de fluxo, em triplicatas independentes, conforme descrito por Schweich et al. (2017). Foram semeadas 2x10⁵ de células 4T1 em placas de 6 poços e mantidas em incubadora com 5% CO₂ a 37°C, por 24 horas. Após procedeu-se os tratamentos com cisplatina 50 µg/mL (controle positivo), 1% DMSO (controle negativo) e com a IC₅₀ do composto RC1. Após 24 horas de tratamento as células foram coletadas por dissociação enzimática, centrifugadas a 1200 rpm por 5 minutos e o sobrenadante foi descartado. O pellet foi ressuscitado em 100µL de PBS e transferido para um criotubo. A aquisição de 10.000 eventos foi realizada em citômetro BD Accuri® C6 e, em seguida, analisada pelo Software BD Accuri® C6.

Ciclo celular

Para verificar a influência dos tratamentos sobre o ciclo celular, 5µL de RNase (2mg/mL) foram adicionados ao criotubo contendo 100µL de suspensão celular (em PBS) e incubou-se a 37°C, 5% de CO₂, por 30 minutos. Em seguida, acrescentou 100µL da solução de lise (20mg de Citrato de Sódio Dihidratado, 20µL de Triton X 100 e 20 mL de PBS) e 5µL de Iodeto de Propídio (50µg/mL). O criotubo foi incubado no gelo por 30 minutos protegido da luz antes da aquisição (Schweich et al., 2017).

Apoptose

Para a detecção de apoptose foi utilizado o Kit de Detecção de Apoptose PE Annexin V (BD Pharmingen™). Para tanto, 100µL de suspensão celular foi homogeneizado com 100µL de solução tampão (1x) e 5µL de Anexina V. O criotubo foi incubado em gelo por 15 minutos. Em seguida, acrescentou-se 5µL de 7-aminoactinomycin D (7AAD) e procedeu-se a aquisição imediatamente (Schweich et al., 2017). O estado celular foi definido conforme descrito por Savio et al. (2014), com modificações. As células não marcadas pelos corantes (Anexina V e 7AAD) foram classificadas como viáveis; as marcadas apenas pela anexina V foram classificadas em apoptose inicial; as células marcadas por ambos marcadores (Anexina V e 7-AAD) foram classificadas em apoptose tardia; e as marcadas apenas por 7AAD foram classificadas como necróticas.

Integridade de Membrana

Para verificação da integridade da membrana foram utilizados 100µL de suspensão celular e 25µL Iodeto de Propídeo (50µg/mL). Após 5 minutos em incubação à temperatura ambiente procedeu-se a aquisição (Schweich et al., 2017).

Expressão gênica - qPCR

A expressão gênica foi avaliada por qPCR. Um total de 2x10⁵ células foram distribuídas em placas de 6 poços e tratadas com 1% DMSO (controle negativo) e com a IC50 do composto RC1. Após 12 horas de tratamento, o RNA total foi extraído por meio de um método in house, utilizando tampão de lise à base de tiocianato de guanidina (Tiocianato de guanidina 5mol/L, Tris HCL 11,2g/L pH6,4, EDTA NaOH 7,43 g/L, 7,8mLTriton X-100). As amostras foram extraídas em triplicata, utilizando 200µL da suspensão celular em 200µL do Tampão de Lise. Após homogeneização por 10 minutos foram adicionados 50µL de beads magnética (Nuclisens®, bioMérieux) e deixado em repouso durante 10 minutos. As impurezas (restos celulares) foram extraídas em rack magnetizada (Promega) realizando duas lavagens com tampão de lise. O excesso de tiocianato de guanidina e sais foram retirados com lavagens de álcool 70% ultrapuro. As beads receberam lavagens com acetona PA, foram aquecidas por um

minuto à 60°C em equipamento de banho seco DB-HC (Loccus®, Brasil) e o material genético foi eluído com 30µL TE (bioMérieux®). Após extração foi realizado tratamento com RQ1 RNase-Free DNase (cat. no. M6101, Promega®) de acordo com as especificações do fabricante. Após a etapa de degradação do DNA, a qualidade do material extraído foi analisada por meio do quociente A260/A280 e A230/A260 em espectrofotômetro NanoVue™ Plus (GE Healthcare – Life Sciences®) e a integridade em gel de agarose desnaturante (1%).

O DNA complementar (cDNA) foi obtido em termociclador T100™ (Thermal Cycler, Bio-Rad™) utilizando 250ng de RNA acrescido de 0,5µg de random primer, água ultra pura livre de RNase/DNase, 5µl GoScript™ Tampão 5X, 3,8 mM MgCl₂, 0,5 mM DNTPs, 20 unidades do inibidor de RNase e 1µl de GoScript™ Reverse (todos componentes Promega). A mistura foi incubada por 25°C durante 5 minutos, seguido de 42°C por 60 minutos e 70°C por 15 minutos.

As reações de qPCR foram realizadas em triplicatas no aparelho Rotor Gene® (Qiagen). Os genes analisados estão descritos na Tabela 1. Foram testados genes envolvidos nos processos de danos no DNA (p53, p21, ATR, ATM e GADD45) e apoptose (BAX, BAK, BCL-2, CASP9, CASP7 e CASP3). Para as reações de qPCR foram utilizados 10µl de master mix GoTaq®, 2 pmol de cada oligonucleotídeo, 500ng de cDNA e água livre de ribonuclease q.s.p. 20 µl (cat. no. A6002, Promega®). A mistura foi submetida a 95°C por 5 minutos e 40 ciclos, de 95°C por 2 segundos e 60°C por 30 segundos. Ao final a curva de Melting foi realizada para avaliar a especificidade dos produtos formados. O gene da Beta-actina (ACTB) foi utilizado como normalizador (housekeeping) e os resultados analisados em software Rotor Gene® (Qiagen) v2.3.1.

4.3 Ensaios in vivo

Animais e condições de alojamento

O experimento foi conduzido de acordo com a Declaração Universal dos Direitos dos Animais, após aprovação da Comissão de Ética no Uso de Animais da Universidade Federal de Mato Grosso do Sul registrado (protocolo 921/2017), no Laboratório de Biotecnologia da Reprodução de Pequenos Ruminantes (BIOCAPRI). Os animais foram mantidos em caixas de propileno recobertas por maravalha e alimentados com ração comercial (Nuvital®) e água filtrada ad libitum. A temperatura e luminosidade foram controladas, para tanto, os animais estavam mantidos sob condições padronizadas de climatização (caixa ventilada ALESCO®): fotoperíodo de doze horas (12 horas de claro: 12 horas de escuro), com temperatura mantendo-se em torno de 22 ± 2°C e umidade relativa de 55 ± 10%.

Agentes químicos

O tratamento quimioterápico foi realizado com cisplatina (Fauldcispla®, Libbs) na dose de 6mg/Kg de peso corpóreo (p.c.) (Berno et al., 2016), via intraperitoneal (i.p.), em uma aplicação no 1º dia experimental.

O composto teste, RC1, foi diluído em DMSO (1%) e administrado nas doses de 3, 6 e 12 mg/Kg (p.c.; i.p.).

Delineamento experimental

Foram utilizados 40 camundongos *Mus musculus* da variedade Swiss, machos, em idade reprodutiva com peso médio de 35g. Os animais foram distribuídos aleatoriamente em 8 grupos experimentais: Grupo Controle (NC) – os animais receberam solução fisiológica (1% DMSO) via intraperitoneal na porção de 0,1ml/10g de peso corpóreo (p.c.); Controle Positivo (PC) – os animais receberam cisplatina na dose de 6mg/Kg (p.c., i.p.); Grupos RC1 – os animais receberam o composto teste em 3 diferentes doses D1 (3mg/Kg), D2 (6mg/Kg) e D3 (12mg/Kg) via intraperitoneal; Grupos Associados (ASS1, ASS2 e ASS3) – os animais receberam cisplatina na dose de 6mg/Kg (p.c., i.p.) e o RC1 nas 3 diferentes doses (D1, D2 e D3) via intraperitoneal.

A coleta de sangue para o ensaio de micronúcleo foi realizada por punção da veia caudal em 24, 48 e 72 horas após a aplicação dos tratamentos (T1, T2 e T3, respectivamente), enquanto a coleta para o ensaio do cometa ocorreu apenas em T1. Após 72 horas da administração dos tratamentos, os animais foram submetidos à eutanásia por deslocamento cervical para coleta de órgãos.

Ensaio do Cometa

Uma lâmina pré-coberta com agarose normal (5%) recebeu 20µL de sangue periférico homogeneizado em 120µL de agarose LMP (1,5%) à 37°C. Em seguida, o ensaio do cometa foi realizado conforme descrito por Singh et al. (1988), com adaptações (Oliveira et al., 2009).

A análise e a classificação dos cometas foram realizadas conforme Kobayashi et al. (1995).

Ensaio do Micronúcleo

Utilizou-se a técnica de Hayashi et al. (1990), modificada por Oliveira et al. (2009). Para tanto, em uma lâmina previamente preparada com uma camada de 20µL de Alaranjado de Acridina (1,0mg/mL), uma gota de sangue periférico foi depositada e então recoberta por lamínula. Este material permaneceu em freezer (-20°C) por um período mínimo de 7 dias. A análise foi realizada em microscópio de fluorescência (Bioval® Modelo G2000 A, Brasil) com filtro de excitação 420-490nm e filtro de

barreira 520nm com aumento de 40x. Analisou-se 2000 células/animal.

Fagocitose esplênica

Os ensaios de fagocitose foram realizados de acordo com o procedimento descrito por Schneider et al. (2016). O baço foi macerado em solução fisiológica para a obtenção de uma suspensão homogênea de células e 100 μ L da suspensão celular foram colocadas em uma lâmina previamente corada com alaranjado de acridina (1mg/mL), recoberta por lamínula e acondicionadas em -20°C até o momento da análise. A análise foi realizada em microscópio de fluorescência (Bioval® Modelo G2000 A, Brasil) com filtro de 420-490nm e filtro de barreira de 520nm, em um aumento de 40x. Analisou-se 200 células/animal. A ausência ou presença de fagocitose foi baseada na descrição de Hayashi et al. (1990) com modificações (Carvalho et al., 2015).

4.4 Análise Estatística

Os resultados serão expressos em média \pm erro padrão da média. A determinação da concentração IC50 do RC1 foi realizada pela análise da curva de regressão não linear a partir dos valores de viabilidade celular obtidos no ensaio do MTT por meio do Software GraphPad Prism 5 (Pesarini et al., 2017). A análise estatística foi realizada por ANOVA/Bonferroni e ANOVA/Tukey, com exceção da qPCR que foi analisada por meio do programa REST (Pfaffl et al., 2002). A diferença significativa foi considerada quando o nível de expressão relativa foi igual ou inferior a 0,5 ou igual ou superior a 2 (Biazi et al., 2017), e em todos os ensaios o nível de significância estabelecido foi $p < 0,05$ (Software GraphPad InStat 5).

5. MANUSCRITO

O presente trabalho originou um artigo intitulado “*New Bis copper complex ((Z) - 4 - ((4-chlorophenyl) amino) -4-oxobut-2-enoyl) oxy): cytotoxicity in 4T1 cells and their toxicogenic potential in Swiss mice*” o qual foi publicado na revista *Toxicology and Applied Pharmacology*. Essa revista possui fator de impacto, atribuído pela *Journal Citation Reports* (JCR), de 3,791 e foi classificada pelo Qualis-Periódicos da Coordenação de Aperfeiçoamento de Pessoal de Nível Superior – CAPES, como A2 na área de concentração Ciências Biológicas I.



New Bis copper complex ((Z)-4-((4-chlorophenyl) amino)-4-oxobut-2-enoyl) oxy): Cytotoxicity in 4T1 cells and their toxicogenic potential in Swiss mice

Edwin José Torres de Oliveira^{a,b}, Lucas Roberto Pessatto^{a,b},
Raquel Oliveira Nascimento de Freitas^c, Bruno Ivo Pelizaro^{a,d}, Ana Paula Maluf Rabacow^{a,e},
Juliana Miron Vani^{a,e}, Antônio Carlos Duenhas Monreal^a, Mário Sérgio Mantovani^b,
Ricardo Bentes de Azevedo^f, Andréia Conceição Milan Brochado Antonioli-Silva^{a,e},
Roberto da Silva Gomes^{c,□}, Rodrigo Juliano Oliveira^{a,b,d,e,□□}

^a Centro de Estudos em CÉLULAS Tronco, TERAPIA CELULAR e GENÉTICA TOXICOLÓGICA – CeTroGen, HOSPITAL Universitário MARIA APARECIDA PEDROSSIAN, EMPRESA BRASILEIRA de Serviços HOSPITALARES – EBSEH, CAMPO GRANDE, MATO Grosso do Sul, BRAZIL

^b PROGRAMA de PÓS-GRADUAÇÃO em GENÉTICA e BIOLOGIA MOLECULAR, Centro de CIÊNCIAS BIOLÓGICAS - CCB, DEPARTAMENTO de BIOLOGIA GERAL, UNIVERSIDADE ESTADUAL de LONDRINA - UEL, LONDRINA, BRAZIL

^c LABORATÓRIO de Síntese e Modificação MOLECULAR, FACULDADE de CIÊNCIAS EXATAS e TECNOLOGIA - FACET, UNIVERSIDADE FEDERAL DA GRANDE DOURADOS - UFGD, DOURADOS, MATO Grosso do Sul 79804-970, BRAZIL

^d PROGRAMA de Mestrado em FARMÁCIA, FACULDADE de CIÊNCIAS FARMACÉUTICAS, Alimentos e Nutrição – FACFAN, UNIVERSIDADE FEDERAL de MATO Grosso do Sul – UFMS, CAMPO GRANDE, MATO Grosso do Sul, BRAZIL

^e FACULDADE de MEDICINA Dr. Hélio MANDETTA, PROGRAMA de PÓS-GRADUAÇÃO em SAÚDE e Desenvolvimento NA Região Centro-Oeste, CAMPO GRANDE, MATO Grosso do Sul, BRAZIL

^f DEPARTAMENTO de GENÉTICA e MORFOLOGIA, Instituto de CIÊNCIAS BIOLÓGICAS - IB, UNIVERSIDADE de BRASÍLIA - UNB, BRASÍLIA, Distrito FEDERAL, BRAZIL

ARTICLE INFO

Keywords:

Copper(II) Complexes
DNA Damage
Cell Cycle
Apoptosis
Antitumor Activity
Breast Cancer

ABSTRACT

Copper (II) complexes are promising in the development of new synthetic models for cancer treatment. In this context, we synthesized a new copper complex containing the pharmacophore group 1,4-dioxo-2-butenyl, the Bis (((Z)-4-((4-chlorophenyl) amino)-4-oxobut-2-enoyl)oxy) copper compound and we evaluated its antitumor activity in 4 T1 murine mammary adenocarcinoma cells and their toxicogenic effect in Swiss mice. The compound demonstrated cytotoxicity and genotoxicity to 4 T1 cells, and after cell cycle arrest in G1, which occurred by the increase in *ATM* and *p21* expression, it induced the cells to apoptosis by increasing *BAX* and *CASPASE-7*. *In vivo* the compound was genotoxic in mice but did not show permanent damage, observed by the absence of increased micronucleus frequency, and did not induce changes in the biometric parameters of the animals. These results indicate that the new copper complex, described firstly in this work, presents therapeutic potential for breast cancer.

1. Introduction

Cancer is a major public health issue on a global scale. Worldwide, cancer incidence could potentially increase to as many as 17 million new cases per year by 2020 (GLOBOCAN, 2012) and > 20 million by 2025 (Stewart and Wild, 2014). In men, lung and prostate cancer is more prevalent, while in women breast cancer is more common

(Stewart and Wild, 2014). Ferlay et al. (2015) reported that breast cancer alone accounts for 25% of all cancer cases among females and over 522 thousand women died from this disease in 2012.

One of the main modes of medical intervention in the treatment of cancer is chemotherapy, which consists of the use of drugs (chemotherapeutic), for the elimination of neoplastic cells. Cisplatin and its analogues are widely used in the treatment of various types of cancer,

[□] Corresponding author at: Faculdade de Ciências Exatas e Tecnologia - FACET, Universidade Federal da Grande Dourados - UFGD, Rodovia Dourados - Itahum, Dourados, MS 79804-970, Brazil.

^{□□} Correspondence to: Faculdade de Medicina Dr. Hélio Mandetta, Universidade Federal de Mato Grosso do Sul. Cidade Universitária, Campo Grande, MS 79070-900, Brazil.

E-MAIL ADDRESSES: robertogomes@ufgd.edu.br (R. da Silva Gomes), rodrigo.oliveira@ufms.br (R.J. Oliveira).

including breast cancer (Dasari and Bernard Tchounwou, 2014; Tsimberidou et al., 2009). However, several adverse effects are reported, such as ototoxicity, nephrotoxicity, neurotoxicity, bone marrow suppression, and gastrointestinal disorders (Martins et al., 2017). In addition to these compounds, the literature reports that copper complexes have antitumor activity (Gao et al., 2011; Pivetta et al., 2012; Thalamuthu et al., 2013), including for breast cancer (Fan et al., 2017; Gouda et al., 2018; Manikandamathavan et al., 2017; Sangeetha and Murali, 2017). Therefore, the coordination of metals to drugs is a possibility to expand the therapies for the treatment of this disease.

In addition to metals there are also important pharmacophoric groups with cytotoxic and anticancer activity (Jha et al., 2010). A good example is the derivatives of maleamic acids, such as chalcones (Mitra et al., 2015), which possess the 1,4-dioxo-2-butenyl group and which demonstrated potent anticancer activity, *in vitro* and *in vivo*, moreover they are not toxic in mice (Rodrigues et al., 2011).

Several research groups seek, through new natural or synthetic compounds, to solve the inherent challenges of side effects, resistance of tumor cells and non-specificity of chemotherapeutics. In this context, our research group proposed to design a new compound based on the anticancer actions of copper and the pharmacophoric group 1,4-dioxo-2-butenyl. For this reason, the present work evaluated the antitumor activity of the new copper (III) complex, Bis(((Z)-4-((4-chlorophenyl)amino)-4-oxobut-2-enoyl)oxy)copper (RC1), in murine mammary adenocarcinoma cells 4 T1, as well as its toxicogenic effect in *Swiss* mice.

2. Methods

2.1. Synthetic chemistry

To obtain the compound, 2.5 mmol of maleic anhydride was reacted with 2.5 mmol of p-chloroaniline in ether at room temperature for approximately 3 h. The precipitate was filtered, washed with cold water and dried at room temperature. Then, 2.5 mmol of sodium hydroxide (NaOH) in ethanol was added to the reaction mixture at room temperature and stirred for 1 h and thereafter 1.25 mmol of copper (II) sulfate pentahydrated ($\text{CuSO}_4 \cdot 5\text{H}_2\text{O}$) was added and the reaction mixture was incubated for more 2 h. The obtained blue precipitate was filtered and dried at room temperature.

2.2. *In vitro* ASSAY

2.2.1. Cell culture conditions

The 4 T1 murine mammary adenocarcinoma cell line (ATCC number CRL-2539) were grown in a 75cm² culture flask in Dulbecco's Modified Eagle Medium (DMEM) (Gibco®, Life Technologies, Grand Island, NY) supplemented with 10% foetal bovine serum (Gibco®), 0,1% penicillin 10.000 U/streptomycin 10.000 µg/mL (BR30110-01, LGC Biotecnologia) at 37 °C in a humidified atmosphere containing 5% CO₂. Upon reaching 80% confluency, the cells were collected by enzymatic dissociation (trypsin 0.025% at 37 °C), and placed in plates with variable counts, according to the need of each experiment.

2.2.2. CHEMICAL AGENTS

Cisplatin (Fauldcispla®, Libbs) was used as a positive control at 50 µg/mL concentration (Lee et al., 2009). As test substance the RC1 compound diluted in 1% dimethylsulfoxide (Synth®) was used and as a negative control DMEM medium with 1% DMSO.

2.2.3. Cytotoxicity ASSAY (MTT- THIAZOLYL Blue TETRAZOLIUM Bromide)

The cytotoxic potential was evaluated by the MTT colorimetric test 3-(4,5-Dimethyl-2-thiazolyl)-2,5-diphenyl-2H-tetrazolium bromide, performed as described by Schweich et al. (2017), with modifications. Cells were seeded at a density of 2.5×10^4 cells/well in 96 well culture plates and incubated with 5% CO₂ at 37 °C for 24 h for stabilization. Thereafter, the treatments were performed with 50 µg/mL

of cisplatin, nine concentrations of compound RC1 (3.125, 6.25, 12.5, 25, 50, 100, 250, 500 and 1000 µg/mL) and negative control cells received 1% DMSO. The cytotoxicity was evaluated at 24, 48 and 72 h. The IC₅₀ was calculated according to Pesarini et al. (2017) and used in the others *in vitro* experiments.

2.2.4. *In vitro* comet ASSAY

The comet assay was performed according to Oliveira et al. (2014). For the comet assay, 4 T1 cells were grown in 6-well plates (1.5×10^5 cells/well) for a complete cycle (24 h) before treatments. The treatments, negative control (1% DMSO), positive control (50 µg/mL cisplatin) and IC₅₀ of RC1 were performed in independent triplicates. After the 4 h treatment, the cells were collected by enzymatic dissociation (trypsin 0.025% at 37 °C), centrifuged at 1200 rpm for 5 min and the supernatant was discarded. The cells were resuspended in 500 µL of DMEM and a 20 µL aliquot plus 120 µL of low melting point agarose (1.5%) was deposited on a pre-coated slide with normal agarose (5%). After lysis (Oliveira et al., 2007) and electrophoresis (Navarro et al., 2014) the slides were neutralized, dried and fixed with absolute ethanol.

The analysis was performed under a fluorescence microscope (Bioval® Model G2000 A, Brazil) using 100 µL of ethidium bromide (20×10^{-3} mg/mL). 100 comets/treatment/repetition were analyzed (40× magnification, 420-490 nm excitation filter and 520 nm barrier), which were classified in class 0 - nucleoids without comet tail; Class 1 - Comet tail less than or equal to nucleoid diameter; class 2 - tail of the comet larger or up to twice the diameter of the nucleoid; and class 3 - comet tail larger than twice the nucleoid diameter (Kobayashi et al., 1995). The genomic damage Score was determined by multiplying the number of damaged cells in each class by the number of damage classes (Hoff Brait et al., 2015; Oliveira et al., 2007).

2.2.5. QUALITATIVE EVALUATION of cell DEATH

For qualitative and morphological analysis of the influence of RC1 on 4 T1 cells, 2×10^5 cells were plated in 6-well plates containing a coverslip at their base and maintained in incubator with 5% CO₂ at 37 °C for 24 h for stabilization. After adherence, treatments with 50 µg/mL of cisplatin (positive control), 1% DMSO (negative control) and IC₅₀ of compound RC1 were performed. After 24 h of treatment, the coverslips were collected and processed according to the protocol described by Schweich et al. (2017). After three washes with PBS, the coverslips were removed from the culture dishes and fixed in Carnoy fixative for 5 min. The coverslip was rapidly dipped into each of the plates containing decreasing concentrations of ethanol (95% to 25%), followed by washing with McIlvaine Buffer for 5 min, staining with acridine orange (0.01%, 5 min) and washing again with the buffer. The analysis was performed under a fluorescence microscope with excitation filter 420-490 nm and 520 nm barrier filter.

2.2.6. DIFFERENTIAL AND QUANTITATIVE EVALUATION of cell DEATH

For qualitative and morphological analysis of the influence of RC1 on 4 T1 cells, 2×10^5 cells were plated in 6-well plates and incubated with 5% CO₂ at 37 °C for 24 h. After that, the treatment was performed with 50 µg/mL of cisplatin (positive control), 1% DMSO (negative control) and with the IC₅₀ of compound RC1. After 24 h the cells were collected by enzymatic cleavage (0.025% trypsin at 37 °C), centrifuged at 1200 rpm for 5 min and the supernatant was discarded. Then, 50 µL of the solution was homogenized with 2 µL of dye (100 µg/mL of Acridine Orange and 100 µg/mL of Ethoxide Bromide, both diluted in PBS). This cell suspension was then placed on a glass slide covered by cover slip and analyzed under a fluorescence microscope with excitation filter 420-490 nm and 520 nm barrier filter.

Cell classification was performed according to the following description: (I) living cells with functional membrane have uniform green coloration in their nucleus; (II) cells in initial apoptosis with functional membrane, but with DNA fragmentation, show a green coloration in

Table 1
Primer sequences (5'– 3') used in real-time PCR.

Gene	Forward	Reverse	Size (pb)
ACTB	GGAAATCGTGCCTGACAT	AGGAAGGAAGGCTGGAAG	183
p53	TACCACCATCCACTACAAC	GACAGGCACAAACACGCAC	145
p21	TAGCAGCGGAACAAGGAG	AAACGGGAACCAGGACAC	249
ATR	CCTTCAGATTCCCTTGAATAC	GCAGTTCATGTTTIGATGAG	137
ATM	ACCATTGTAGAGGTCCTTC	GTCTCATTAAAGACACCGTTCAG	148
GADD45	TCAGCGCACGATCACTGTC	CCAGCAGGCACAACACCAC	82
BAX	CCT TCT TTG AGT TCG GTG	TTCAGTACTCAGTCATCCAC	100
BAK	CTGTTTGAGAGTGGCATC	ATGCTGGTAGACGTGTAG	84
BCL-2	GGACGAACTGGACAGTAAC	GCAAAGTAGAAAAGGGCGACAAC	127
CASP9	CTCTACTTCCAGGTTGA	TTTCCCGAAACAGCATT	195
CASP7	TCACCATGCGATCCATCAAGACCA	TTTGCTGTTCCGTTTCGAACGCC	148
CASP3	ATCATACATGGAAGCGAATC	ATACATAAACCCATCTCAGGA	86

nucleus and cytoplasm, with a visible marginalization of their nuclear content; (III) cells in final apoptosis present orange-stained areas both in the cytoplasm and in the sites where the chromatin is condensed in the nucleus, which distinguishes them from necrotic cells; (IV) necrotic cells have uniform orange staining in the nucleus (Oliveira et al., 2007). 100 cells/treatment were counted. The experiments were performed in independent triplicate.

2.2.7. Flow cytometry ASSAYS

The cell cycle experiments, apoptosis and membrane integrity were performed by flow cytometry in independent triplicates, as described by Schweich et al. (2017). 2×10^5 of 4 T1 cells were seeded in 6 well plates and incubated with 5% CO₂ at 37 °C for 24 h. After that, the treatments with 50 µg/mL of cisplatin (positive control), 1% DMSO (negative control) and with the IC₅₀ of compound RC1 were performed. After 24 h the cells were collected by enzymatic cleavage, centrifuged at 1200 rpm for 5 min and the supernatant was discarded. The pellet was resuspended in 100 µL of PBS and transferred to a cryotube. The acquisition of 10.000 events was performed on a BD Accuri® C6 cytometer and then analyzed by BD Accuri® C6 Software.

2.2.7.1. Cell cycle. To verify the influence of the treatments on the cell cycle, 5 µL of RNase (2 mg/mL) were added to the cryotube containing 100 µL of cell suspension (in PBS) and incubated at 37 °C, 5% CO₂, for 30 min. Then, 100 µL of the lysis solution (20 mg Sodium Citrate Dihydrate, 20 µL Triton X 100 and 20 mL PBS) and 5 µL of Propidium Iodide (50 µg / mL) were added. The cryotube was incubated on ice for 30 min protected from light prior to acquisition (Schweich et al., 2017).

2.2.7.2. Apoptosis. The Annexin V Apoptosis PE Detection Kit (BD Pharmingen™) was used for the detection of apoptosis. To this end, 100 µL of cell suspension was homogenized with 100 µL of buffer solution (1×) and 5 µL of Annexin V. The cryotube was incubated on ice for 15 min. Then, 5 µL of 7-aminoactinomycin D (7AAD) was added and the acquisition was done immediately (Schweich et al., 2017). Cell status was defined as described by Savio et al. (2014), with modifications. The cells not labeled by the dyes (Annexin V and 7AAD) were classified as viable; those labeled only by annexin V were classified as initial apoptosis; cells labeled by both markers (Annexin V and 7-AAD) were classified as late apoptosis; and those marked only by 7AAD were classified as necrotic.

2.2.7.3. MEMBRANE integrity. To verify membrane integrity, 100 µL of cell suspension and 25 µL Propionate Iodide (50 µg/mL) were used. After 5 min of incubation at room temperature the acquisition was made (Schweich et al., 2017).

2.2.8. Gene expression – qPCR

Gene expression was evaluated by qPCR. In a 6 well plates a total of 2×10^5 cells/well were seeded and treated with a 1% DMSO (negative

control) and with IC₅₀ of RC1. After 12 h, the total RNA was extract by an in house method using a lyses buffer containing guanidine isothiocyanate (GuSCN 5 mol/L, Tris HCL 11.2 g/L pH 6.4, EDTA NaOH 7.43 g/L, 7.8mL Triton X-100). Each sample was extracted in triplicate. 200 µL of lysis buffer was added in 200 µL of cell suspension. After 10 min of homogenization, it was added 50 µL of magnetic beads (Nuclisens®, bioMérieux) and allowed to stand for 10 min. The impurities (cell debris) were extracted by magnetized rack (Promega®) by performing two washes with lysis buffer. Excess of guanidine thiocyanate and salts were withdrawn with 70% ultrapure alcohol washings. The beads were washed with acetone PA, heated for one minute at 60 °C in dry bath equipment DB-HC (Loccus®, Brazil) and the genetic material was eluted with 30 µL of TE (bioMérieux®). After extraction, RQ1 RNase-Free DNase (cat. no. M6101, Promega®) was performed according to the manufacturer's specifications. After the DNA degradation step, the quality of the extracted material was analyzed by ratio of the quotient A260/A280 and A230/A260 in a NanoVue™ Plus spectrophotometer (GE Healthcare - Life Sciences®) and the integrity in denaturing agarose gel (1%). Complementary DNA (cDNA) was obtained on T100™ thermal cycler (Thermal Cycler, Bio-Rad™) using 250 ng of RNA plus 0.5 µg of random primer, ultra-pure RNase/DNase free water, 5 µL of GoScript™ 5× Buffer 3.8 mM of MgCl₂, 0.5 mM of DNTPs, 20 units of the RNase inhibitor and 1 µL of GoScript™ Reverse (all Promega components). The mixture was incubated at 25 °C for 5 min, followed by 42 °C for 60 min and 70 °C for 15 min. The qPCR reactions were performed in triplicates in the Rotor Gene® equipment (Qiagen). The genes analyzed are described in Table 1. The tested genes were involved in DNA damage processes (*p53*, *p21*, *ATR*, *ATM* AND *GADD45*) and apoptosis (*BAX*, *BAK*, *BCL-2*, *CASP9*, *CASP7* AND *CASP3*). For the qPCR reactions, it was used 10 µL of GoTaq® master mix, 2 pmol of each oligonucleotide, 500 ng of cDNA and free of ribonuclease water q.s.p. 20 µL (cat. no. A6002, Promega®). The mixture was subjected to 95 °C for 5 min and 40 cycles, 95 °C for 2 s and 60 °C for 30 s. At the end, the Melting curve was performed to evaluate the specificity of the products formed. The Beta-actin gene (*ACTB*) was used as housekeeping and the results were analyzed in Rotor Gene® SOFTWARE (Qiagen) v2.3.1.

2.3. In vivo ASSAYS

2.3.1. ANIMALS AND ACCOMMODATION conditions

The experiment was conducted in accordance with the Universal Declaration of the Rights of the Animals, after approval of the Ethical Committee on the Use of Animals of the Federal University of Mato Grosso do Sul registered (protocol 921/2017). The animals were kept in polypropylene boxes coated with wood shavings and fed with commercial feed (Nuvital®) and filtered water *ad libitum*. The temperature and luminosity were controlled, for that the animals were kept under standard conditions of air conditioning (ventilated box ALESCO®): photoperiod of twelve hours (12 h of light: 12 h of darkness), with temperature keeping around 22 ± 2 °C and relative humidity of

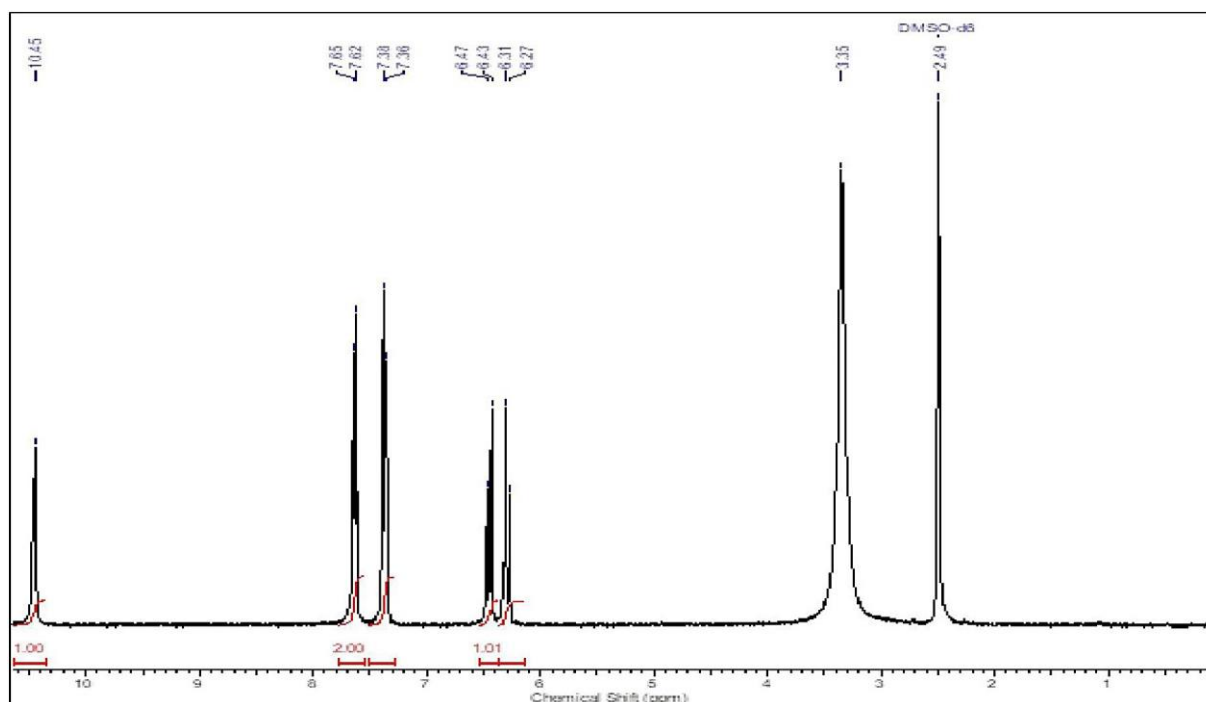


Fig. 1. ^1H NMR spectra of RC1 in $\text{DMSO-}d_6$ at 300 MHz.

$55 \pm 10\%$.

2.3.2. CHEMICAL AGENTS

The chemotherapeutic treatment was performed with cisplatin (Fauldcispla®, Libbs) at a dose of 6 mg/kg body weight (b.w.) (Bernó et al., 2016), intraperitoneally (i.p.), in an application on the 1st experimental day.

The test compound, RC1, was diluted in DMSO (1%) and administered in the doses of 3, 6 and 12 mg/kg (b.w., i.p.).

2.3.3. EXPERIMENTAL design

We used 40 Swiss male mice (*Mus musculus*) at reproductive age with 35 g average weight. The animals were randomly distributed into eight experimental groups: Control Group (NC) - the animals received physiological solution (1% DMSO) at 0.1 mL/10 g body weight (b.w., i.p.); Positive Control (PC) - animals received cisplatin at 6 mg/kg (b.w., i.p.); Groups RC1 - animals received the test compound in 3 different doses D1 (3 mg/kg), D2 (6 mg/kg) and D3 (12 mg/kg) (i.p.); Associated Groups, positive control and test chemical combined, (ASS1, ASS2 and ASS3) - the animals received cisplatin at the dose of 6 mg/kg (b.w., i.p.) and the RC1 at the 3 different doses D1 (ASS1), D2 (ASS2) and D3 (ASS3) intraperitoneally (i.p.).

Blood collection for the micronucleus assay was performed by caudal vein puncture at 24, 48 and 72 h after application of the treatments (T1, T2 and T3, respectively), when the collection for the comet assay occurred only in T1. After 72 h of treatments administration, the animals were submitted to euthanasia by cervical dislocation for collection of organs.

2.3.4. Comet ASSAY in PERIPHERAL blood

It was pipet 20 μL of homogenized peripheral blood in 120 μL of LMP agarose (1.5%) onto the (5%) agarose-covered surface of a pre-coated slide at 37 °C. Then, the comet assay was performed as described by Singh et al. (1988), with adaptations (Oliveira et al., 2009).

The analysis and classification of comets were performed according to Kobayashi et al. (1995).

2.3.5. Micronucleus ASSAY

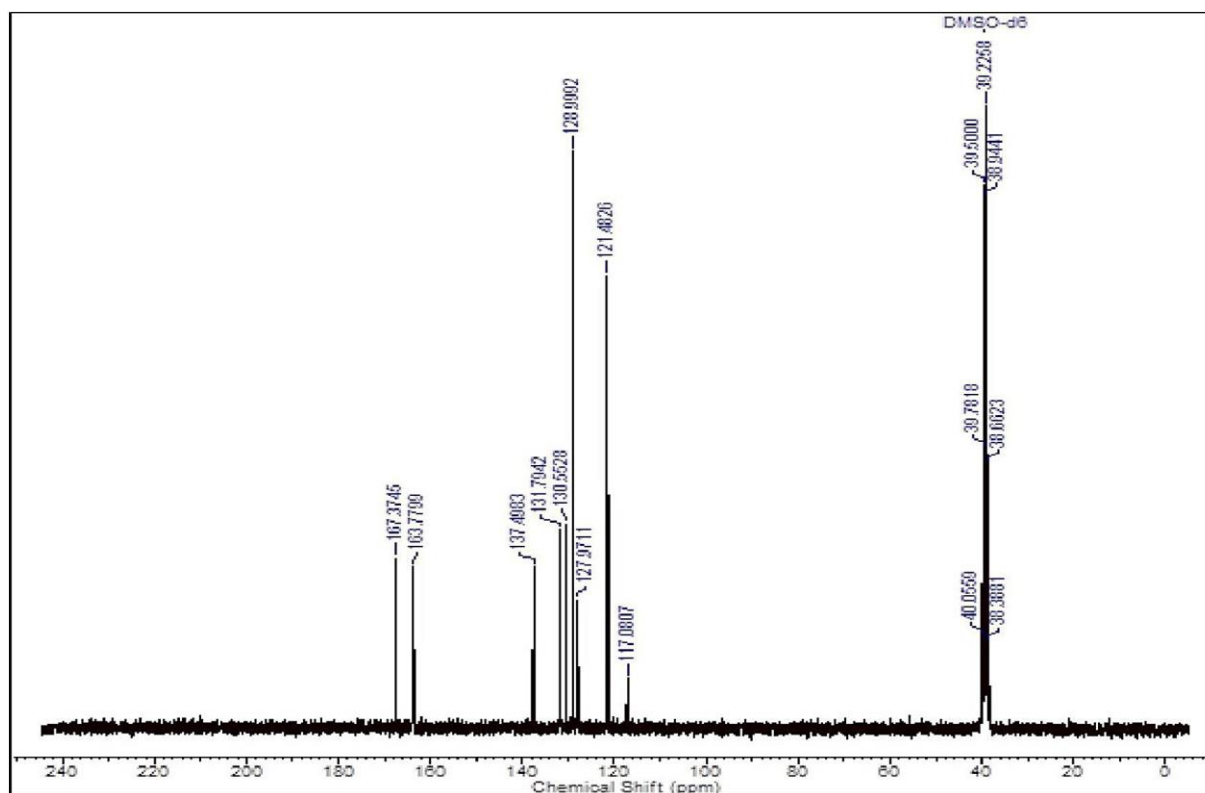
For this purpose, the technique of Hayashi et al. (1990) modified by Oliveira et al. (2009) was used. One drop of peripheral blood was deposited in a slide previously prepared with a layer of 20 μL of Acridine Orange (1.0 mg/mL), and then covered by coverslip. This material remained in freezer ($-20\text{ }^\circ\text{C}$) for a minimum period of 7 days. The analysis was performed under a fluorescence microscope (Bioval® Model G2000 A, Brazil) with excitation filter 420–490 nm and 520 nm barrier filter with a 40 \times magnification. 2000 cells/animal were analyzed.

2.3.6. Splenic PHAGOCYTOSIS

Phagocytosis assays were performed according to the procedure described by Schneider et al. (2016). The spleen was macerated in physiological solution to obtain a homogenous suspension of cells and 100 μL of the cell suspension were placed on a lamina previously stained with acridine orange (1 mg/mL), covered by coverslip and conditioned at $-20\text{ }^\circ\text{C}$ until analysis. The analysis was performed under a fluorescence microscope (Bioval® Model G2000 A, Brazil) with a 420–490 nm filter and a 520 nm barrier filter, at a 40 \times magnification. 200 cells/animal was analyzed. The absence or presence of phagocytosis was based on the description of Hayashi et al. (1990) with modifications (Carvalho et al., 2015).

2.4. STATISTICAL ANALYSIS

Results were expressed as mean \pm standard error of the mean. The determination of the IC_{50} concentration of RC1 was performed by analyzing the non-linear regression curve from the cell viability values obtained in the MTT assay using the GraphPad Prism 5 SOFTWARE (Pesarini et al., 2017). Statistical analysis was performed by ANOVA/Bonferroni and ANOVA/Tukey, with the exception of qPCR that was analyzed by the REST program (Pfaffl et al., 2002). The significant difference was considered when the level of relative expression was equal to or ≤ 0.5 or equal to or > 2 (Biazi et al., 2017), and in all trials the established level of significance was $p < 0,05$ (SOFTWARE GraphPad InStat 5).

Fig. 2. ^{13}C NMR spectra of RC1 in $\text{DMSO-}d_6$ at 75 MHz.

3. Results

3.1. RC1 synthesis

^1H and ^{13}C NMR spectra (Figs. 1 and 2) were obtained in a Bruker Avance 300 spectrometer at the Institute of Chemistry of the Federal University of Mato Grosso do Sul (UFMS), in $\text{DMSO-}d_6$, operating at 300.132 and 75.476 MHz, respectively. The chemical shifts (δ) of ^1H and ^{13}C are given on the ppm scale and were referenced to tetramethylsilane (TMS).

^1H NMR ($\text{DMSO-}d_6$, 300 MHz) δ (ppm): 3.35 (s, NH), 6.29 (d, 1H, $J = 12$ Hz), 6.45 (d, 1H, $J = 12$ Hz), 7.37 (m, 2H), 7.64 (m, 2H), 10.45 (sl, OH). ^{13}C NMR ($\text{DMSO-}d_6$, 75 MHz) δ (ppm): 117.1 (C), 121.5 (CH), 128.9 (CH), 130.6 (CH), 131.8 (CH), 137.5 (C), 163.8 (C=O), 167.4 (C=O).

Infrared spectra were recorded at room temperature in the infrared absorption spectrometer - Jasco IR-6200 (FACET - UFGD) in the range of 4000 to 400 cm^{-1} . The samples were prepared by dispersion in potassium bromide (KBr) and pelleted, which were placed directly in the optical path of the equipment for transmittance reading (%T).

The IR data (Table 2) of the complex in addition to presenting the major bands of the ligand showed evident shifts of the carboxyl $\nu_{\text{C=O}}$ band from 1705 cm^{-1} to 1557-1541 cm^{-1} , indicating the possible formation of coordination binding by this group of the ligand, since the complex was formed by deprotonation of the carboxyl. It is also possible to notice the presence of less intense bands around 1690 to 1640 cm^{-1} , attributed to $\nu_{\text{C=O}}$ amide. For these bands there were no significant shifts, suggesting that this group interacts poorly with the metal and that there is probably no coordinate bond formation by this region of the ligand molecule.

Table 2

Frequencies (ν , cm^{-1}) of selected vibration bands in the IR spectra of RC1.

Vibration band	ν (cm^{-1})
ν_{NH}	3274
$\nu_{\text{as=C-H}}$	3077, 3057, 3012
$\nu_{\text{s=C-H}}$	2975, 2876
Combination bands or harmonic	3200, 2251 a 1733
$\nu_{\text{C=O}}$	1705, 1699
$\nu_{\text{C=C}}$ alkene <i>cis</i>	1627
$\nu_{\text{C=C}}$ aromatic <i>p</i> -substituted	1601 e 1488
δ_{NH} in-plane	1552, 1522
$\nu_{\text{C-N}}$	1398 a 1320
$\nu_{\text{C-O}}$	1294 a 1198
$\nu_{\text{C-Cl}}$	1093
δ_{OeH} out-of-plane	972
δ_{CeH} aromatic out-of-plane, <i>p</i> -substituted	858
δ_{CeH} alkene <i>cis</i> out-of-plane	699
δ_{NH} out-of-plane	669 a 609
$\delta_{\text{C=C}}$ alkene or aromatic out-of-plane	512,444

3.2. In vitro ASSAYS

3.2.1. Cytotoxicity of compound RC1

RC1 compound is cytotoxic to 4 T1 cells at the three times tested (Fig. 3a). The IC_{50} in 24 h was 72 $\mu\text{g/mL}$ (Fig. 3b) and, at in the all-time points, concentrations > 25 $\mu\text{g/mL}$ caused cell death ($p < 0.05$) in a dose-dependent manner (Fig. 3c). The IC_{50} of the RC1 compound at the 48 h treatment was 71.2 $\mu\text{g/mL}$ whereas, for the 72 h the IC_{50} was 63.3 $\mu\text{g/mL}$.

3.2.2. DNA DAMAGE

DNA damage, evaluated by the comet assay in 4 T1 cells (Fig. 4a), demonstrated that the RC1 compound induces (Fig. 4b) the same frequency of damage as the positive control (Fig. 4c). However, the RC1 DNA damage score is higher ($p < .05$) than the cisplatin score (Fig. 4d).

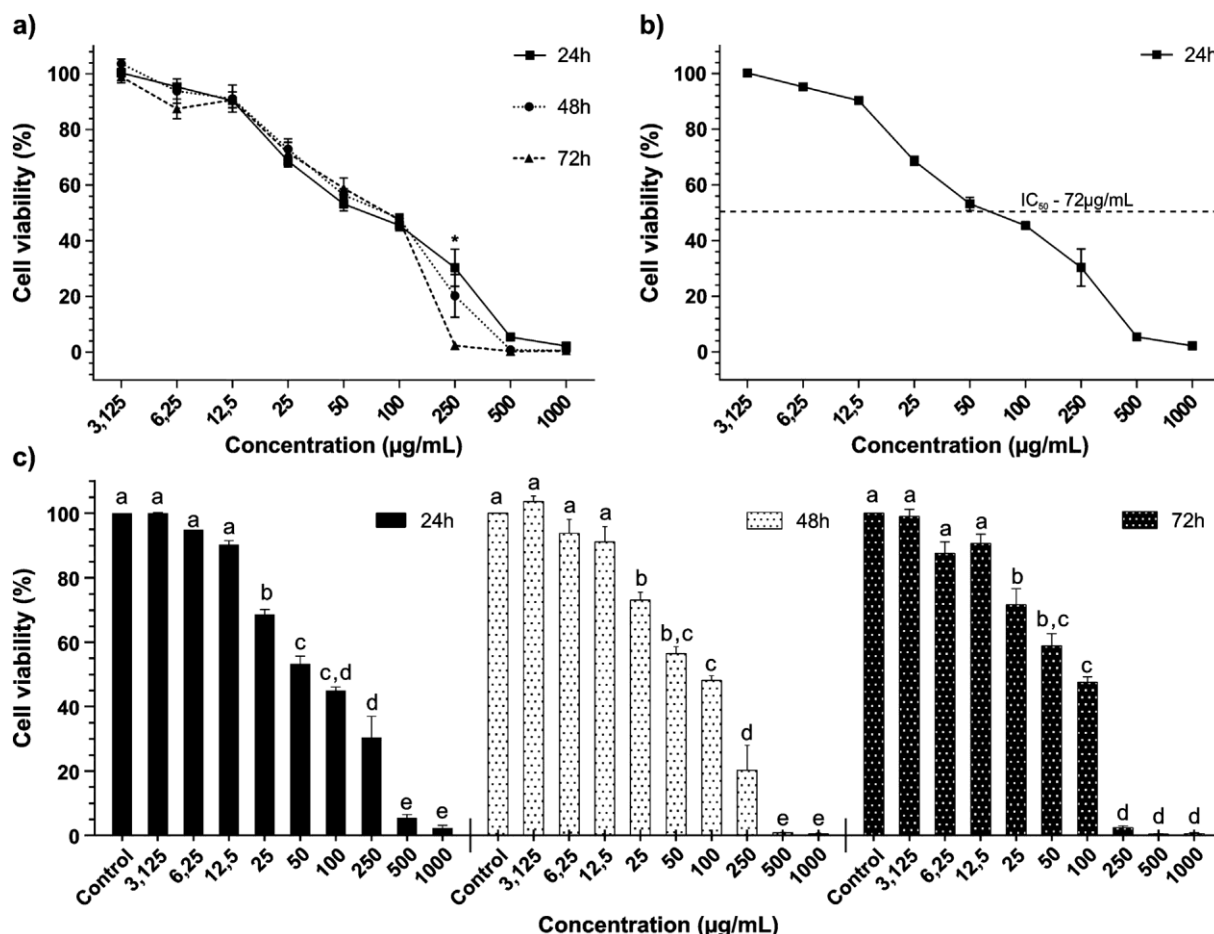


Fig. 3. Cytotoxicity of RC1 compound in 4 T1 murine mammary adenocarcinoma cells.

RC1 compound induces cell cycle arrest in 4 T1 cells (Fig. 4e). Cells treated with RC1 had G1 cell cycle arrest ($p < 0.05$) and G1, S and G2/M cell percentages were 46.27% ($p < 0.05$), 18.90% ($p < 0.05$) and 7.73% ($p > 0.05$), respectively. For this treatment 27.10% of the cells in Sub G1 were still observed ($p < 0.05$). In cells treated with cisplatin there was accumulation of cells in G2/M and the percentages of cells in G1, S and G2/M were 30.20% ($p > 0.05$), 20.93% ($p > 0.05$), 42.00% ($p > 0.05$), respectively. For this treatment, 6.87% of the cells in Sub G1 ($p < 0.05$) were still observed (Fig. 4f).

Analysis of the qPCR assay demonstrated significant increase in the expression of *p21* (8.31 \times), *ATM* (2.44 \times) and *GADD45* (2.65 \times) genes. There was also an increase in *p53* (1.45 \times) and a decrease in *ATR* (-1.35 \times) in a non-significant manner (Fig. 4g).

3.2.3. Apoptosis

RC1 compound induces apoptosis in 4 T1 cells and this was demonstrated by the cytological technique of *in situ* apoptosis (qualitative evaluation) (Fig. 5a). In the differential cytological apoptosis/necrosis test (quantitative evaluation) (Fig. 5b) there was no significant difference between the RC1 and PC treatments, but both were different ($p < 0.05$) from the NC with an increase in apoptosis frequency of 11.94 \times and 12.02 \times , respectively. In the apoptosis assay by flow cytometric were observed (Fig. 5c), 28.6% of the cells in initial apoptosis, 6.6% of final apoptosis and 5.6% in necrosis for treatment with cisplatin, whereas, cells treated with compound RC1 showed 43.1% in initial apoptosis, 9.9% in final apoptosis and 1.4% in necrosis.

RC1 compound did not alter the membrane integrity of 4 T1 cells. Membrane integrity test (Fig. 5d), evaluated by flow cytometry, demonstrated no difference ($p > 0.05$) in the treatments of PC and RC1 in relation to the control.

Analysis of apoptosis gene expression (Fig. 5e) demonstrated that the RC1 compound induced a significant increase in the expression of *BAX* (2.38 \times) and *CASP7* (4.45 \times) genes, and increase of *BAK* (1.98 \times), *CASP9* (1.10 \times), *CASP3* (0.99 \times) and decrease of *BCL-2* (-1.19 \times) in a non-significant manner.

3.3. *In vivo* ASSAYS

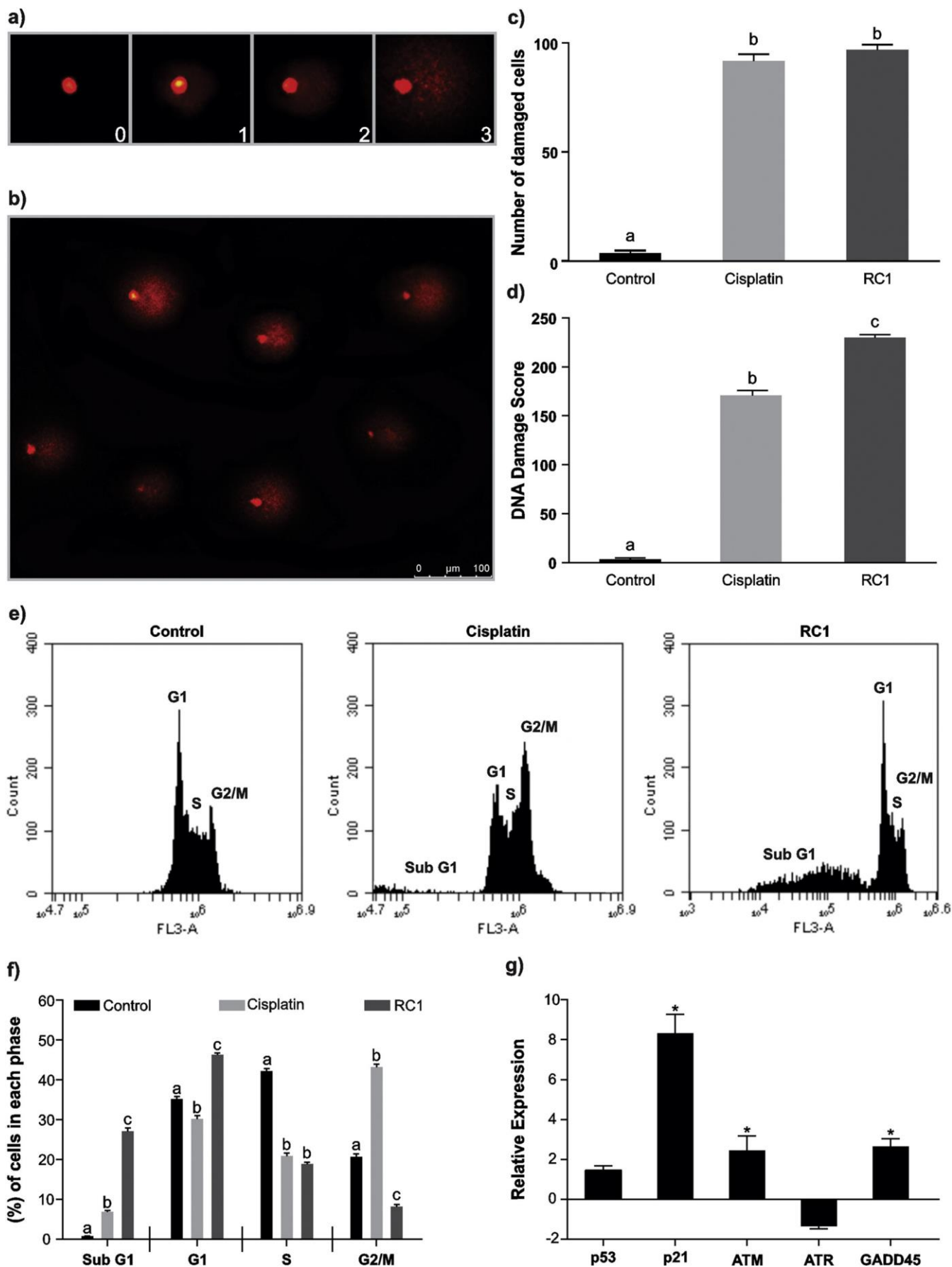
3.3.1. Biometric PARAMETERS

The initial weight of the animals did not present statistically significant differences between the experimental groups. Regarding the final weight of the animals, only the PC group and the ASS3 group presented differences ($p < 0.05$) in relation to the NC (Table 3).

In the analysis of the absolute weight of the organs, it was possible to observe that the PC group presented differences ($p < 0.05$) in liver and kidney weight, and D3 group in spleen weight. The ASS2 group presented differences ($p < 0.05$) in heart weight and the ASS3 in heart and liver weight. Regarding to the analysis of the relative weight of the organs, statistically significant differences were observed for the spleen and heart in groups D3 and ASS2, respectively (Table 3).

3.3.2. Genotoxicity EVALUATION

The RC1 compound is genotoxic in mice ($p < 0.05$). RC1 caused an increase in the frequency of damages of 5.38 \times , 6.22 \times and 6.61 \times for doses D1, D2 and D3, respectively. The PC group and the groups ASS1, ASS2 and Ass3 showed an increase of 22.66 \times , 21.22 \times , 21.83 \times and 24.0 \times , these variations are significant in relation to the NC, but not in relation to the PC. When the score was evaluated, it was observed an increase of 26.5 \times , 6.72 \times , 7.61 \times , 8.27 \times , 23.94 \times , 24.50 \times and 28.05 \times for PC, D1, D2 D3, ASS1, ASS2 and ASS3, respectively



(CAPTION on next PAGE)

Fig. 4. Analysis of genomic damage induced 822 by RC1 compound in 4 T1 murine mammary adenocarcinoma cells.

(A) criterion for classification of genomic damage by comet assay means, where 0 represents nucleoid with no damage and 1, 2 and 3, the respective damage classes; (B) nucleoids with genomic damage induced by compound RC1 after 4 h of 827 treatment; (C) percentage of cells with DNA damage observed by the comet assay; (D) score of genomic damage in 4 T1 cells treated with IC50 of RC1 compound; (E) graphs of the cell cycle analysis of 4 T1 cells treated with negative control, cisplatin and IC50 of RC1 compound; (F) Percentage of cells in each phase of the cell cycle after treatments with negative control, cisplatin and IC 50 of compound RC1. Different letters indicate statistically significant differences ($p < 0.05$; ANOVA/Bonferroni); (G) gene expression related to DNA damage and repair of 4 T1 cells treated with IC50 of RC1 compound. As normalizer was used the ACTB gene and * indicate statistically significant differences ($p < 0.05$, REST). Needs color printing.

(Table 4).

The RC1 compound did not increased the frequency of micronuclei in peripheral blood samples of mice. In the three times tested, doses D1, D2 and D3 presented frequencies ranging from 3.40 ± 0.81 to 7.40 ± 1.08 . In the combination of RC1 and cisplatin, a discrete increase in the frequency of micronuclei was observed in 48 h for ASS2 and ASS3 and for the three doses in 72 h (Table 5).

3.3.3. Splenic PHAGOCYTOSIS

There was an increase ($p < 0.05$) in phagocytosis frequency in the cisplatin-treated, RC1 and ASS1 groups. The groups ASS2 and ASS3 did not present significant differences in relation to NC (Fig. 6).

4. Discussion

The present work was described the synthesis of the copper complex RC1, and evaluate its antitumor activity and toxicogenic action in 4 T1 adenocarcinoma cells murine mammary in Swiss mice.

Several studies report the antitumor activity of copper (II) complex (Facchin et al., 2016; Fan et al., 2017; Gouda et al., 2018; Kosiha et al., 2017; Lakshmipraba et al., 2013; Manikandamathavan et al., 2017; Sangeetha and Murali, 2017), which is related to DNA cleavage (Bhat et al., 2017) and/or the formation of reactive oxygen species (ROS), that cause genomic and mitochondrial. (Liu et al., 2015).

The genotoxicity of RC1 compound was observed in both, *in vitro* and *in vivo* assays. The results of the *in vitro* comet assay indicate genotoxic activity of compound RC1 in 4 T1 tumor cells, with a higher score than the chemotherapeutic cisplatin. While in *in vivo* the chemotherapeutic agent was remarkably more genotoxic. This finding corroborates the results of other groups (Acilan et al., 2017; Bhat et al., 2017; Dallavalle et al., 2002; Marzano et al., 2009) that indicate lower action of copper (II) complexes in normal cells, than in tumor cells. This prominent effect of copper (II) complexes on tumor cells probably occurs because of the greater tolerance of normal cells to the DNA oxidation process (Acilan et al., 2017).

DNA damage caused by RC1 compound induced *in vitro*, G1 cell cycle arrest, preventing the progression of the cell cycle to S phase. The gene expression assay demonstrated increase expression of *ATM*, *GADD45* and *p21*, these genes inhibits the activity of *Cdk2* (Massagué, 2004; Nash et al., 2001), resulting in disruption of the DNA replication process, cell cycle arrest in G1 and senescence (Bertoli et al., 2013; Ueda et al., 2017). Cisplatin, which develops its antitumor action by binding to the purine bases, blocking DNA replication (Wang and Lippard, 2005), induced cell cycle arrest in G2/M, which corroborates other studies that evaluated the influence of this chemotherapeutic on the cell cycle (Łakomska et al., 2014; Wang and Lippard, 2005). Regardless of the stage in which the cell stops its cell cycle, when there is no DNA repair, the cell must be induced to cell death (Bertoli et al., 2013; Massagué, 2004; Oliveira et al., 2014; Roos and Kaina, 2006; Wang and Lippard, 2005).

It is expected that treatments with chemotherapeutic compounds induce cell death *via* apoptosis, which does not result in an inflammatory process (Ooi and Ma, 2013), as in cases of cell death due to necrosis (Urru et al., 2018). Lakshmipraba et al. (2015) described the synthesis, cytotoxic and genotoxic activity of a copper (II) complex in MCF-7 cells. However, when analyzing the type of cell death, they

found cells in apoptosis and in necrosis, different from that observed in the cytotoxic activity of RC1 compound, which induced cell death mediated only by apoptosis, and without altering cell membrane integrity. Apoptosis, induced by RC1 compound, was demonstrated by *in situ* and differential apoptosis/necrosis cytological techniques, as well as by the cytometric assay.

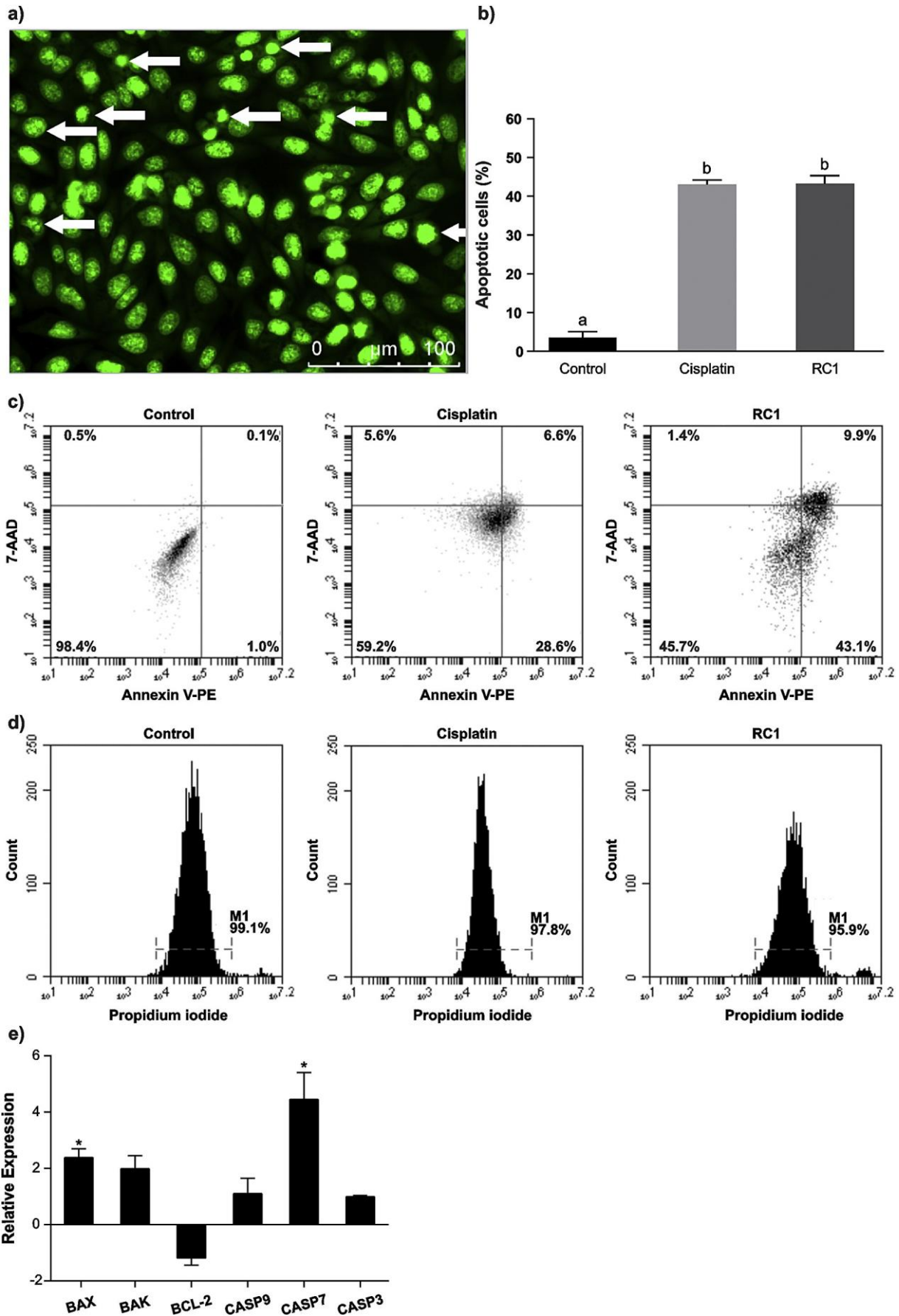
The process of cell death by apoptosis is complex and multigenic. Mitochondria have a central role in triggering apoptosis and their integrity is mediated by BCL-2 activity (Márquez-Jurado et al., 2018). The decrease in BCL-2 expression and the increase of the pro-apoptotic BAX gene probably induced lesions in the mitochondrial membrane of 4T1 cells, with consequent release of cytochrome C. The release of cytochrome C from mitochondria to the cytosol, in addition to activation of caspases, blocks the transport of electrons, preventing the production of energy, which compromises cellular viability (Amarante-Mendes and Green, 1999; Gogvadze and Orrenius, 2006). The RC1 compound induced apoptosis in 4 T1 cells *via* caspase-7, which is an effector caspase, as well as caspase-3, and although no significant increase occurred in the gene expression assay, caspase-7 appears to have been activated by caspase-9 (Domracheva et al., 2017; Márquez-Jurado et al., 2018).

Copper (II) complexes are considered promising in the development of new treatments for various neoplasms (Koňariková et al., 2016). Regulatory agencies require that, prior to human testing, the compound is administered to animals, mainly to assess their toxicity and genotoxicity (ANVISA, 2013; European Commission, 2006; U.S. Department of Health and Human Services et al., 2012).

When the ~~weight~~ ^{strength} of the animals was evaluated, only cisplatin-treated animals, those treated with cisplatin and those treated with the highest dose of RC1 showed reduction. Therefore, this reduction, which may be indicative of toxicity (De David et al., 2014; Ishikawa et al., 2017), has no direct correlation with RC1. When we evaluated the absolute and relative organ weights, the only significant differences were the reduction of relative heart weight and relative spleen weight gain in groups ASS2 and D3, respectively. In relation to the group treated with the highest dose of RC1, it is suggested that the increase of the spleen size of the animals of this group can be correlated with the significant increase of splenic cells in phagocytic activity of group in relation to the NC group, which induces leukocyte migration (de Araújo et al., 2017; Luchini et al., 2008). The splenic phagocytosis may occur in response to DNA damage, as a cellular mechanism of defense against genotoxic agents (Bazo et al., 2002; Carvalho et al., 2015; Ishii et al., 2011; Navarro et al., 2014).

The cisplatin, which was already confirmed *in vitro* as genotoxic in 4 T1 cells, also showed action *in vivo* and increased the frequency of comets and micronuclei *in vivo*. However, in any of the times tested, the RC1 compound had a frequency of micronuclei in different amounts of the negative control group, despite having increased comet frequency *in vivo*, suggesting that cells with DNA lesions, observed by the comet assay were phagocytosed, or that genomic damage was corrected by the DNA repair machinery (Bazo et al., 2002; Carvalho et al., 2015; Ishii et al., 2011; Navarro et al., 2014). However, despite this possibility, the toxicity of cisplatin is well described in the literature (Ciarimboli, 2014) and among its toxic effects nephrotoxicity is highlighted (Pabla et al., 2009).

The RC1 compound did not reduce the genotoxicity of cisplatin observed by the *in vivo* comet assay but prolonged the metabolism of



(CAPTION on next PAGE)

Fig. 5. Apoptosis in 4 T1 cells induced by compound RC1.

(A) cells in apoptosis after treatment with IC50 of RC1 840 compound; (B) percentage of cells in apoptosis after treatment with DMSO (negative control), cisplatin and IC50 of RC1 compound. Different letters indicate statistically significant differences ($p < 0.05$, ANOVA/Bonferroni); (C) percentage of viable cells in initial apoptosis, late apoptosis and necrosis following treatments with 1% DMSO, cisplatin and IC50 of RC1 compound.; (D) membrane integrity analysis of 4 T1 cells performed on flow cytometry with propidium iodide after treatments; (E) expression of apoptosis-related genes in 4 T1 cells after treatment with IC50 of RC1 compound. Needs color printing.

Table 3

Comparison of the biometric parameters between the experimental groups.

Biometric Parameters					
Experimental groups		Initial weight (g)		Final weight (g)	
NC		38,00 ± 1,44 ^a		39,60 ± 1,17 ^a	
PC		35,60 ± 0,74 ^a		34,20 ± 0,37 ^b	
D1		38,50 ± 1,22 ^a		38,80 ± 0,97 ^a	
D2		35,20 ± 0,96 ^a		36,00 ± 0,63 ^{a,b}	
D3		36,20 ± 0,58 ^a		36,80 ± 0,73 ^{a,b}	
ASS1		38,00 ± 0,77 ^a		36,40 ± 0,80 ^{a,b}	
ASS2		38,40 ± 1,60 ^a		37,00 ± 1,50 ^{a,b}	
ASS3		37,40 ± 0,68 ^a		35,20 ± 0,94 ^b	
Absolute weight organs (g)					
	Heart	Lung	Spleen	Liver	Kidneys
NC	0,23 ± 0,01 ^a	0,27 ± 0,00 ^a	0,17 ± 0,01 ^{a,b,c}	2,26 ± 0,05 ^a	0,57 ± 0,03 ^a
PC	0,19 ± 0,01 ^{a,b}	0,25 ± 0,02 ^a	0,13 ± 0,00 ^c	1,74 ± 0,02 ^b	0,46 ± 0,02 ^b
D1	0,21 ± 0,01 ^{a,b}	0,26 ± 0,02 ^a	0,21 ± 0,01 ^{b,d}	2,43 ± 0,09 ^a	0,58 ± 0,01 ^a
D2	0,21 ± 0,00 ^{a,b}	0,25 ± 0,01 ^a	0,19 ± 0,01 ^b	1,84 ± 0,03 ^{a,b}	0,56 ± 0,01 ^a
D3	0,20 ± 0,00 ^{a,b}	0,26 ± 0,01 ^a	0,26 ± 0,02 ^d	2,35 ± 0,17 ^a	0,57 ± 0,02 ^a
ASS1	0,21 ± 0,00 ^{a,b}	0,26 ± 0,01 ^a	0,17 ± 0,01 ^{a,b,c}	1,86 ± 0,09 ^{a,b}	0,48 ± 0,00 ^{a,b}
ASS2	0,16 ± 0,01 ^b	0,24 ± 0,01 ^a	0,16 ± 0,01 ^{a,b,c}	1,85 ± 0,09 ^{a,b}	0,51 ± 0,03 ^{a,b}
ASS3	0,17 ± 0,01 ^b	0,26 ± 0,00 ^a	0,11 ± 0,00 ^c	1,69 ± 0,12 ^b	0,48 ± 0,03 ^{a,b}
Relative weight organs (g)					
	Heart	Lung	Spleen	Liver	Kidneys
NC	0,006 ± 0,0003 ^a	0,007 ± 0,0002 ^{a,b}	0,004 ± 0,0003 ^{a,b}	0,057 ± 0,0009 ^{a,b}	0,014 ± 0,0008 ^{a,b}
PC	0,006 ± 0,0003 ^a	0,007 ± 0,0005 ^{a,b}	0,004 ± 0,0001 ^{a,b}	0,051 ± 0,0006 ^a	0,013 ± 0,0009 ^{a,b}
D1	0,005 ± 0,0002 ^{a,b}	0,006 ± 0,0004 ^b	0,005 ± 0,0003 ^{a,b}	0,056 ± 0,0014 ^{a,b}	0,013 ± 0,0002 ^{a,b}
D2	0,005 ± 0,0002 ^{a,b}	0,007 ± 0,0004 ^{a,b}	0,005 ± 0,0003 ^a	0,051 ± 0,0009 ^a	0,012 ± 0,0004 ^b
D3	0,006 ± 0,0003 ^{a,b}	0,007 ± 0,0003 ^{a,b}	0,007 ± 0,0008 ^c	0,064 ± 0,0035 ^b	0,015 ± 0,0006 ^a
ASS1	0,006 ± 0,0002 ^a	0,007 ± 0,0003 ^{a,b}	0,004 ± 0,0004 ^{a,b}	0,050 ± 0,0016 ^a	0,013 ± 0,0001 ^{a,b}
ASS2	0,004 ± 0,0001 ^b	0,006 ± 0,0003 ^{a,b}	0,004 ± 0,0003 ^{a,b}	0,052 ± 0,0042 ^a	0,014 ± 0,0004 ^{a,b}
ASS3	0,005 ± 0,0003 ^{a,b}	0,008 ± 0,0002 ^a	0,003 ± 0,0002 ^b	0,052 ± 0,0025 ^a	0,015 ± 0,0006 ^a

Biometric parameters of mice treated with saline (DMSO 1%), cisplatin (6 mg/kg), different doses of compound RC1 (D1, D2 and D3) and different doses of RC1 associated with cisplatin (6 mg/kg) were used. The results are presented in Mean ± SEM. Different letters indicate statistically significant differences ($p \leq 0.05$; ANOVA/Tukey Kramer).

Table 4

Mean ± standard error, frequency of damaged cells, distribution between damage classes and score related to the comet assay.

Experimental group	Damaged cells ¹	Damaged class				Score ¹
		0	1	2	3	
NC	3.60 ± 0.50 ^a	96.40 ± 0.50	3.60 ± 0.50	0.00 ± 0.00	0.00 ± 0.00	3.60 ± 0.51 ^a
PC	81.60 ± 5.16 ^b	18.40 ± 5.16	70.20 ± 4.07	9 ± 1.48	2.40 ± 0.50	95.4 ± 6.98 ^b
D1	19.40 ± 2.04 ^c	80.60 ± 2.04	15.20 ± 1.02	3.60 ± 0.81	0.60 ± 0.40	24.2 ± 3.54 ^c
D2	22.40 ± 0.51 ^c	77.60 ± 0.51	18.60 ± 0.50	2.60 ± 0.24	1.20 ± 0.37	27.4 ± 1.12 ^c
D3	23.80 ± 1.50 ^c	76.20 ± 1.50	19.00 ± 1.05	3.60 ± 0.60	1.20 ± 0.37	29.8 ± 2.63 ^c
ASS1	76.40 ± 2.06 ^b	23.60 ± 2.06	68.60 ± 1.69	5.80 ± 1.24	2.00 ± 0.45	86.2 ± 3.61 ^b
ASS2	78.60 ± 2.04 ^b	21.40 ± 2.04	70.80 ± 1.31	6.00 ± 0.94	1.80 ± 0.37	88.2 ± 3.34 ^b
ASS3	86.40 ± 1.29 ^b	13.60 ± 1.29	75.60 ± 1.50	7.00 ± 1.40	3.80 ± 0.59	101.0 ± 2.92 ^b

Frequency of cells with genomic damage, distribution between classes and score of the comet assay performed with peripheral blood of mice treated with saline (DMSO 1%), cisplatin (6 mg/kg) different doses of compound RC1 (D1, D2 and D3) and different doses of RC1 associated with cisplatin (6 mg/kg). The results are presented in Mean ± EPM. Different letters indicate statistically significant differences ($p \leq 0.05$; ANOVA/Tukey Kramer).

the chemotherapeutic by increasing the frequency of micronuclei in the ASS2 and ASS3 groups within 48 h and of all associated groups within 72 h. This effect may be due to the competitiveness of the RC1 compound and cisplatin, since cisplatin is transported by copper receptors (Ishida et al., 2002). According to Ciarimboli (2014) several carriers are described for cisplatin, such as the copper-1 carrier (Ctr1), the copper-2 carrier (Ctr2), the ATP7A and ATP7B type P copper transport ATPases, the organic cation transporter-2 (OCT2) and the multidrug and toxin

extrusion transporter 1 (MATE1). The transporters OCTs and MATE1 are highly expressed in the liver and kidneys (Ciarimboli, 2008; Pabla et al., 2009), which justifies the increased time of cisplatin metabolism in the liver and kidneys for later elimination of the organism. Thus, there is an increase in cisplatin circulation time which would explain the increase in micronuclei frequency in the last evaluation times (48 and 72 h) since this compound is a direct acting genotoxic agent (Wang and Lippard, 2005).

Table 5

Frequency of micronuclei in the peripheral blood of mice treated with RC1 compound.

Experimental group	Mean ± EPM		
	24H	48H	72H
NC	3,20 ± 0,66 ^a	4,20 ± 0,80 ^a	3,80 ± 0,58 ^a
PC	79,20 ± 4,46 ^b	73,00 ± 1,00 ^b	69,80 ± 1,39 ^b
D1	3,80 ± 0,73 ^a	3,80 ± 0,58 ^a	4,40 ± 0,60 ^a
D2	3,40 ± 0,81 ^a	5,40 ± 0,51 ^a	4,60 ± 0,51 ^a
D3	5,20 ± 0,73 ^a	7,40 ± 1,08 ^a	5,20 ± 0,66 ^a
ASS1	73,60 ± 2,90 ^b	76,60 ± 0,93 ^{b,c}	80,00 ± 0,70 ^c
ASS2	79,60 ± 5,24 ^b	78,60 ± 0,93 ^c	79,00 ± 0,71 ^c
ASS3	84,40 ± 3,72 ^b	79,00 ± 1,43 ^c	79,60 ± 0,75 ^c

Frequency of micronucleus in peripheral blood in mice treated with saline (DMSO 1%), cisplatin (6 mg/kg), different doses of the RC1 compound (D1, D2 and D3) and different doses of RC1 compound associated with cisplatin (6 mg/kg). The results are presented in Mean ± SEM. Different letters indicate statistically significant differences ($p \leq 0.05$; ANOVA/Tukey Kramer).

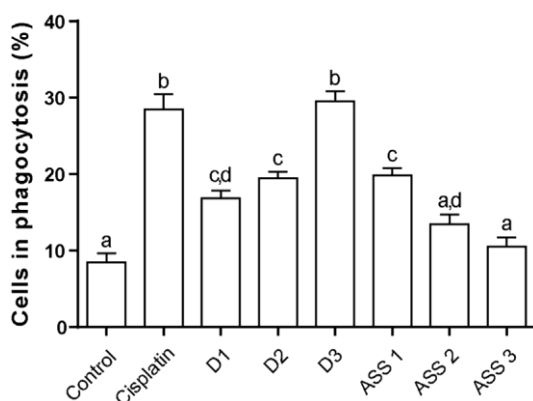


Fig. 6. Analysis of splenic phagocytosis in Swiss mice treated with RC1 compound.

Percentage of cells with phagocytotic characteristics in DMSO, cisplatin (positive control) the RC1 compound at three different doses (D1, D2 and D3) and the three doses of RC1 compound associated with dose of cisplatin. Different letters indicate statistically significant differences ($p \leq 0.05$; ANOVA/Tukey Kramer).

The results presented in this study indicate that the RC1 compound possesses therapeutic potential, as it presented toxicity to 4 T1 murine mammary adenocarcinoma cells. The toxicity was triggered by DNA damage, which induced cell cycle arrest in G1, that was mediated by ATM and p21 expression, with subsequent cell death by mitochondrial apoptosis, which occurred due to increased expression of BAX and Caspase-7, and decrease in BCL-2 gene expression. Notably, in *in vivo*, the compound was less genotoxic than cisplatin, did not increase the frequency of micronuclei, thus DNA damage was not permanent, and at the doses tested there were no changes in biometric parameters.

Conflict of interest

The authors declare that there is no conflict of interest in the present study.

References

Acilan, C., Cevatemre, B., Adiguzel, Z., Karakas, D., Ulukaya, E., Ribeiro, N., Correia, I., Pessoa, J.C., 2017. Synthesis, biological characterization and evaluation of molecular mechanisms of novel copper complexes as anticancer agents. *Biochim. Biophys. Acta* 1861, 218–234. <https://doi.org/10.1016/j.bbagen.2016.10.014>.

Amarante-Mendes, G.P., Green, D.R., 1999. The regulation of apoptotic cell death. *Brazilian J. Med. Biol. Res. = Rev. Bras. Pesqui. Médicas e Biológicas/Soc. Bras. Biofísica* 32, 1053–1061. <https://doi.org/10.1590/S0100-879X199900900001>.

ANVISA, 2013. Guia para a condução de estudos não clínicos de toxicologia e segurança

farmacológica necessários ao desenvolvimento de medicamentos. Versão 2, 1–48.

Bazo, A.P., Rodrigues, M.A.M., Sforzin, J.M., De Camargo, J.L.V., Ribeiro, L.R., Salvadori, D.M.F., 2002. Protective action of propolis on the rat colon carcinogenesis. *Teratog. Carcinog. Mutagen.* 22, 183–194. <https://doi.org/10.1002/tcm.10011>.

Berno, C.R., Rós, B., DdaSilveira, I.O.M.F., Coelho, H.R., Antonioli, A.C.M.B., Beatriz, A., Dde Lima, D.P., Monreal, A.C.D., Sousa, F.G., Dda Silva Gomes, R., Oliveira, R.J., 2016. 4-Aminoantipyrine reduces toxic and genotoxic effects of doxorubicin, cisplatin, and cyclophosphamide in male mice. *Mutat. Res. - Genet. Toxicol. Environ. Mutagen.* 805, 19–24. <https://doi.org/10.1016/j.mrgentox.2016.05.009>.

Bertoli, C., Skotheim, J.M., De Bruin, R.A.M., 2013. Control of cell cycle transcription during G1 and S phases. *Nat. Rev. Mol. Cell Biol.* <https://doi.org/10.1038/nrm3629>.

Bhat, G.A., Maqbool, R., Dar, A.A., Ul Hussain, M., Murugavel, R., 2017. Selective formation of discrete versus polymeric copper organophosphates: DNA cleavage and cytotoxic activity. *Dalt. Trans.* 46, 13409–13420. <https://doi.org/10.1039/C7DT02763J>.

Biazi, B.I., D'Epiro, G.F.R., Zanetti, T.A., de Oliveira, M.T., Ribeiro, L.R., Mantovani, M.S., 2017. Risk assessment via metabolism and cell growth inhibition in a HepG2/C3A cell line upon treatment with Arpadol and its active component Harpagoside. *Phyther. Res.* 31, 387–394. <https://doi.org/10.1002/ptr.5757>.

Carvalho, P.C., Santos, E.A., Schneider, B.U.C., Matuo, R., Pesarini, J.R., Cunha-Laura, A.L., Monreal, A.C.D., Lima, D.P., Antonioli, A.C.M.B., Oliveira, R.J., 2015. Diaryl sulfide analogs of combretastatin A-4: Toxicogenetic, immunomodulatory and apoptotic evaluations and prospects for use as a new chemotherapeutic drug. *Environ. Toxicol. Pharmacol.* 40, 715–721. <https://doi.org/10.1016/j.etap.2015.08.028>.

Ciarimboli, G., 2008. Organic cation transporters. *Xenobiotica.* <https://doi.org/10.1080/00498250701882482>.

Ciarimboli, G., 2014. Membrane transporters as mediators of cisplatin side-effects. In: *Anticancer Research*, pp. 547–550.

Dallavalle, F., Gaccioli, F., Franchi-Gazzola, R., Lanfranchi, M., Marchiò, L., Pellinghelli, M.A., Tegoni, M., 2002. Synthesis, molecular structure, solution equilibrium, and antiproliferative activity of thioxotriazoline and thioxotriazole complexes of copper (II) and palladium(II). *J. Inorg. Biochem.* 92, 95–104. [https://doi.org/10.1016/S0162-0134\(02\)00545-7](https://doi.org/10.1016/S0162-0134(02)00545-7).

Dasari, S., Bernard Tchounwou, P., 2014. Cisplatin in cancer therapy: molecular mechanisms of action. *Eur. J. Pharmacol.* <https://doi.org/10.1016/j.ejphar.2014.07.025>.

de Araújo, F.H.S., de Figueiredo, D.R., Auharek, S.A., Pesarini, J.R., Meza, A., Gomes, R., Monreal, A.C.D., Antonioli-Silva, A.C.M.B., Dde Lima, D.P., Kassuya, C.A.L., Beatriz, A., Oliveira, R.J., 2017. In vivo chemotherapeutic insight of a novel isocoumarin (3-hexyl-5,7-dimethoxy-isochromen-1-one): genotoxicity, cell death induction, leukometry and phagocytic evaluation. *Genet. Mol. Biol.* 40, 665–675. <https://doi.org/10.1590/1678-4685-gmb-2016-0316>.

De David, N., De Oliveira Mauro, M., Gonçalves, C.A., Pesarini, J.R., Strapasson, R.L.B., Kassuya, C.A.L., Stefanello, M.É.A., Cunha-Laura, A.L., Monreal, A.C.D., Oliveira, R.J., 2014. Gochnatia polymorpha ssp. floccosa: bioprospecting of an anti-inflammatory phytotherapy for use during pregnancy. *J. Ethnopharmacol.* 154, 370–379. <https://doi.org/10.1016/j.jep.2014.04.005>.

Domracheva, I., Kanepe-Lapsa, I., Jacekiva, L., Vasiljeva, J., Arsenyan, P., 2017. Selenopheno quinolones and coumarins promote cancer cell apoptosis by ROS depletion and caspase-7 activation. *Life Sci.* 186, 92–101. <https://doi.org/10.1016/j.lfs.2017.08.011>.

European Commission, 2006. European Medicines Agency. pp. 1–12. <https://doi.org/10.1136/bmj.333.7574.873-a>.

Facchin, G., Veiga, N., Kramer, M.G., Batista, A.A., Várnagy, K., Farkas, E., Moreno, V., Torre, M.H., 2016. Experimental and theoretical studies of copper complexes with isomeric dipeptides as novel candidates against breast cancer. *J. Inorg. Biochem.* 162, 52–61. <https://doi.org/10.1016/j.jinorgbio.2016.06.005>.

Fan, L., Tian, M., Liu, Y., Deng, Y., Liao, Z., Xu, J., 2017. Salicylate dot Phenanthroline copper (II) complex induces apoptosis in triple-negative breast cancer cells. *Oncotarget* 8, 29823–29832. <https://doi.org/10.18632/oncotarget.16161>.

Ferlay, J., Soerjomataram, I., Dikshit, R., Eser, S., Mathers, C., Rebelo, M., Parkin, D.M., Forman, D., Bray, F., 2015. Cancer incidence and mortality worldwide: sources, methods and major patterns in GLOBOCAN 2012. *Int. J. Cancer* 136, E359–E386. <https://doi.org/10.1002/ijc.29210>.

Gao, E.J., Lin, L., Zhang, Y., Wang, R.S., Zhu, M.C., Liu, S.H., Sun, T.D., Jiao, W., Andrey, V.Z., 2011. Synthesis, characterization, and study on HeLa cells activity of a dinuclear complex [Cu4(phen)4(H2O)2](pyri)3H2O. *Eur. J. Med. Chem.* 46, 2546–2554. <https://doi.org/10.1016/j.ejmech.2011.03.044>.

Gogvadze, V., Orrenius, S., 2006. Mitochondrial regulation of apoptotic cell death. *Chem. Biol. Interact.* 163, 4–14. <https://doi.org/10.1016/j.cbi.2006.04.010>.

Gouda, A.M., El-Ghamry, H.A., Bawazeer, T.M., Farghaly, T.A., Abdalla, A.N., Aslam, A., 2018. Antitumor activity of pyrrolizidines and their Cu(II) complexes: design, synthesis and cytotoxic screening with potential apoptosis-inducing activity. *Eur. J. Med. Chem.* <https://doi.org/10.1016/j.ejmech.2018.01.009>.

Hayashi, M., Morita, T., Kodama, Y.K., Sofuni, T., Ishidate, M.J., 1990. The micronucleus assay with mouse peripheral blood reticulocytes using acridine orange-coated slides. *Mutat. Res. Toxicol.* 278, 127–130. [https://doi.org/10.1016/0165-1218\(92\)90222-L](https://doi.org/10.1016/0165-1218(92)90222-L).

Hoff Brait, D.R., Mattos Vaz, M.S., da Silva Arrigo, J., Borges De Carvalho, L.N., Souza De Araújo, F.H., Vani, J.M., da Silva Mota, J., Cardoso, C.A.L., Oliveira, R.J., Negrão, F.J., Kassuya, C.A.L., Arena, A.C., 2015. Toxicological analysis and anti-inflammatory effects of essential oil from Piper vicosanum leaves. *Regul. Toxicol. Pharmacol.* 73, 699–705. <https://doi.org/10.1016/j.yrtph.2015.10.028>.

Ishida, S., Lee, J., Thiele, D.J., Herskowitz, I., 2002. Uptake of the anticancer drug cisplatin mediated by the copper transporter Ctrl1 in yeast and mammals. *Proc. Natl. Acad. Sci.* 99, 14298–14302. <https://doi.org/10.1073/pnas.162491399>.

- Ishii, P.L., Prado, C.K., Mauro, M., Carreira, C.M., Mantovani, M.S., Ribeiro, L.R., Dichi, J.B., Oliveira, R.J., 2011. Evaluation of Agaricus blazei in vivo for antigenotoxic, anticarcinogenic, phagocytic and immunomodulatory activities. *Regul. Toxicol. Pharmacol.* 59, 412–422. <https://doi.org/10.1016/j.yrtph.2011.01.004>.
- Ishikawa, R.B., Leitão, M.M., Kassuya, R.M., Macorini, L.F., Moreira, F.M.F., Cardoso, C.A.L., Coelho, R.G., Pott, A., Gelfuso, G.M., Croda, J., Oliveira, R.J., Kassuya, C.A.L., 2017. Anti-inflammatory, antimycobacterial and genotoxic evaluation of *Doliocarpus dentatus*. *J. Ethnopharmacol.* 204, 18–25. <https://doi.org/10.1016/j.jep.2017.04.004>.
- Jha, A., Mukherjee, C., Prasad, A.K., Parmar, V.S., Vadaparti, M., Das, U., De Clercq, E., Balzarini, J., Stables, J.P., Shrivastav, A., Sharma, R.K., Dimmock, J.R., 2010. Derivatives of aryl amines containing the cytotoxic 1,4-dioxo-2-butenyl pharmacophore. *Bioorganic Med. Chem. Lett.* 20, 1510–1515. <https://doi.org/10.1016/j.bmcl.2010.01.098>.
- Kobayashi, H., Sugiyama, C., Morikawa, Y., Hayashi, M., Sofuni, T., 1995. A comparison between manual microscopic analysis and computerized image analysis in the single cell gel electrophoresis assay. *MMS Commun.* 3, 103–115.
- Koňariková, K., Perdíkari, G.A., Gbelcová, H., Andrežalová, L., Švédá, M., Ruml, T., Laubertová, L., Režnáková, S., Žitňanová, L., 2016. Autophagy in MCF-7 cancer cells induced by copper complexes. *Pharmacol. Reports* 68, 1221–1224. <https://doi.org/10.1016/j.pharep.2016.07.011>.
- Kosiba, A., Parthiban, C., Elango, K.P., 2017. Synthesis, characterization and DNA binding/cleavage, protein binding and cytotoxicity studies of Co(II), Ni(II), Cu(II) and Zn(II) complexes of aminonaphthoquinone. *J. Photochem. Photobiol. B Biol.* 168, 165–174. <https://doi.org/10.1016/j.jphotobiol.2017.02.010>.
- Lakomska, I., Hoffmann, K., Wojtczak, A., Sitkowski, J., Maj, E., Wietrzyk, J., 2014. Cytotoxic malonate platinum(II) complexes with 1,2,4-triazolo[1,5-a]pyrimidine derivatives: structural characterization and mechanism of the suppression of tumor cell growth. *J. Inorg. Biochem.* 141, 188–197. <https://doi.org/10.1016/j.jinorgbio.2014.08.005>.
- Lakshmi Praba, J., Arunachalam, S., Riyasdeen, A., Dhivya, R., Vignesh, S., Akbarsha, M.A., James, R.A., 2013. DNA/RNA binding and anticancer/antimicrobial activities of polymer-copper(II) complexes. *Spectrochim. Acta* 109, 23–31. <https://doi.org/10.1016/j.saa.2013.02.020>.
- Lakshmi Praba, J., Arunachalam, S., Riyasdeen, A., Dhivya, R., Akbarsha, M.A., 2015. Polyethyleneimine anchored copper(II) complexes: synthesis, characterization, in vitro DNA binding studies and cytotoxicity studies. *J. Photochem. Photobiol. B Biol.* 142, 59–67. <https://doi.org/10.1016/j.jphotobiol.2014.11.005>.
- Lee, H.L., Er, H.M., Radhakrishnan, A.K., 2009. In vitro anti-proliferative and antioxidant activities of stem extracts of *Pereskia bleo* (Kunth) DC (Cactaceae). *Malaysian J. Sci.* 28, 225–239.
- Liu, N., Huang, H., Dou, Q.P., Liu, J., 2015. Inhibition of 19S proteasome-associated deubiquitinases by metal-containing compounds. *Oncoscience* 2, 457–466. <https://doi.org/10.18632/oncoscience.167>.
- Luchini, A.C., Rodrigues-Orsi, P., Cestari, S.H., Seito, L.N., Witaicenis, A., Pellizzon, C.H., Di Stasi, L.C., 2008. Intestinal anti-inflammatory activity of coumarin and 4-hydroxycoumarin in the trinitrobenzenesulphonic acid model of rat colitis. *Biol. Pharm. Bull.* 31, 1343–1350. <https://doi.org/10.1248/bpb.31.1343>.
- Manikandamathavan, V.M., Thangaraj, M., Weyhermuller, T., Parameswari, R.P., Punitha, V., Murthy, N.N., Nair, B.U., 2017. Novel mononuclear Cu(II) terpyridine complexes: impact of fused ring thiophene and thiazole head groups towards DNA/BSA interaction, cleavage and anti-proliferative activity on HepG2 and triple negative CAL-51 cell line. *Eur. J. Med. Chem.* 135, 434–446. <https://doi.org/10.1016/j.ejmech.2017.04.030>.
- Márquez-Jurado, S., Díaz-Colunga, J., das Neves, R.P., Martínez-Lorente, A., Almazán, F., Guantes, R., Iborra, F.J., 2018. Mitochondrial levels determine variability in cell death by modulating apoptotic gene expression. *Nat. Commun.* 9, 389. <https://doi.org/10.1038/s41467-017-02787-4>.
- Martins, M.J.B., Batista, A.M.A., Brito, Y.N.F., Soares, P.M.G., Martins, C., Ribeiro, R., Brito, G.A., Dde Freitas, M.R., 2017. Effect of remote ischemic preconditioning on systemic toxicity and ototoxicity induced by cisplatin in rats: role of TNF- α and nitric oxide. *Orl* 60125001, 336–346. <https://doi.org/10.1159/000485514>.
- Marzano, C., Pellei, M., Tisato, F., Santini, C., 2009. Copper complexes as anticancer agents. *Anti Cancer Agents Med. Chem.* 9, 185–211. <https://doi.org/10.2174/187152009787313837>.
- Massagué, J., 2004. G1 cell-cycle control and cancer. *Nature*. <https://doi.org/10.1038/nature03094>.
- Mitra, A.K., Agrahari, V., Mandal, A., Cholkar, K., Natarajan, C., Shah, S., Joseph, M., Trinh, H.M., Vaishya, R., Yang, X., Hao, Y., Khurana, V., Pal, D., 2015. Novel delivery approaches for cancer therapeutics. *J. Control. Release* 219, 248–268. <https://doi.org/10.1016/j.jconrel.2015.09.067>.
- Nash, P., Tang, X., Orlicky, S., Chen, Q., Gertler, F.B., Mendenhall, M.D., Sicheri, F., Pawson, T., Tyers, M., 2001. Multisite phosphorylation of a CDK inhibitor sets a threshold for the onset of DNA replication. *Nature* 414, 514–521. <https://doi.org/10.1038/35107009>.
- Navarro, S.D., Beatriz, A., Meza, A., Pesarini, J.R., Gomes, R.D.S., Karaziack, C.B., Cunha-Laura, A.L., Monreal, A.C.D., Romão, W., Lacerda Júnior, V., Mauro, M.D.O., Oliveira, R.J., 2014. A new synthetic resorcinoic lipid 3-Heptyl-3,4,6-trimethoxy-3H-isobenzofuran-1-one: evaluation of toxicology and ability to potentiate the mutagenic and apoptotic effects of cyclophosphamide. *Eur. J. Med. Chem.* 75, 132–142. <https://doi.org/10.1016/j.ejmech.2014.01.057>.
- Oliveira, R.J., Matuo, R., da Silva, A.F., Matiazzi, H.J., Mantovani, M.S., Ribeiro, L.R., 2007. Protective effect of β -glucan extracted from *Saccharomyces cerevisiae*, against DNA damage and cytotoxicity in wild-type (k1) and repair-deficient (xrs5) CHO cells. *Toxicol. Vitr.* 21, 41–52. <https://doi.org/10.1016/j.tiv.2006.07.018>.
- Oliveira, R.J., Salles, M.J.S., da Silva, A.F., Kanno, T.Y.N., Lourenço, A.C., Freiria, G.A., Matiazzi, H.J., Ribeiro, L.R., Mantovani, M.S., 2009. Effects of the polysaccharide β -glucan on clastogenic and teratogenicity caused by acute exposure to cyclophosphamide in mice. *Regul. Toxicol. Pharmacol.* 53, 164–173. <https://doi.org/10.1016/j.yrtph.2008.12.007>.
- Oliveira, R.J., Mantovani, M.S., Da Silva, A.F., Pesarini, J.R., Mauro, M.O., Ribeiro, L.R., 2014. Compounds used to produce cloned animals are genotoxic and mutagenic in mammalian assays in vitro and in vivo. *Brazilian J. Med. Biol. Res.* 47, 287–298. <https://doi.org/10.1590/1414-431X20143301>.
- Ooi, H.K., Ma, L., 2013. Modeling heterogeneous responsiveness of intrinsic apoptosis pathway. *BMC Syst. Biol.* 7. <https://doi.org/10.1186/1752-0509-7-65>.
- Pabla, N., Murphy, R.F., Liu, K., Dong, Z., 2009. The copper transporter Ctr1 contributes to cisplatin uptake by renal tubular cells during cisplatin nephrotoxicity. *Am. J. Physiol. Physiol.* 296, F505–F511. <https://doi.org/10.1152/ajprenal.90545.2008>.
- Pesarini, J.R., Oliveira, R.J., Pessatto, L.R., Milan Brochado Antoniolli-Silva, A.C., Felicidade, I., Nardi, N.B., Camassola, M., Mantovani, M.S., Ribeiro, L.R., 2017. Vitamin D: correlation with biochemical and body composition changes in a southern Brazilian population and induction of cytotoxicity in mesenchymal stem cells derived from human adipose tissue. *Biomed Pharmacother* 91, 861–871. <https://doi.org/10.1016/j.biopha.2017.05.013>.
- Pfaffl, M.W., Horgan, G.W., Dempfle, L., 2002. Relative expression software tool (REST) for group-wise comparison and statistical analysis of relative expression results in real-time PCR. *Nucleic Acids Res.* 30, e36. <https://doi.org/10.1093/nar/30.9.e36>.
- Pivetta, T., Isaia, F., Verani, G., Cannas, C., Serra, L., Castellano, C., Demartin, F., Pilla, F., Manca, M., Pani, A., 2012. Mixed-1,10-phenanthroline-cu(II) complexes: synthesis, cytotoxic activity versus hematological and solid tumor cells and complex formation equilibria with glutathione. *J. Inorg. Biochem.* 114, 28–37. <https://doi.org/10.1016/j.jinorgbio.2012.04.017>.
- Rodrigues, J., Abramjuk, C., Vásquez, L., Gamboa, N., Domínguez, J., Nitzsche, B., Höpfner, M., Georgieva, R., Bäumler, H., Stephan, C., Jung, K., Lein, M., Rabien, A., 2011. New 4-maleamic acid and 4-maleamide peptidyl chalcones as potential multitarget drugs for human prostate cancer. *Pharm. Res.* 28, 907–919. <https://doi.org/10.1007/s11095-010-0347-8>.
- Roos, W.P., Kaina, B., 2006. DNA damage-induced cell death by apoptosis. *Trends Mol. Med.* <https://doi.org/10.1016/j.molmed.2006.07.007>.
- Sangeetha, S., Murali, M., 2017. Non-covalent DNA binding, protein interaction, DNA cleavage and cytotoxicity of [Cu(quamol)Cl] \cdot H₂O. *Int. J. Biol. Macromol.* <https://doi.org/10.1016/j.ijbiomac.2017.10.131>.
- Savio, A.L.V., da Silva, G.N., de Camargo, E.A., Salvadori, D.M.F., 2014. Cell cycle kinetics, apoptosis rates, DNA damage and TP53 gene expression in bladder cancer cells treated with allyl isothiocyanate (mustard essential oil). *Mutat. Res. - Fundam. Mol. Mech. Mutagen.* 762, 40–46. <https://doi.org/10.1016/j.mrfmmm.2014.02.006>.
- Schneider, B.U.C., Meza, A., Beatriz, A., Pesarini, J.R., de Carvalho, P.C., de Oliveira Mauro, M., Karaziack, C.B., Cunha-Laura, A.L., Monreal, A.C.D., Matuo, R., de Lima, D.P., Oliveira, R.J., 2016. Cardanol: Toxicogenic assessment and its effects when combined with cyclophosphamide. *Genet. Mol. Biol.* 39, 279–289. <https://doi.org/10.1590/1678-4685-GMB-2015-0170>.
- Schweich, L.D.C., Oliveira, E.J.T.D., Pesarini, J.R., Hermeto, L.C., Camassola, M., Nardi, N.B., Brochado, T.M.M., Antoniolli-Silva, A.C.M.B., Oliveira, R.J., 2017. All-trans retinoic acid induces mitochondria-mediated apoptosis of human adipose-derived stem cells and affects the balance of the adipogenic differentiation. *Biomed Pharmacother* 96, 1267–1274. <https://doi.org/10.1016/j.biopha.2017.11.087>.
- Singh, N.P., McCoy, M.T., Tice, R.R., Schneider, E.L., 1988. A simple technique for quantitation of low levels of DNA damage in individual cells. *Exp. Cell Res.* 175, 184–191. [https://doi.org/10.1016/0014-4827\(88\)90265-0](https://doi.org/10.1016/0014-4827(88)90265-0).
- Stewart, B.W., Wild, C.P., 2014. *World cancer report 2014*. In: *World Health Organization*, pp. 1–2.
- Thalamuthu, S., Annaraj, B., Vasudevan, S., Sengupta, S., Neelakantan, M.A., 2013. DNA binding, nuclease, and colon cancer cell inhibitory activity of a Cu(II) complex of a thiazolidine-4-carboxylic acid derivative. *J. Coord. Chem.* 66, 1805–1820. <https://doi.org/10.1080/00958972.2013.791393>.
- Tsimberidou, A.M., Braithe, F., Stewart, D.J., Kurzrock, R., 2009. Ultimate fate of oncology drugs approved by the US food and drug administration without a randomized trial. *J. Clin. Oncol.* <https://doi.org/10.1200/JCO.2009.23.6018>.
- U.S. Department of Health and Human Services, FDA, CDER, CBER, 2012. *S2(R1) genotoxicity testing and data interpretation for pharmaceuticals intended for human use*. *Guid. Ind.* 2, 1–31.
- Ueda, T., Kohama, Y., Kuge, A., Kido, E., Sakurai, H., 2017. GADD45 family proteins suppress JNK signaling by targeting MKK7. *Arch. Biochem. Biophys.* 635, 1–7. <https://doi.org/10.1016/j.abb.2017.10.005>.
- Urru, S.A.M., Gallus, S., Bosetti, C., Moi, T., Medda, R., Sollai, E., Murgia, A., Sanges, F., Pira, G., Manca, A., Palmas, D., Floris, M., Asunis, A.M., Atzori, F., Carru, C., D'Incalci, M., Ghiani, M., Marras, V., Onnis, D., Santona, M.C., Sarobba, G., Valle, E., Canu, L., Cossu, S., Bulfone, A., Rocca, P.C., De Miglio, M.R., Orrù, S., 2018. Clinical and pathological factors influencing survival in a large cohort of triple-negative breast cancer patients. *BMC Cancer* 18. <https://doi.org/10.1186/s12885-017-3969-y>.
- Wang, D., Lippard, S.J., 2005. Cellular processing of platinum anticancer drugs. *Nat. Rev. Drug Discov.* <https://doi.org/10.1038/nrd1691>.
- GLOBOCAN, 2012. World Health Organization, Global Cancer Observatory - Online analysis prediction. Available at: http://globocan.iarc.fr/Pages/summary_table_site_sel.aspx, Accessed date: 4 January 2018.

6. REFERÊNCIAS UTILIZADAS NA DISSERTAÇÃO

ALLEMANI, C. et al. Global surveillance of cancer survival 1995-2009: analysis of individual data for 25,676,887 patients from 279 population-based registries in 67 countries (CONCORD-2). **Lancet**, v. 385, n. 9972, p. 977–1010, 2015.

Anasamy, T.; Thy, C. K.; Lo, K. M.; Chee, C. F.; Yeap, S. K.; Kamalidehghan, B.; Chung, L. Y. Tribenzyltin carboxylates as anticancer drug candidates: Effect on the cytotoxicity, mobility and invasiveness of breast cancer cell lines. **Europ. J. Med. Chem.**, v. 125, p. 770-783, 2016.

Banti, C.N.; Hadjikakou, S.K.. Anti-proliferative and anti-tumor activity of silver (I) compounds. **Metallomics**, v. 5, p. 569-596, 2013.

BARR, F. A.; GRUNEBERG, U. Cytokinesis: Placing and Making the Final Cut Cell, 2007.

BERNO, C. R. et al. 4-Aminoantipyrine reduces toxic and genotoxic effects of doxorubicin, cisplatin, and cyclophosphamide in male mice. **Mutation Research - Genetic Toxicology and Environmental Mutagenesis**, v. 805, p. 19–24, 2016.

DE ALMEIDA, V. L. et al. Câncer e agentes antineoplásicos ciclo-celular específicos e ciclo-celular não específicos que interagem com o DNA: Uma introdução. **Quimica Nova**, v. 28, n. 1, p. 118–129, 2005.

FAN, L. et al. Salicylate dot Phenanthroline copper (II) complex induces apoptosis in triple-negative breast cancer cells. **Oncotarget**, v. 8, n. 18, p. 29823–29832, 2017.

Fonseca, T.G.; Morais, M. B.; Rocha, T.; Abessa, D. M.; Aureliano, M.; Bebianno, M.J. Ecotoxicological assessment of the anticancer drug cisplatin in the polychaete *Nereis diversicolor*. **Sci. Total Environ.**, v. 575, p. 162-172, 2016.

GALLORINI, M.; CATALDI, A.; DI GIACOMO, V. Cyclin-dependent kinase modulators and cancer therapy. **BioDrugs**, 2012.

GAO, E. J. et al. Synthesis, characterization, and study on HeLa cells activity of a dinuclear complex [Cu₂(phen)₄(H₂O)₂](pyri)·3H₂O. **European Journal of Medicinal Chemistry**, v. 46, n. 6, p. 2546–2554, 2011.

GOUDA, A. M. et al. Antitumor activity of pyrrolizines and their Cu(II) complexes:

Design, synthesis and cytotoxic screening with potential apoptosis-inducing activity. **European Journal of Medicinal Chemistry**, n. li, 2018.

GLOBOCAN, 2012. World Health Organization, Global Cancer Observatory - Online analysis prediction. Available at. http://globocan.iarc.fr/Pages/summary_table_site_sel.aspx, Accessed date: 4 January 2018.

HAHN, W. C.; WEINBERG, R. A. Rules for making human tumor cells. **The New England journal of medicine**, v. 347, n. 20, p. 1593–1603, nov. 2002.

HUANG, X. et al. The association between RFC1 G80A polymorphism and cancer susceptibility: Evidence from 33 studies. **Journal of Cancer**, v. 7, n. 2, p. 144–152, 2016.

INCA, 2019. Instituto Nacional de Câncer. Disponível em <https://www.inca.gov.br/sites/ufu.sti.inca.local/files//media/document//estimativa-incidencia-de-cancer-no-brasil-2018.pdf>. Acessado em 29 de janeiro de 2019.

Jha, A.; Mukherjee, C.; Prasad, A. K.; Parmar, V. S.; Vadaparti, M.; Das, U.; De Clercq, E.; Balzarini, J.; Stables, J. P.; Shrivastav, A.; Sharma, R. K.; Dimmock, J. R.. Derivatives of aryl amines containing the cytotoxic 1,4-dioxo-2-butenyl pharmacophore. **Bioorg. Med. Chem. Letter**, v. 20, p. 1510-1515, 2010.

KLEIN, G. Cancer, apoptosis, and nonimmune surveillance. **Cell Death and Differentiation**, v. 11, n.1, p. 13–17, 2004.

LAMSON, D. W.; BRIGNALL, M. S. Antioxidants in cancer therapy; their actions and interactions with oncologic therapies Alternative. **Medicine Review**, 1999.

MANIKANDAMATHAVAN, V. M. et al. Novel mononuclear Cu (II) terpyridine complexes: Impact of fused ring thiophene and thiazole head groups towards DNA/BSA interaction, cleavage and antiproliferative activity on HepG2 and triple negative CAL-51 cell line. **European Journal of Medicinal Chemistry**, v. 135, p. 434–446, 2017.

MALUMBRES, M.; BARBACID, M. Mammalian cyclin-dependent kinases. **Trends in Biochemical Sciences**, 2005.

Matos, M.R.P.N. Complexos metálicos na terapêutica do cancro. *Biol. Soc. Portug. Quím.*, v. 85, 2002.

NAVARRO, S. D. et al. Resorcinolic lipid 3-heptyl-3,4,6-trimethoxy-3H-sobenzofuran-1-one is a strategy for melanoma treatment. **Life Sciences**, 2018.

OLIVEIRA, R. J. et al. Pre-treatment with glutamine reduces genetic damage due to cancer treatment with cisplatin. **Genetics and Molecular Research**, v. 12, n. 4, p. 6040–6051, 2013.

Oliveira, E.J.T.; Pessatto, L.R.; De Freitas, R.O.N.; Pelizaro, B.I.; Rabacow, A.P.M.; Vani, J.M.; Monreal, A.C.D.; Mantovani, M.S.; De Azevedo, R.B.; Antonioli-Silva, A.C.M.B.; Gomes, R.S; Oliveira, R.J.. New Bis copper complex ((Z) -4 - ((4-chlorophenyl) amino) -4-oxobut-2-enoyl) oxy): Cytotoxicity in 4T1 cells and their toxicogenic potential in Swiss mice. **Toxicol. Appl. Pharmacol.**, v. 356, p. 127-138, 2018a.

Oliveira, R.J.; Baise, E.; Mauro, M.O.; Pesarini, J.R.; Matuo, R.; Silva, A.F.; Ribeiro, L.R.; Mantovani, M.S.. Evaluation of chemopreventive activity of glutamine by the comet and the micronucleus assay in mice's peripheral blood. **Environ. Toxicol. Pharmacol.**, v.28, p.120-124, 2009.

Oliveira, R.J.; Leite, N. C.; Pesarini, J.R.; Oliveira, B.C.; Berno, C.R.; Araujo, F.H.S.; Silveira, I.O.M.F.; Nascimento, R.O.; Antonioli-Silva, A.C.M.B.; Monreal, A.C.D. ; Beatriz, A.; Lima, D.P.; Gomes, R.S.. Assessment of genetic integrity, splenic phagocytosis and cell death potential of (Z)-4-((1,5-dimethyl-3-oxo-2-phenyl-2,3-dihydro-1H-pyrazol-4-yl) amino)-4-oxobut-2-enoic acid and its effect when combined with commercial chemotherapeutics. **Genet. Mol. Biol.**, v. 19, p. 1/1678-4685-GMB-13, 2018b.

Oliveira, R.J.; Matuo, R.; Silva, A.F.; Matiazi, H.J.; Mantovani, M.S.; Ribeiro, L.R.. Protective effect of beta-glucan extracted from *Saccharomyces cerevisiae*, against DNA damage and cytotoxicity in wild-type (k1) and repair-deficient (xrs5) CHO cells. **Toxicol. in Vitro**, v.21, p.41-52, 2007.

Oliveira, R.J.; Pereira, F.P.A.N.; Winckd, C.R.; Berno, C.R.; Pesarini, J.R.; Antonioli-Silva, A.C.M.B.; Monreal, A.C.D.; Beatriz, A.; Lima, D.P.; Gomes, R.S.. Assessment of the toxicogenic, immunostimulatory and apoptotic effects of the ester (Z)-methyl 4-((1,5-dimethyl-3-oxo-2-phenyl-2,3-dihydro-1H-pyrazol-4-yl)amino)-4-oxobut-2-anoate in combination with cisplatin, cyclophosphamide and doxorubicin. **Genet. Biol. Mol.**, Impress. 2018.

OPAS, 2019. Organização Pan-Americana de Saúde. Disponível em <https://www.paho.org/bra/>. Acessado em 29 de janeiro de 2019.

PESSOA ROCHA, D. et al. Coordenação de metais a antibióticos como uma estratégia de combate à resistência bacteriana. **Química Nova**, 2011.

PITOT, H. C. Pathways of progression in hepatocarcinogenesis. **Lancet (London, England)**, v. 358, n. 9285, p. 859–860, set. 2011.

PIVETTA, T. et al. Mixed-1,10-phenanthroline-Cu(II) complexes: Synthesis, cytotoxic activity versus hematological and solid tumor cells and complex formation equilibria with glutathione. **Journal of Inorganic Biochemistry**, v. 114, p. 28–37, 2012.

Rabacow, A.P.M.; MEZA, A.; De Oliveira, E.J.T.; De David, N.; Vitor, N.; Antonioli-Silva, A.C.M.B.; MATOS, M.F.C.; PERDOMO, R.T.; Gomes, R.S.; Lima, D.P.; BEATRIZ, A.; Oliveira, R.J.. Evaluation of the Antitumor Potential of the Resorcinolic Lipid 3-Heptyl-3,4,6-trimethoxy-3H-isobenzofuran-1-one in Breast Cancer Cells. **Anticancer Res.**, v. 38, p. 4565-4576, 2018.

Reichel, V.; Burghard, S.; John, I.; Huber, O.. P-glycoprotein and breast cancer resistance protein expression and function at the blood-brain barrier and blood-cerebrospinal fluid barrier (choroid plexus) in streptozotocin-induced diabetes in rats. **Brain Res.**, v. 25; p.238-245, 2011.

Reis M. Farmacogenética aplicada ao câncer. Quimioterapia individualizada e especificidade molecular. **Medicina**, v. 39, p. 577-586, 2006.

Rocha, D.; Pinto, G. F.; Ruggiero, R.; De Oliveira, C. A.; Guerra, W.; Fontes, A. P. S.; Tavares, T. T.; Marzano, I. M.; Pereira-Maia, E. C.. Coordenação de metais a antibióticos como uma estratégia de combate à resistência bacteriana. **Química Nova**. v. 34, p. 111-118, 2011.

SANGEETHA, S.; MURALI, M. Non-covalent DNA binding, protein interaction, DNA cleavage and cytotoxicity of [Cu(quamol)Cl]-H₂O. **International Journal of Biological Macromolecules**, 2017.

SCHWARTZ, G. K.; SHAH, M. A. Targeting the cell cycle: a new approach to cancer therapy. *Journal of clinical oncology: official journal of the American Society of* **Clinical Oncology**, v. 23, n. 36, p. 9408–21, 2005.

Shahsavani, M. B.; Ahmadi, S.; Aseman, M. D.; Nabavizadeh, S. M.; Rashidi, M.; Asadi, Z.; Erfani, N.; Ghasemi, A.; Saboury, A. A.; Niazi, A.; Bahaoddini, A.; Yousefi, R.. Anticancer activity assessment of two novel binuclear platinum (II) complexes. **J. Photoch. Photob.**, v. 161, p. 345-354, 2016.

Sharma, N. K.; Ameta, R. K.; Singh, M.. Spectrophotometric and physicochemical studies of newly synthesized anticancer Pt (IV) complexes and their interactions with CT-DNA. **J. Mol. Liquids.**, v. 222, p. 752-761, 2016.

STEWART, B. W.; WILD, C. P. World cancer report 2014. World Health Organization, p. 1–2, 2014.

STEWART, Z. A.; WESTFALL, M. D.; PIETENPOL, J. A. Cell-cycle dysregulation and anticancer therapy. **Trends in Pharmacological Sciences**, 2003.

Takimoto, Y.; Imai, T.; Kondo, M.; Hanada, Y.; Uno, A.; Ishida, Y.; Kamakura, T.; Kitahara, T.; Inohara, H.; Shimada, S.. Cisplatin-induced toxicity decreases the mouse vestibule-ocular reflex. **Toxicol. Letter.**, v. 262, p. 49-54, 2016.

THALAMUTHU, S. et al. DNA binding, nuclease, and colon cancer cell inhibitory activity of a Cu(II) complex of a thiazolidine-4-carboxylic acid derivative. **Journal of Coordination Chemistry**, v. 66, n. 10, p. 1805–1820, 2013a.

THALAMUTHU, S. et al. DNA binding, nuclease, and colon cancer cell inhibitory activity of a Cu(II) complex of a thiazolidine-4-carboxylic acid derivative. **Journal of Coordination Chemistry**, v. 66, n. 10, p. 1805–1820, 2013b.

WAGNER-SOUZA, K. et al. Resistance to thapsigargin-induced intracellular calcium mobilization in a multidrug resistant tumour cell line. **Molecular and Cellular Biochemistry**, v. 252, n. 1–2, p. 109–116, 2003.

Wang, Q. W.; Lam, P. L.; Wong, R. S.; Cheng, G. Y.; Lam, K. H.; Bian, Z. X.; Ho, C. L.; Feng, Y. H.; Gambari, R.; Lo, Y. H.; Wong, W. Y.; Chui, C. H. Synthesis of platinum (II) and palladium (II) complexes with 9,9-dihexyl-4,5-diazafluorene and their in vivo antitumor activity against Hep3B xenografted mice. **Europ. J. Med. Chem.**, v. 124, p. 537-543, 2016.

WORLD HEALTH ORGANIZATION. Cancer Fact Sheet N297. Disponível em: <<http://www.who.int/mediacentre/factsheets/fs297/en/>>. Acessado em 29 de janeiro de 2019.

VIDEIRA, M.; REIS, R. L.; BRITO, M. A. Deconstructing breast cancer cell biology and the mechanisms of multidrug resistance. **Biochimica et Biophysica. Acta - Reviews on Cancer**, 2014.

7. ANEXO 1: CERTIFICADO DA COMISSÃO DE ÉTICA NO USO DE ANIMAIS – CEUA



Serviço Público Federal
Ministério da Educação
Fundação Universidade Federal de Mato Grosso do Sul



C E R T I F I C A D O

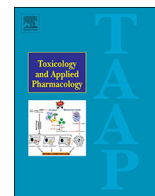
Certificamos que a proposta intitulada “Avaliação toxicogenética de compostos baseados em ligantes contendo o grupo farmacofórico 1,4dioxo-butenil”, registrada com o nº 921/2017, sob a responsabilidade de **Rodrigo Juliano Oliveira** - que envolve a utilização de animais pertencentes ao filo Chordata, subfilo Vertebrata, para fins de pesquisa científica – encontra-se de acordo com os preceitos da Lei nº 11.794, de 8 de outubro de 2008, do Decreto nº 6.899, de 15 de julho de 2009, e com as normas editadas pelo Conselho Nacional de Controle de Experimentação Animal (CONCEA), e foi aprovado pela COMISSÃO DE ÉTICA NO USO DE ANIMAIS/CEUA DA UNIVERSIDADE FEDERAL DE MATO GROSSO DO SUL/UFMS, na 1ª reunião ordinária do dia 21/02/2018.

FINALIDADE	() Ensino (x) Pesquisa Científica
Vigência da autorização	20/01/2018 a 31/12/2020
Espécie/Linhagem/Raça	<i>Mus musculus</i> / BALB/c <i>Mus musculus</i> / C57BL/6
Nº de animais	Machos 200 / Machos 160 = 360
Peso/Idade	30g / 60 dias 25g / 60 dias
Sexo	Machos
Origem	Biotério Central/INBIO/UFMS

Joice Stein

Coordenadora da CEUA/UFMS
Campo Grande, 23 de fevereiro de 2018.

Comissão de Ética no Uso de Animais/CEUA
<http://www.propp.ufms.br/ceua>
ceua.propp@ufms.br
fone (67) 3345-7925



New Bis copper complex ((Z) -4 - ((4-chlorophenyl) amino) -4-oxobut-2-enoyl) oxy): Cytotoxicity in 4T1 cells and their toxicogenic potential in Swiss mice

Edwin José Torres de Oliveira^{a,b}, Lucas Roberto Pessatto^{a,b},
Raquel Oliveira Nascimento de Freitas^c, Bruno Ivo Pelizaro^{a,d}, Ana Paula Maluf Rabacow^{a,e},
Juliana Miron Vani^{a,e}, Antônio Carlos Duenhas Monreal^a, Mário Sérgio Mantovani^b,
Ricardo Bentes de Azevedo^f, Andréia Conceição Milan Brochado Antonioli-Silva^{a,e},
Roberto da Silva Gomes^{c,*}, Rodrigo Juliano Oliveira^{a,b,d,e,**}

^a Centro de Estudos em Células Tronco, Terapia Celular e Genética Toxicológica – CeTroGen, Hospital Universitário Maria Aparecida Pedrossian, Empresa Brasileira de Serviços Hospitalares – EBSEH, Campo Grande, Mato Grosso do Sul, Brazil

^b Programa de Pós-graduação em Genética e Biologia Molecular, Centro de Ciências Biológicas - CCB, Departamento de Biologia Geral, Universidade Estadual de Londrina - UEL, Londrina, Brazil.

^c Laboratório de Síntese e Modificação Molecular, Faculdade de Ciências Exatas e Tecnologia - FACET, Universidade Federal da Grande Dourados - UFGD, Dourados, Mato Grosso do Sul 79804-970, Brazil

^d Programa de Mestrado em Farmácia, Faculdade de Ciências Farmacêuticas, Alimentos e Nutrição – FACFAN, Universidade Federal de Mato Grosso do Sul – UFMS, Campo Grande, Mato Grosso do Sul, Brazil

^e Faculdade de Medicina Dr. Hélio Mandetta, Programa de Pós-graduação em Saúde e Desenvolvimento na Região Centro-Oeste, Campo Grande, Mato Grosso do Sul, Brazil

^f Departamento de Genética e Morfologia, Instituto de Ciências Biológicas - IB, Universidade de Brasília - UNB, Brasília, Distrito Federal, Brazil

ARTICLE INFO

Keywords:

Copper(II) Complexes
DNA Damage
Cell Cycle
Apoptosis
Antitumor Activity
Breast Cancer

ABSTRACT

Copper (II) complexes are promising in the development of new synthetic models for cancer treatment. In this context, we synthesized a new copper complex containing the pharmacophore group 1,4-dioxo-2-butenyl, the Bis (((Z)-4-((4-chlorophenyl) amino)-4-oxobut-2-enoyl)oxy) copper compound and we evaluated its antitumor activity in 4 T1 murine mammary adenocarcinoma cells and their toxicogenic effect in Swiss mice. The compound demonstrated cytotoxicity and genotoxicity to 4 T1 cells, and after cell cycle arrest in G1, which occurred by the increase in *ATM* and *p21* expression, it induced the cells to apoptosis by increasing *BAX* and *caspase-7*. *In vivo* the compound was genotoxic in mice but did not show permanent damage, observed by the absence of increased micronucleus frequency, and did not induce changes in the biometric parameters of the animals. These results indicate that the new copper complex, described firstly in this work, presents therapeutic potential for breast cancer.

1. Introduction

Cancer is a major public health issue on a global scale. Worldwide, cancer incidence could potentially increase to as many as 17 million new cases per year by 2020 (GLOBOCAN, 2012) and > 20 million by 2025 (Stewart and Wild, 2014). In men, lung and prostate cancer is more prevalent, while in women breast cancer is more common

(Stewart and Wild, 2014). Ferlay et al. (2015) reported that breast cancer alone accounts for 25% of all cancer cases among females and over 522 thousand women died from this disease in 2012.

One of the main modes of medical intervention in the treatment of cancer is chemotherapy, which consists of the use of drugs (chemotherapeutic), for the elimination of neoplastic cells. Cisplatin and its analogues are widely used in the treatment of various types of cancer,

* Corresponding author at: Faculdade de Ciências Exatas e Tecnologia - FACET, Universidade Federal da Grande Dourados - UFGD, Rodovia Dourados - Itahum, Dourados, MS 79804-970, Brazil.

** Correspondence to: Faculdade de Medicina Dr. Hélio Mandetta, Universidade Federal de Mato Grosso do Sul. Cidade Universitária, Campo Grande, MS 79070-900, Brazil.

E-mail addresses: robertogomes@ufgd.edu.br (R. da Silva Gomes), rodrigo.oliveira@ufms.br (R.J. Oliveira).

<https://doi.org/10.1016/j.taap.2018.08.004>

Received 2 May 2018; Received in revised form 2 August 2018; Accepted 3 August 2018

Available online 06 August 2018

0041-008X/ © 2018 Published by Elsevier Inc.

including breast cancer (Dasari and Bernard Tchounwou, 2014; Tsimberidou et al., 2009). However, several adverse effects are reported, such as ototoxicity, nephrotoxicity, neurotoxicity, bone marrow suppression, and gastrointestinal disorders (Martins et al., 2017). In addition to these compounds, the literature reports that copper complexes have antitumor activity (Gao et al., 2011; Pivetta et al., 2012; Thalamuthu et al., 2013), including for breast cancer (Fan et al., 2017; Gouda et al., 2018; Manikandamathavan et al., 2017; Sangeetha and Murali, 2017). Therefore, the coordination of metals to drugs is a possibility to expand the therapies for the treatment of this disease.

In addition to metals there are also important pharmacophoric groups with cytotoxic and anticancer activity (Jha et al., 2010). A good example is the derivatives of maleamic acids, such as chalcones (Mitra et al., 2015), which possess the 1,4-dioxo-2-butenyl group and which demonstrated potent anticancer activity, *in vitro* and *in vivo*, moreover they are not toxic in mice (Rodrigues et al., 2011).

Several research groups seek, through new natural or synthetic compounds, to solve the inherent challenges of side effects, resistance of tumor cells and non-specificity of chemotherapeutics. In this context, our research group proposed to design a new compound based on the anticancer actions of copper and the pharmacophoric group 1,4-dioxo-2-butenyl. For this reason, the present work evaluated the antitumor activity of the new copper (III) complex, Bis((Z)-4-((4-chlorophenyl)amino)-4-oxobut-2-enyl)oxy)copper (RC1), in murine mammary adenocarcinoma cells 4 T1, as well as its toxicogenic effect in Swiss mice.

2. Methods

2.1. Synthetic chemistry

To obtain the compound, 2.5 mmol of maleic anhydride was reacted with 2.5 mmol of p-chloroaniline in ether at room temperature for approximately 3 h. The precipitate was filtered, washed with cold water and dried at room temperature. Then, 2.5 mmol of sodium hydroxide (NaOH) in ethanol was added to the reaction mixture at room temperature and stirred for 1 h and thereafter 1.25 mmol of copper (II) sulfate pentahydrated ($\text{CuSO}_4 \cdot 5\text{H}_2\text{O}$) was added and the reaction mixture was incubated for more 2 h. The obtained blue precipitate was filtered and dried at room temperature.

2.2. *In vitro* assay

2.2.1. Cell culture conditions

The 4 T1 murine mammary adenocarcinoma cell line (ATCC number CRL-2539) were grown in a 75cm² culture flask in Dulbecco's Modified Eagle Medium (DMEM) (Gibco®, Life Technologies, Grand Island, NY) supplemented with 10% foetal bovine serum (Gibco®), 0,1% penicillin 10.000 U/streptomycin 10.000 µg/mL (BR30110-01, LGC Biotecnologia) at 37 °C in a humidified atmosphere containing 5% CO₂. Upon reaching 80% confluency, the cells were collected by enzymatic dissociation (trypsin 0.025% at 37 °C), and placed in plates with variable counts, according to the need of each experiment.

2.2.2. Chemical agents

Cisplatin (Fauldcispla®, Libbs) was used as a positive control at 50 µg/mL concentration (Lee et al., 2009). As test substance the RC1 compound diluted in 1% dimethylsulfoxide (Synth®) was used and as a negative control DMEM medium with 1% DMSO.

2.2.3. Cytotoxicity assay (MTT- Thiazolyl Blue Tetrazolium Bromide)

The cytotoxic potential was evaluated by the MTT colorimetric test 3-(4,5-Dimethyl-2-thiazolyl)-2,5-diphenyl-2H-tetrazolium bromide, performed as described by Schweich et al. (2017), with modifications. Cells were seeded at a density of 2.5×10^4 cells/well in 96 well culture plates and incubated with 5% CO₂ at 37 °C for 24 h for stabilization. Thereafter, the treatments were performed with 50 µg/mL

of cisplatin, nine concentrations of compound RC1 (3.125, 6.25, 12.5, 25, 50, 100, 250, 500 and 1000 µg/mL) and negative control cells received 1% DMSO. The cytotoxicity was evaluated at 24, 48 and 72 h. The IC₅₀ was calculated according to Pesarini et al. (2017) and used in the others *in vitro* experiments.

2.2.4. *In vitro* comet assay

The comet assay was performed according to Oliveira et al. (2014). For the comet assay, 4 T1 cells were grown in 6-well plates (1.5×10^5 cells/well) for a complete cycle (24 h) before treatments. The treatments, negative control (1% DMSO), positive control (50 µg/mL cisplatin) and IC₅₀ of RC1 were performed in independent triplicates. After the 4 h treatment, the cells were collected by enzymatic dissociation (trypsin 0.025% at 37 °C), centrifuged at 1200 rpm for 5 min and the supernatant was discarded. The cells were resuspended in 500 µL of DMEM and a 20 µL aliquot plus 120 µL of low melting point agarose (1.5%) was deposited on a pre-coated slide with normal agarose (5%). After lysis (Oliveira et al., 2007) and electrophoresis (Navarro et al., 2014) the slides were neutralized, dried and fixed with absolute ethanol.

The analysis was performed under a fluorescence microscope (Bioval® Model G2000 A, Brazil) using 100 µL of ethidium bromide (20×10^{-3} mg/mL). 100 comets/treatment/repetition were analyzed (40× magnification, 420–490 nm excitation filter and 520 nm barrier), which were classified in class 0 - nucleoids without comet tail; Class 1 - Comet tail less than or equal to nucleoid diameter; class 2 - tail of the comet larger or up to twice the diameter of the nucleoid; and class 3 - comet tail larger than twice the nucleoid diameter (Kobayashi et al., 1995). The genomic damage Score was determined by multiplying the number of damaged cells in each class by the number of damage classes (Hoff Brait et al., 2015; Oliveira et al., 2007).

2.2.5. Qualitative evaluation of cell death

For qualitative and morphological analysis of the influence of RC1 on 4 T1 cells, 2×10^5 cells were plated in 6-well plates containing a coverslip at their base and maintained in incubator with 5% CO₂ at 37 °C for 24 h for stabilization. After adherence, treatments with 50 µg/mL of cisplatin (positive control), 1% DMSO (negative control) and IC₅₀ of compound RC1 were performed. After 24 h of treatment, the coverslips were collected and processed according to the protocol described by Schweich et al. (2017). After three washes with PBS, the coverslips were removed from the culture dishes and fixed in Carnoy fixative for 5 min. The coverslip was rapidly dipped into each of the plates containing decreasing concentrations of ethanol (95% to 25%), followed by washing with McIlvaine Buffer for 5 min, staining with acridine orange (0.01%, 5 min) and washing again with the buffer. The analysis was performed under a fluorescence microscope with excitation filter 420–490 nm and 520 nm barrier filter.

2.2.6. Differential and quantitative evaluation of cell death

For qualitative and morphological analysis of the influence of RC1 on 4 T1 cells, 2×10^5 cells were plated in 6-well plates and incubated with 5% CO₂ at 37 °C for 24 h. After that, the treatment was performed with 50 µg/mL of cisplatin (positive control), 1% DMSO (negative control) and with the IC₅₀ of compound RC1. After 24 h the cells were collected by enzymatic cleavage (0.025% trypsin at 37 °C), centrifuged at 1200 rpm for 5 min and the supernatant was discarded. Then, 50 µL of the solution was homogenized with 2 µL of dye (100 µg/mL of Acridine Orange and 100 µg/mL of Ethoxide Bromide, both diluted in PBS). This cell suspension was then placed on a glass slide covered by cover slip and analyzed under a fluorescence microscope with excitation filter 420–490 nm and 520 nm barrier filter.

Cell classification was performed according to the following description: (I) living cells with functional membrane have uniform green coloration in their nucleus; (II) cells in initial apoptosis with functional membrane, but with DNA fragmentation, show a green coloration in

Table 1
Primer sequences (5'– 3') used in real-time PCR.

Gene	Forward	Reverse	Size (pb)
ACTB	GGAAATCGTGCGTGACAT	AGGAAGGAAGGCTGGAAG	183
p53	TACCACCATCCACTACAACCT	GACAGGCACAAACACGCAC	145
p21	TAGCAGCGGAACAAGGAG	AAACGGGAACCAAGGACAC	249
ATR	CCTTCAGATTTCCCTTGAATAC	GCAGTTCATGTTTTGATGAG	137
ATM	ACCATTGTAGAGGTCCTTC	GTCTCATTAAAGACACCGTTGAG	148
GADD45	TCAGCGCAGCATCACTGTC	CCAGCAGGCACAACACCAC	82
BAX	CCT TCT TTG AGT TCG GTG	TTCAGGTACTCAGTCATCCAC	100
BAK	CTGTTTGAGAGTGGCATC	ATGCTGGTAGACGTGTAG	84
BCL-2	GGACGAACTGGACAGTAAC	GCAAAGTAGAAAAGGGCGACAAC	127
CASP9	CTCTACTTTCCAGGTGA	TTTCCACCGAAACAGCATT	195
CASP7	TCACCATGCGATCCATCAAGACCA	TTTGCTGTTCCGTTTCCGAACGCC	148
CASP3	ATCATACATGGAAGCGAATC	ATACATAAACCCATCTCAGGA	86

nucleus and cytoplasm, with a visible marginalization of their nuclear content; (III) cells in final apoptosis present orange-stained areas both in the cytoplasm and in the sites where the chromatin is condensed in the nucleus, which distinguishes them from necrotic cells; (IV) necrotic cells have uniform orange staining in the nucleus (Oliveira et al., 2007). 100 cells/treatment were counted. The experiments were performed in independent triplicate.

2.2.7. Flow cytometry assays

The cell cycle experiments, apoptosis and membrane integrity were performed by flow cytometry in independent triplicates, as described by Schweich et al. (2017). 2×10^5 of 4T1 cells were seeded in 6 well plates and incubated with 5% CO₂ at 37 °C for 24 h. After that, the treatments with 50 µg/mL of cisplatin (positive control), 1% DMSO (negative control) and with the IC₅₀ of compound RC1 were performed. After 24 h the cells were collected by enzymatic cleavage, centrifuged at 1200 rpm for 5 min and the supernatant was discarded. The pellet was resuspended in 100 µL of PBS and transferred to a cryotube. The acquisition of 10.000 events was performed on a BD Accuri® C6 cytometer and then analyzed by BD Accuri® C6 Software.

2.2.7.1. Cell cycle. To verify the influence of the treatments on the cell cycle, 5 µL of RNase (2 mg/mL) were added to the cryotube containing 100 µL of cell suspension (in PBS) and incubated at 37 °C, 5% CO₂, for 30 min. Then, 100 µL of the lysis solution (20 mg Sodium Citrate Dihydrate, 20 µL Triton X 100 and 20 mL PBS) and 5 µL of Propidium Iodide (50 µg / mL) were added. The cryotube was incubated on ice for 30 min protected from light prior to acquisition (Schweich et al., 2017).

2.2.7.2. Apoptosis. The Annexin V Apoptosis PE Detection Kit (BD Pharmingen™) was used for the detection of apoptosis. To this end, 100 µL of cell suspension was homogenized with 100 µL of buffer solution (1 ×) and 5 µL of Annexin V. The cryotube was incubated on ice for 15 min. Then, 5 µL of 7-aminoactinomycin D (7AAD) was added and the acquisition was done immediately (Schweich et al., 2017). Cell status was defined as described by Savio et al. (2014), with modifications. The cells not labeled by the dyes (Annexin V and 7AAD) were classified as viable; those labeled only by annexin V were classified as initial apoptosis; cells labeled by both markers (Annexin V and 7AAD) were classified as late apoptosis; and those marked only by 7AAD were classified as necrotic.

2.2.7.3. Membrane integrity. To verify membrane integrity, 100 µL of cell suspension and 25 µL Propionate Iodide (50 µg/mL) were used. After 5 min of incubation at room temperature the acquisition was made (Schweich et al., 2017).

2.2.8. Gene expression – qPCR

Gene expression was evaluated by qPCR. In a 6 well plates a total of 2×10^5 cells/well were seeded and treated with a 1% DMSO (negative

control) and with IC₅₀ of RC1. After 12 h, the total RNA was extract by an in house method using a lyses buffer containing guanidine isothiocyanate (GuSCN 5 mol/L, Tris HCL 11.2 g/L pH 6.4, EDTA NaOH 7.43 g/L, 7.8mL Triton X-100). Each sample was extracted in triplicate. 200 µL of lysis buffer was added in 200 µL of cell suspension. After 10 min of homogenization, it was added 50 µL of magnetic beads (Nuclisens®, bioMérieux) and allowed to stand for 10 min. The impurities (cell debris) were extracted by magnetized rack (Promega®) by performing two washes with lysis buffer. Excess of guanidine thiocyanate and salts were withdrawn with 70% ultrapure alcohol washings. The beads were washed with acetone PA, heated for one minute at 60 °C in dry bath equipment DB-HC (Loccus®, Brazil) and the genetic material was eluted with 30 µL of TE (bioMérieux®). After extraction, RQ1 RNase-Free DNase (cat. no. M6101, Promega®) was performed according to the manufacturer's specifications. After the DNA degradation step, the quality of the extracted material was analyzed by ratio of the quotient A260/A280 and A230/A260 in a NanoVue™ Plus spectrophotometer (GE Healthcare - Life Sciences®) and the integrity in denaturing agarose gel (1%). Complementary DNA (cDNA) was obtained on T100™ thermal cycler (Thermal Cycler, Bio-Rad™) using 250 ng of RNA plus 0.5 µg of random primer, ultra-pure RNase/DNase free water, 5 µL of GoScript™ 5 × Buffer 3.8 mM of MgCl₂, 0.5 mM of DNTPs, 20 units of the RNase inhibitor and 1 µL of GoScript™ Reverse (all Promega components). The mixture was incubated at 25 °C for 5 min, followed by 42 °C for 60 min and 70 °C for 15 min. The qPCR reactions were performed in triplicates in the Rotor Gene® equipment (Qiagen). The genes analyzed are described in Table 1. The tested genes were involved in DNA damage processes (*p53*, *p21*, *ATR*, *ATM* and *GADD45*) and apoptosis (*BAX*, *BAK*, *BCL-2*, *CASP9*, *CASP7* and *CASP3*). For the qPCR reactions, it was used 10 µL of GoTaq® master mix, 2 pmol of each oligonucleotide, 500 ng of cDNA and free of ribonuclease water q.s.p. 20 µL (cat. no. A6002, Promega®). The mixture was subjected to 95 °C for 5 min and 40 cycles, 95 °C for 2 s and 60 °C for 30 s. At the end, the Melting curve was performed to evaluate the specificity of the products formed. The Beta-actin gene (*ACTB*) was used as housekeeping and the results were analyzed in Rotor Gene® software (Qiagen) v2.3.1.

2.3. In vivo assays

2.3.1. Animals and accommodation conditions

The experiment was conducted in accordance with the Universal Declaration of the Rights of the Animals, after approval of the Ethical Committee on the Use of Animals of the Federal University of Mato Grosso do Sul registered (protocol 921/2017). The animals were kept in polypropylene boxes coated with wood shavings and fed with commercial feed (Nuvital®) and filtered water *ad libitum*. The temperature and luminosity were controlled, for that the animals were kept under standard conditions of air conditioning (ventilated box ALESCO®): photoperiod of twelve hours (12 h of light: 12 h of darkness), with temperature keeping around 22 ± 2 °C and relative humidity of

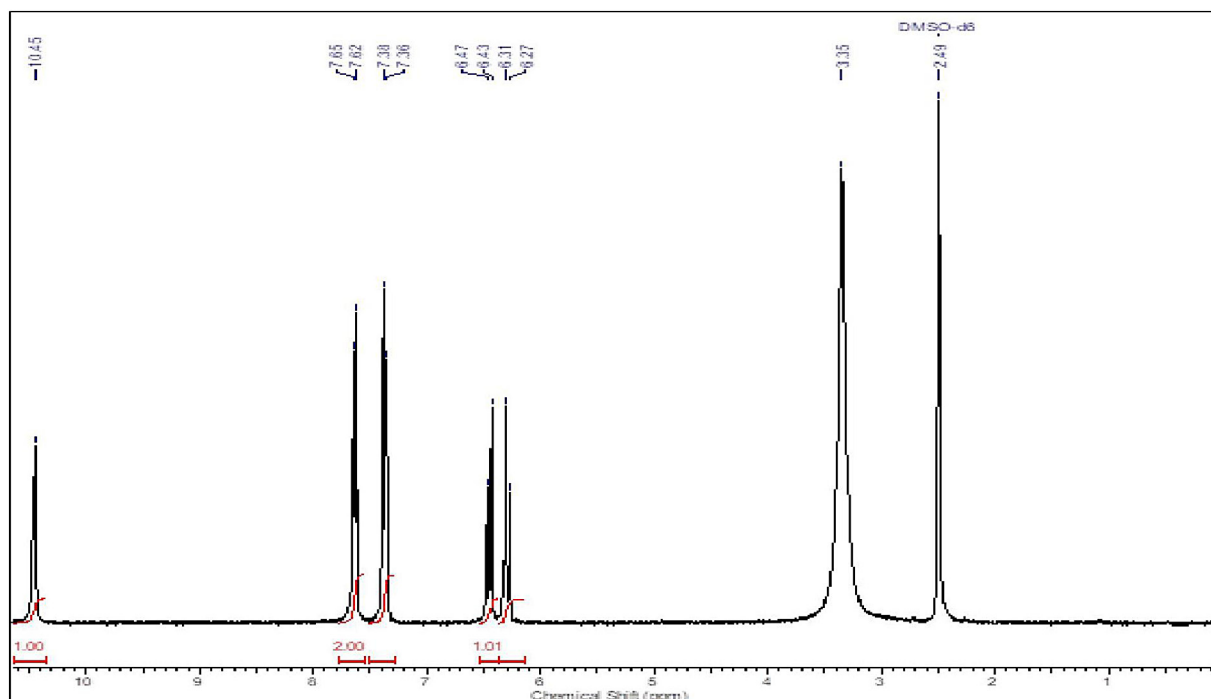


Fig. 1. ^1H NMR spectra of RC1 in $\text{DMSO}-d_6$ at 300 MHz.

$55 \pm 10\%$.

2.3.2. Chemical agents

The chemotherapeutic treatment was performed with cisplatin (Fauldcispla®, Libbs) at a dose of 6 mg/kg body weight (b.w.) (Berno et al., 2016), intraperitoneally (i.p.), in an application on the 1st experimental day.

The test compound, RC1, was diluted in DMSO (1%) and administered in the doses of 3, 6 and 12 mg/kg (b.w., i.p.).

2.3.3. Experimental design

We used 40 Swiss male mice (*Mus musculus*) at reproductive age with 35 g average weight. The animals were randomly distributed into eight experimental groups: Control Group (NC) - the animals received physiological solution (1% DMSO) at 0.1 mL/10 g body weight (b.w., i.p.); Positive Control (PC) - animals received cisplatin at 6 mg/kg (b.w., i.p.); Groups RC1 - animals received the test compound in 3 different doses D1 (3 mg/kg), D2 (6 mg/kg) and D3 (12 mg/kg) (i.p.); Associated Groups, positive control and test chemical combined, (ASS1, ASS2 and ASS3) - the animals received cisplatin at the dose of 6 mg/kg (b.w., i.p.) and the RC1 at the 3 different doses D1 (ASS1), D2 (ASS2) and D3 (ASS3) intraperitoneally (i.p.).

Blood collection for the micronucleus assay was performed by caudal vein puncture at 24, 48 and 72 h after application of the treatments (T1, T2 and T3, respectively), when the collection for the comet assay occurred only in T1. After 72 h of treatments administration, the animals were submitted to euthanasia by cervical dislocation for collection of organs.

2.3.4. Comet assay in peripheral blood

It was pipet 20 μL of homogenized peripheral blood in 120 μL of LMP agarose (1.5%) onto the (5%) agarose-covered surface of a pre-coated slide at 37 °C. Then, the comet assay was performed as described by Singh et al. (1988), with adaptations (Oliveira et al., 2009).

The analysis and classification of comets were performed according to Kobayashi et al. (1995).

2.3.5. Micronucleus assay

For this purpose, the technique of Hayashi et al. (1990) modified by Oliveira et al. (2009) was used. One drop of peripheral blood was deposited in a slide previously prepared with a layer of 20 μL of Acridine Orange (1.0 mg/mL), and then covered by coverslip. This material remained in freezer ($-20\text{ }^\circ\text{C}$) for a minimum period of 7 days. The analysis was performed under a fluorescence microscope (Bioval® Model G2000 A, Brazil) with excitation filter 420–490 nm and 520 nm barrier filter with a 40 \times magnification. 2000 cells/animal were analyzed.

2.3.6. Splenic phagocytosis

Phagocytosis assays were performed according to the procedure described by Schneider et al. (2016). The spleen was macerated in physiological solution to obtain a homogenous suspension of cells and 100 μL of the cell suspension were placed on a lamina previously stained with acridine orange (1 mg/mL), covered by coverslip and conditioned at $-20\text{ }^\circ\text{C}$ until analysis. The analysis was performed under a fluorescence microscope (Bioval® Model G2000 A, Brazil) with a 420–490 nm filter and a 520 nm barrier filter, at a 40 \times magnification. 200 cells/animal was analyzed. The absence or presence of phagocytosis was based on the description of Hayashi et al. (1990) with modifications (Carvalho et al., 2015).

2.4. Statistical analysis

Results were expressed as mean \pm standard error of the mean. The determination of the IC_{50} concentration of RC1 was performed by analyzing the non-linear regression curve from the cell viability values obtained in the MTT assay using the GraphPad Prism 5 Software (Pesarini et al., 2017). Statistical analysis was performed by ANOVA/Bonferroni and ANOVA/Tukey, with the exception of qPCR that was analyzed by the REST program (Pfaffl et al., 2002). The significant difference was considered when the level of relative expression was equal to or < 0.5 or equal to or > 2 (Biazi et al., 2017), and in all trials the established level of significance was $p < 0,05$ (Software GraphPad InStat 5).

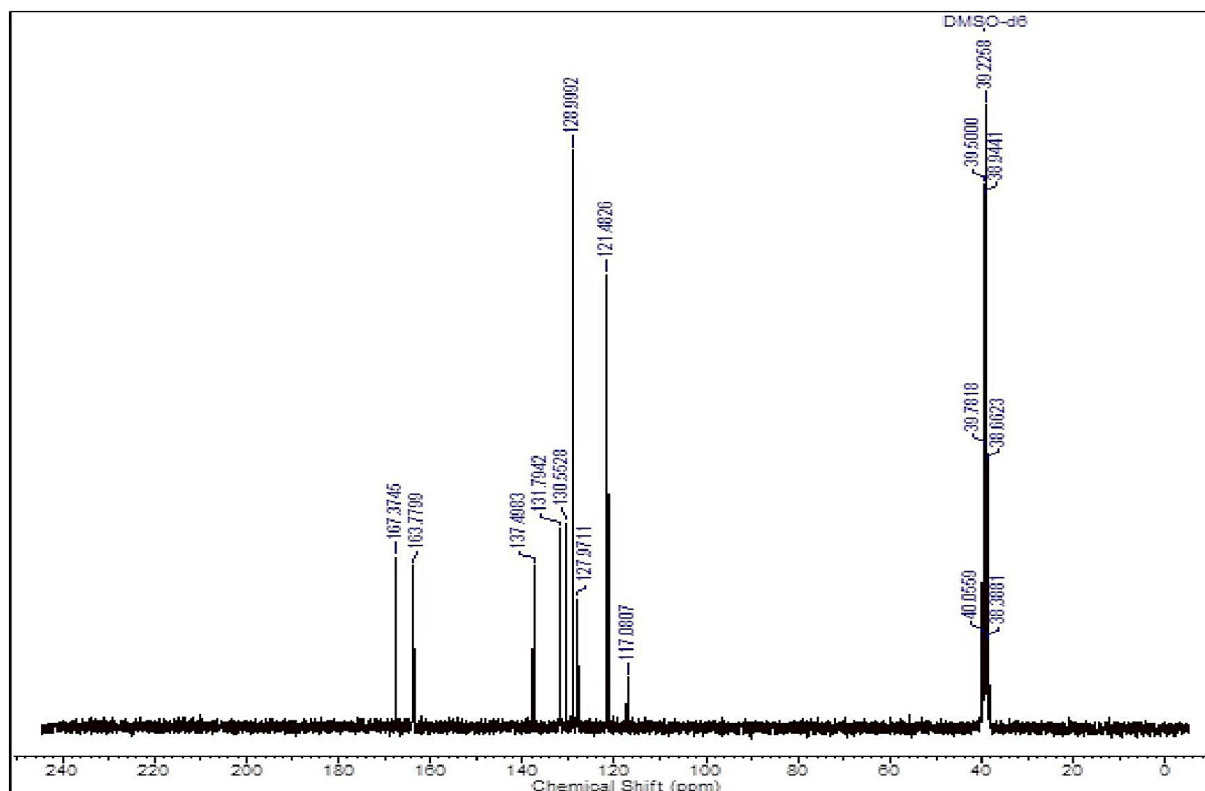


Fig. 2. ^{13}C NMR spectra of RC1 in DMSO- d_6 at 75 MHz.

3. Results

3.1. RC1 synthesis

^1H and ^{13}C NMR spectra (Figs. 1 and 2) were obtained in a Bruker Avance 300 spectrometer at the Institute of Chemistry of the Federal University of Mato Grosso do Sul (UFMS), in DMSO- d_6 , operating at 300.132 and 75.476 MHz, respectively. The chemical shifts (δ) of ^1H and ^{13}C are given on the ppm scale and were referenced to tetramethylsilane (TMS).

^1H NMR (DMSO- d_6 , 300 MHz) δ (ppm): 3.35 (s, NH), 6.29 (d, 1H, $J_{\text{cis}} = 12$ Hz), 6.45 (d, 1H, $J_{\text{cis}} = 12$ Hz), 7.37 (m, 2H), 7.64 (m, 2H), 10.45 (s, OH). ^{13}C NMR (DMSO- d_6 , 75 MHz) δ (ppm): 117.1 (C), 121.5 (CH), 128.9 (CH), 130.6 (CH), 131.8 (CH), 137.5 (C), 163.8 (C = O), 167.4 (C = O).

Infrared spectra were recorded at room temperature in the infrared absorption spectrometer - Jasco IR-6200 (FACET - UFGD) in the range of 4000 to 400 cm^{-1} . The samples were prepared by dispersion in potassium bromide (KBr) and pelleted, which were placed directly in the optical path of the equipment for transmittance reading (%T).

The IR data (Table 2) of the complex in addition to presenting the major bands of the ligand showed evident shifts of the carboxyl $\nu_{\text{C=O}}$ band from 1705 cm^{-1} to 1557–1541 cm^{-1} , indicating the possible formation of coordination binding by this group of the ligand, since the complex was formed by deprotonation of the carboxyl. It is also possible to notice the presence of less intense bands around 1690 to 1640 cm^{-1} , attributed to $\nu_{\text{C=O}}$ amide. For these bands there were no significant shifts, suggesting that this group interacts poorly with the metal and that there is probably no coordinate bond formation by this region of the ligand molecule.

Table 2

Frequencies (ν , cm^{-1}) of selected vibration bands in the IR spectra of RC1.

Vibration band	ν (cm^{-1})
$\nu_{\text{N-H}}$	3274
$\nu_{\text{ass}} = \text{C-H}$	3077, 3057, 3012
$\nu_{\text{s}} = \text{C-H}$	2975, 2876
Combination bands or harmonic	3200, 2251 a 1733
$\nu_{\text{C=O}}$	1705, 1699
$\nu_{\text{C=C}}$ alkene <i>cis</i>	1627
$\nu_{\text{C=C}}$ aromatic <i>p</i> -substituted	1601 e 1488
$\delta_{\text{N-H}}$ in-plane	1552, 1522
$\nu_{\text{C-N}}$	1398 a 1320
$\nu_{\text{C-O}}$	1294 a 1198
$\nu_{\text{C-Cl}}$	1093
$\delta_{\text{O-H}}$ out-of-plane	972
$\delta_{\text{C-H}}$ aromatic out-of-plane, <i>p</i> -substituted	858
$\delta_{\text{C-H}}$ alkene <i>cis</i> out-of-plane	699
$\delta_{\text{N-H}}$ out-of-plane	669 a 609
$\delta_{\text{C=C}}$ alkene or aromatic out-of-plane	512,444

3.2. In vitro assays

3.2.1. Cytotoxicity of compound RC1

RC1 compound is cytotoxic to 4T1 cells at the three times tested (Fig. 3a). The IC_{50} in 24 h was 72 $\mu\text{g}/\text{mL}$ (Fig. 3b) and, at in the all-time points, concentrations > 25 $\mu\text{g}/\text{mL}$ caused cell death ($p < 0.05$) in a dose-dependent manner (Fig. 3c). The IC_{50} of the RC1 compound at the 48 h treatment was 71.2 $\mu\text{g}/\text{mL}$ whereas, for the 72 h the IC_{50} was 63.3 $\mu\text{g}/\text{mL}$.

3.2.2. DNA damage

DNA damage, evaluated by the comet assay in 4T1 cells (Fig. 4a), demonstrated that the RC1 compound induces (Fig. 4b) the same frequency of damage as the positive control (Fig. 4c). However, the RC1 DNA damage score is higher ($p < .05$) than the cisplatin score (Fig. 4d).

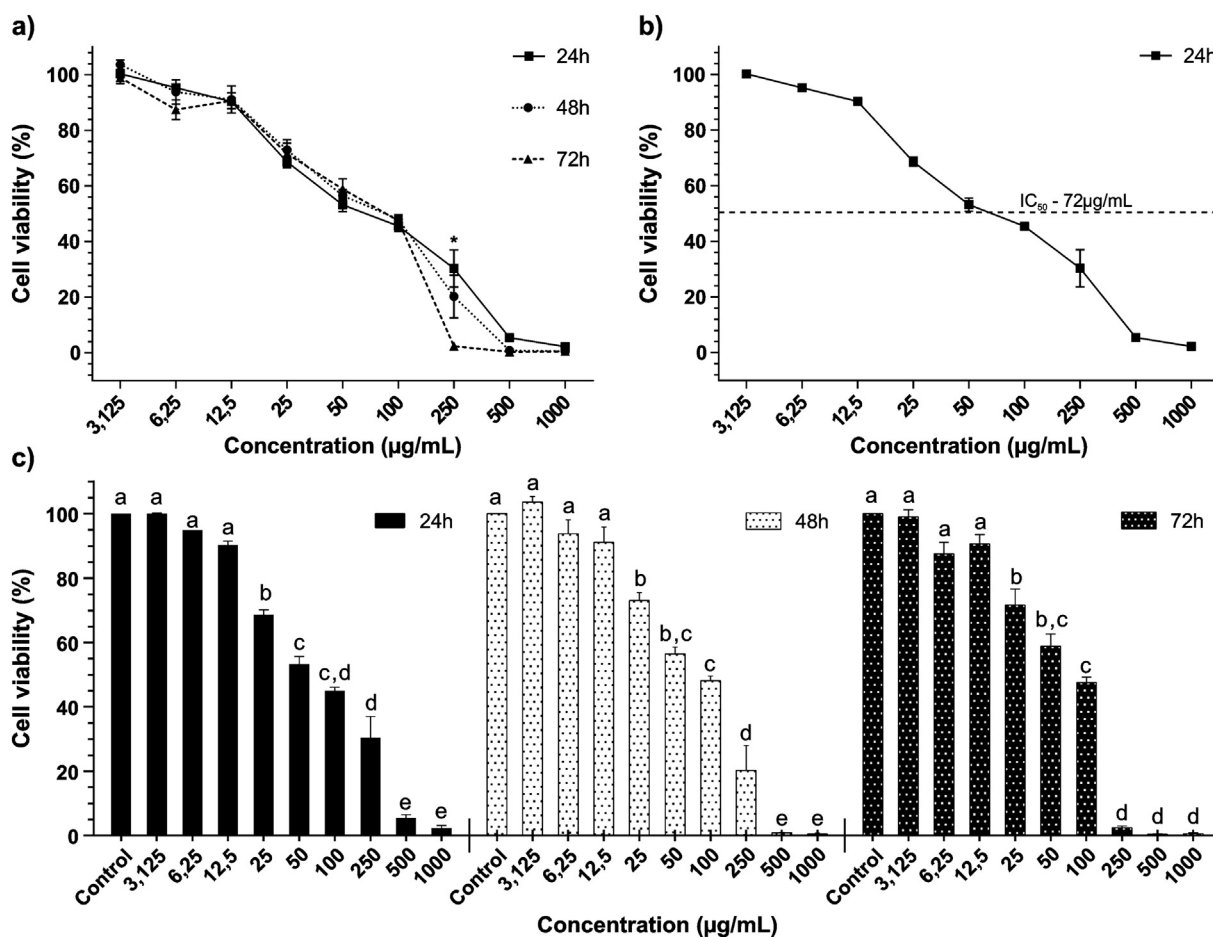


Fig. 3. Cytotoxicity of RC1 compound in 4T1 murine mammary adenocarcinoma cells.

RC1 compound induces cell cycle arrest in 4T1 cells (Fig. 4e). Cells treated with RC1 had G1 cell cycle arrest ($p < 0.05$) and G1, S and G2/M cell percentages were 46.27% ($p < 0.05$), 18.90% ($p < 0.05$) and 7.73% ($p > 0.05$), respectively. For this treatment 27.10% of the cells in Sub G1 were still observed ($p < 0.05$). In cells treated with cisplatin there was accumulation of cells in G2/M and the percentages of cells in G1, S and G2/M were 30.20% ($p > 0.05$), 20.93% ($p > 0.05$), 42.00% ($p > 0.05$), respectively. For this treatment, 6.87% of the cells in Sub G1 ($p < 0.05$) were still observed (Fig. 4f).

Analysis of the qPCR assay demonstrated significant increase in the expression of *p21* ($8.31 \times$), *ATM* ($2.44 \times$) and *GADD45* ($2.65 \times$) genes. There was also an increase in *p53* ($1.45 \times$) and a decrease in *ATR* ($-1.35 \times$) in a non-significant manner (Fig. 4g).

3.2.3. Apoptosis

RC1 compound induces apoptosis in 4T1 cells and this was demonstrated by the cytological technique of *in situ* apoptosis (qualitative evaluation) (Fig. 5a). In the differential cytological apoptosis/necrosis test (quantitative evaluation) (Fig. 5b) there was no significant difference between the RC1 and PC treatments, but both were different ($p < 0.05$) from the NC with an increase in apoptosis frequency of $11.94 \times$ and $12.02 \times$, respectively. In the apoptosis assay by flow cytometric were observed (Fig. 5c), 28.6% of the cells in initial apoptosis, 6.6% of final apoptosis and 5.6% in necrosis for treatment with cisplatin, whereas, cells treated with compound RC1 showed 43.1% in initial apoptosis, 9.9% in final apoptosis and 1.4% in necrosis.

RC1 compound did not alter the membrane integrity of 4T1 cells. Membrane integrity test (Fig. 5d), evaluated by flow cytometry, demonstrated no difference ($p > 0.05$) in the treatments of PC and RC1 in relation to the control.

Analysis of apoptosis gene expression (Fig. 5e) demonstrated that the RC1 compound induced a significant increase in the expression of *BAX* ($2.38 \times$) and *CASP7* ($4.45 \times$) genes, and increase of *BAK* ($1.98 \times$), *CASP9* ($1.10 \times$), *CASP3* ($0.99 \times$) and decrease of *BCL-2* ($-1.19 \times$) in a non-significant manner.

3.3. In vivo assays

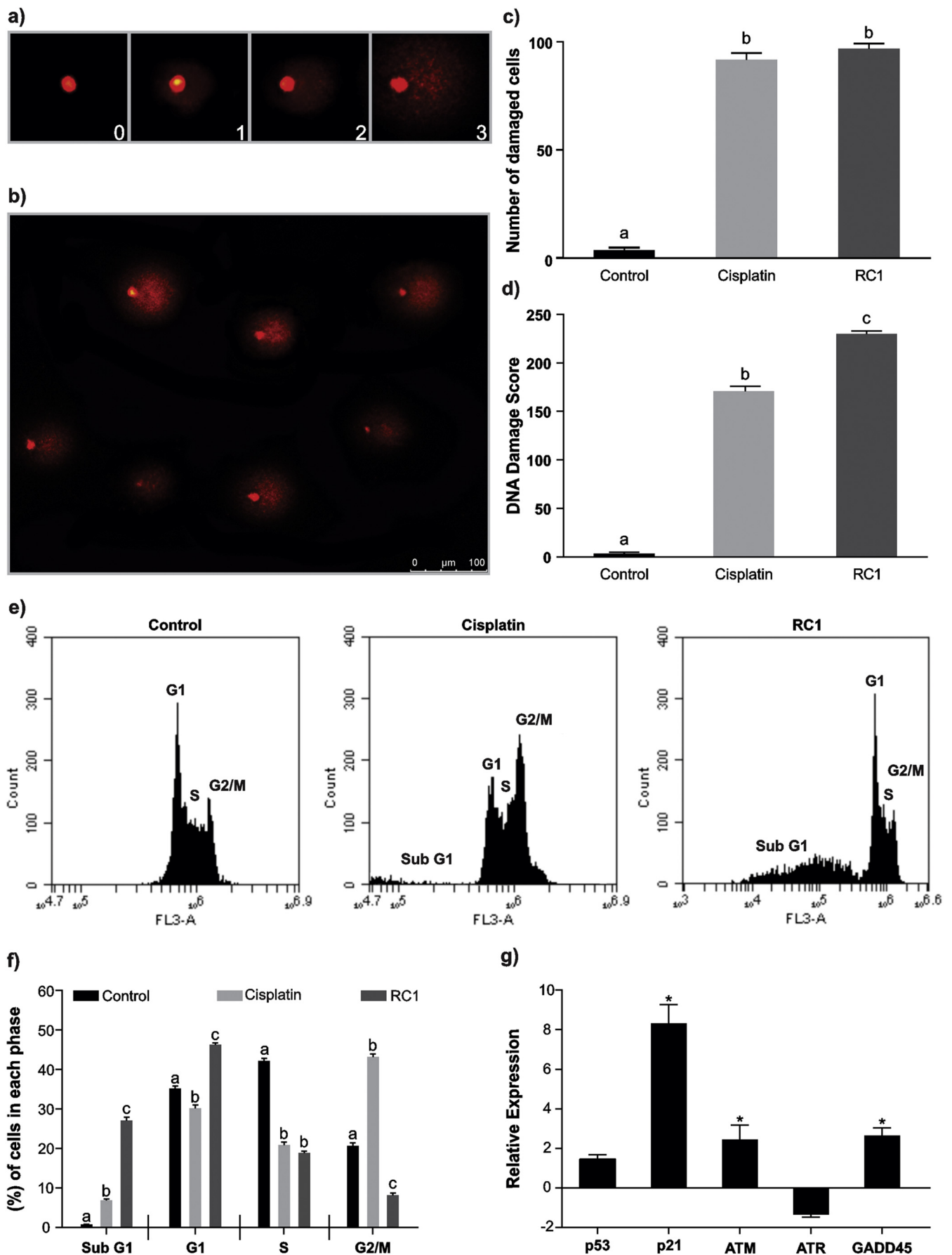
3.3.1. Biometric parameters

The initial weight of the animals did not present statistically significant differences between the experimental groups. Regarding the final weight of the animals, only the PC group and the ASS3 group presented differences ($p < 0.05$) in relation to the NC (Table 3).

In the analysis of the absolute weight of the organs, it was possible to observe that the PC group presented differences ($p < 0.05$) in liver and kidney weight, and D3 group in spleen weight. The ASS2 group presented differences ($p < 0.05$) in heart weight and the ASS3 in heart and liver weight. Regarding to the analysis of the relative weight of the organs, statistically significant differences were observed for the spleen and heart in groups D3 and ASS2, respectively (Table 3).

3.3.2. Genotoxicity evaluation

The RC1 compound is genotoxic in mice ($p < 0.05$). RC1 caused an increase in the frequency of damages of $5.38 \times$, $6.22 \times$ and $6.61 \times$ for doses D1, D2 and D3, respectively. The PC group and the groups ASS1, ASS2 and Ass3 showed an increase of $22.66 \times$, $21.22 \times$, $21.83 \times$ and $24.0 \times$, these variations are significant in relation to the NC, but not in relation to the PC. When the score was evaluated, it was observed an increase of $26.5 \times$, $6.72 \times$, $7.61 \times$, $8.27 \times$, $23.94 \times$, $24.50 \times$ and $28.05 \times$ for PC, D1, D2 D3, ASS1, ASS2 and ASS3, respectively



(caption on next page)

Fig. 4. Analysis of genomic damage induced 822 by RC1 compound in 4 T1 murine mammary adenocarcinoma cells. (A) criterion for classification of genomic damage by comet assay means, where 0 represents nucleoid with no damage and 1, 2 and 3, the respective damage classes; (B) nucleoids with genomic damage induced by compound RC1 after 4 h of 827 treatment; (C) percentage of cells with DNA damage observed by the comet assay; (D) score of genomic damage in 4 T1 cells treated with IC50 of RC1 compound; (E) graphs of the cell cycle analysis of 4 T1 cells treated with negative control, cisplatin and IC50 of RC1 compound; (F) Percentage of cells in each phase of the cell cycle after treatments with negative control, cisplatin and IC 50 of compound RC1. Different letters indicate statistically significant differences ($p < 0.05$; ANOVA/Bonferroni); (G) gene expression related to DNA damage and repair of 4 T1 cells treated with IC50 of RC1 compound. As normalizer was used the ACTB gene and * indicate statistically significant differences ($p < 0.05$, REST). Needs color printing.

(Table 4).

The RC1 compound did not increased the frequency of micronuclei in peripheral blood samples of mice. In the three times tested, doses D1, D2 and D3 presented frequencies ranging from 3.40 ± 0.81 to 7.40 ± 1.08 . In the combination of RC1 and cisplatin, a discrete increase in the frequency of micronuclei was observed in 48 h for ASS2 and ASS3 and for the three doses in 72 h (Table 5).

3.3.3. Splenic phagocytosis

There was an increase ($p < 0.05$) in phagocytosis frequency in the cisplatin-treated, RC1 and ASS1 groups. The groups ASS2 and ASS3 did not present significant differences in relation to NC (Fig. 6).

4. Discussion

The present work was described the synthesis of the copper complex RC1, and evaluate its antitumor activity and toxicogenic action in 4 T1 adenocarcinoma cells murine mammary in Swiss mice.

Several studies report the antitumor activity of copper (II) complex (Facchin et al., 2016; Fan et al., 2017; Gouda et al., 2018; Kosiha et al., 2017; Lakshmipraba et al., 2013; Manikandamathavan et al., 2017; Sangeetha and Murali, 2017), which is related to DNA cleavage (Bhat et al., 2017) and/or the formation of reactive oxygen species (ROS), that cause genomic and mitochondrial. (Liu et al., 2015).

The genotoxicity of RC1 compound was observed in both, *in vitro* and *in vivo* assays. The results of the *in vitro* comet assay indicate genotoxic activity of compound RC1 in 4 T1 tumor cells, with a higher score than the chemotherapeutic cisplatin. While in *in vivo* the chemotherapeutic agent was remarkably more genotoxic. This finding corroborates the results of other groups (Acilan et al., 2017; Bhat et al., 2017; Dallavalle et al., 2002; Marzano et al., 2009) that indicate lower action of copper (II) complexes in normal cells, than in tumor cells. This prominent effect of copper (II) complexes on tumor cells probably occurs because of the greater tolerance of normal cells to the DNA oxidation process (Acilan et al., 2017).

DNA damage caused by RC1 compound induced *in vitro*, G1 cell cycle arrest, preventing the progression of the cell cycle to S phase. The gene expression assay demonstrated increase expression of *ATM*, *GADD45* and *p21*, these genes inhibits the activity of *Cdk2* (Massagué, 2004; Nash et al., 2001), resulting in disruption of the DNA replication process, cell cycle arrest in G1 and senescence (Bertoli et al., 2013; Ueda et al., 2017). Cisplatin, which develops its antitumor action by binding to the purine bases, blocking DNA replication (Wang and Lippard, 2005), induced cell cycle arrest in G2/M, which corroborates other studies that evaluated the influence of this chemotherapeutic on the cell cycle (Łakomska et al., 2014; Wang and Lippard, 2005). Regardless of the stage in which the cell stops its cell cycle, when there is no DNA repair, the cell must be induced to cell death (Bertoli et al., 2013; Massagué, 2004; Oliveira et al., 2014; Roos and Kaina, 2006; Wang and Lippard, 2005).

It is expected that treatments with chemotherapeutic compounds induce cell death *via* apoptosis, which does not result in an inflammatory process (Ooi and Ma, 2013), as in cases of cell death due to necrosis (Urru et al., 2018). Lakshmipraba et al. (2015) described the synthesis, cytotoxic and genotoxic activity of a copper (II) complex in MCF-7 cells. However, when analyzing the type of cell death, they

found cells in apoptosis and in necrosis, different from that observed in the cytotoxic activity of RC1 compound, which induced cell death mediated only by apoptosis, and without altering cell membrane integrity. Apoptosis, induced by RC1 compound, was demonstrated by *in situ* and differential apoptosis/necrosis cytological techniques, as well as by the cytometric assay.

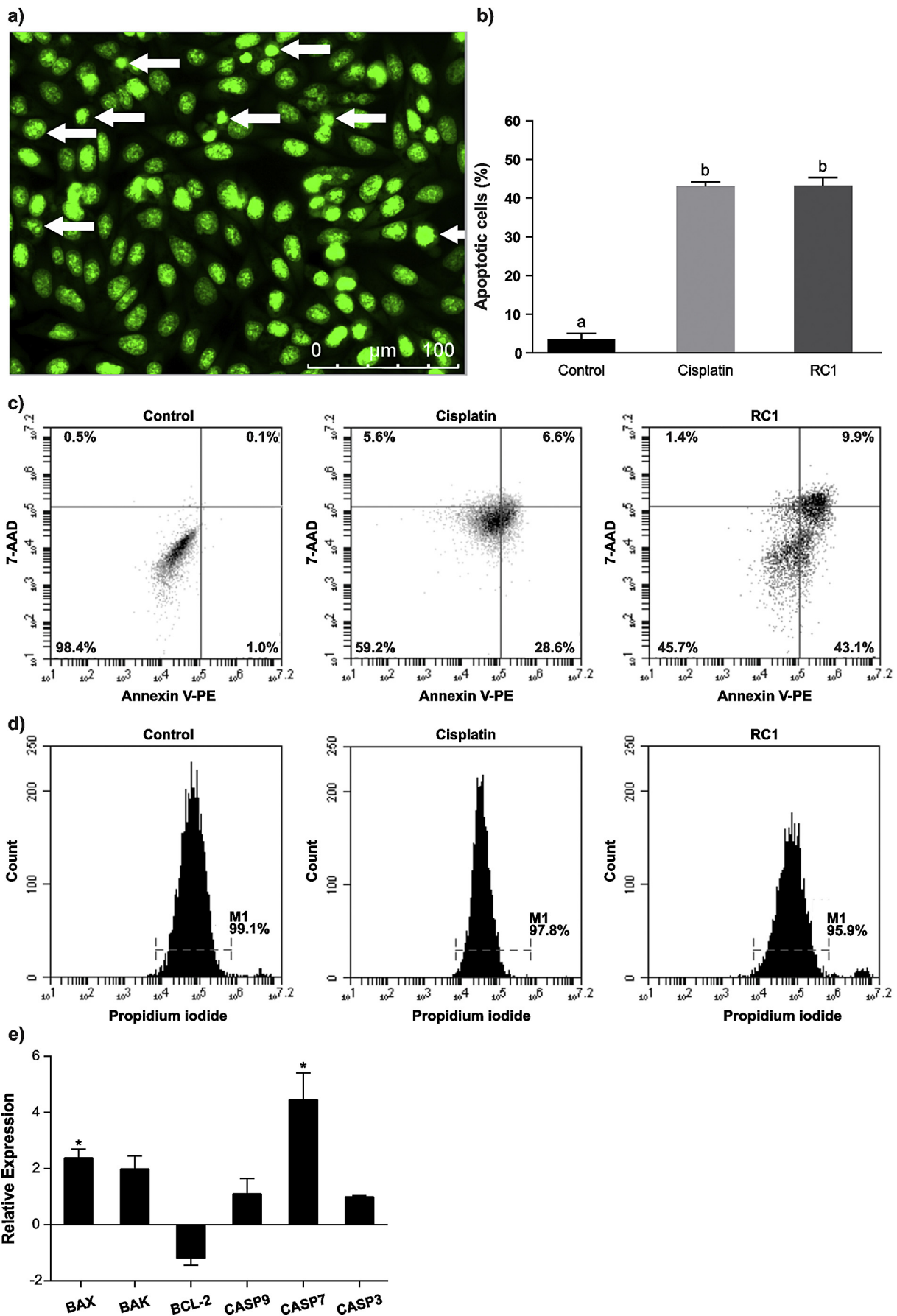
The process of cell death by apoptosis is complex and multigenic. Mitochondria have a central role in triggering apoptosis and their integrity is mediated by BCL-2 activity (Márquez-Jurado et al., 2018). The decrease in BCL-2 expression and the increase of the pro-apoptotic BAX gene probably induced lesions in the mitochondrial membrane of 4T1 cells, with consequent release of cytochrome C. The release of cytochrome C from mitochondria to the cytosol, in addition to activation of caspases, blocks the transport of electrons, preventing the production of energy, which compromises cellular viability (Amarante-Mendes and Green, 1999; Gogvadze and Orrenius, 2006). The RC1 compound induced apoptosis in 4 T1 cells *via* caspase-7, which is an effector caspase, as well as caspase-3, and although no significant increase occurred in the gene expression assay, caspase-7 appears to have been activated by caspase-9 (Domracheva et al., 2017; Márquez-Jurado et al., 2018).

Copper (II) complexes are considered promising in the development of new treatments for various neoplasms (Košariková et al., 2016). Regulatory agencies require that, prior to human testing, the compound is administered to animals, mainly to assess their toxicity and genotoxicity (ANVISA, 2013; European Commission, 2006; U.S. Department of Health and Human Services et al., 2012).

When the final weight of the animals was evaluated, only cisplatin-treated animals, those treated with cisplatin and those treated with the highest dose of RC1 showed reduction. Therefore, this reduction, which may be indicative of toxicity (De David et al., 2014; Ishikawa et al., 2017), has no direct correlation with RC1. When we evaluated the absolute and relative organ weights, the only significant differences were the reduction of relative heart weight and relative spleen weight gain in groups ASS2 and D3, respectively. In relation to the group treated with the highest dose of RC1, it is suggested that the increase of the spleen size of the animals of this group can be correlated with the significant increase of splenic cells in phagocytic activity of group in relation to the NC group, which induces leukocyte migration (de Araújo et al., 2017; Luchini et al., 2008). The splenic phagocytosis may occur in response to DNA damage, as a cellular mechanism of defense against genotoxic agents (Bazo et al., 2002; Carvalho et al., 2015; Ishii et al., 2011; Navarro et al., 2014).

The cisplatin, which was already confirmed *in vitro* as genotoxic in 4 T1 cells, also showed action *in vivo* and increased the frequency of comets and micronuclei *in vivo*. However, in any of the times tested, the RC1 compound had a frequency of micronuclei in different amounts of the negative control group, despite having increased comet frequency *in vivo*, suggesting that cells with DNA lesions, observed by the comet assay were phagocytosed, or that genomic damage was corrected by the DNA repair machinery (Bazo et al., 2002; Carvalho et al., 2015; Ishii et al., 2011; Navarro et al., 2014). However, despite this possibility, the toxicity of cisplatin is well described in the literature (Ciarimboli, 2014) and among its toxic effects nephrotoxicity is highlighted (Pabla et al., 2009).

The RC1 compound did not reduce the genotoxicity of cisplatin observed by the *in vivo* comet assay but prolonged the metabolism of



(caption on next page)

Fig. 5. Apoptosis in 4 T1 cells induced by compound RC1.

(A) cells in apoptosis after treatment with IC50 of RC1 840 compound; (B) percentage of cells in apoptosis after treatment with DMSO (negative control), cisplatin and IC50 of RC1 compound. Different letters indicate statistically significant differences ($p < 0.05$, ANOVA/Bonferroni); (C) percentage of viable cells in initial apoptosis, late apoptosis and necrosis following treatments with 1% DMSO, cisplatin and IC50 of RC1 compound.; (D) membrane integrity analysis of 4 T1 cells performed on flow cytometry with propidium iodide after treatments; (E) expression of apoptosis-related genes in 4 T1 cells after treatment with IC50 of RC1 compound. Needs color printing.

Table 3

Comparison of the biometric parameters between the experimental groups.

Biometric Parameters					
Experimental groups	Initial weight (g)			Final weight (g)	
NC	38,00 ± 1,44 ^a			39,60 ± 1,17 ^a	
PC	35,60 ± 0,74 ^a			34,20 ± 0,37 ^b	
D1	38,50 ± 1,22 ^a			38,80 ± 0,97 ^a	
D2	35,20 ± 0,96 ^a			36,00 ± 0,63 ^{a,b}	
D3	36,20 ± 0,58 ^a			36,80 ± 0,73 ^{a,b}	
ASS1	38,00 ± 0,77 ^a			36,40 ± 0,80 ^{a,b}	
ASS2	38,40 ± 1,60 ^a			37,00 ± 1,50 ^{a,b}	
ASS3	37,40 ± 0,68 ^a			35,20 ± 0,94 ^b	
Absolute weight organs (g)					
	Heart	Lung	Spleen	Liver	Kidneys
NC	0,23 ± 0,01 ^a	0,27 ± 0,00 ^a	0,17 ± 0,01 ^{a,b,c}	2,26 ± 0,05 ^a	0,57 ± 0,03 ^a
PC	0,19 ± 0,01 ^{a,b}	0,25 ± 0,02 ^a	0,13 ± 0,00 ^c	1,74 ± 0,02 ^b	0,46 ± 0,02 ^b
D1	0,21 ± 0,01 ^{a,b}	0,26 ± 0,02 ^a	0,21 ± 0,01 ^{b,d}	2,43 ± 0,09 ^a	0,58 ± 0,01 ^a
D2	0,21 ± 0,00 ^{a,b}	0,25 ± 0,01 ^a	0,19 ± 0,01 ^b	1,84 ± 0,03 ^{a,b}	0,56 ± 0,01 ^a
D3	0,20 ± 0,00 ^{a,b}	0,26 ± 0,01 ^a	0,26 ± 0,02 ^d	2,35 ± 0,17 ^a	0,57 ± 0,02 ^a
ASS1	0,21 ± 0,00 ^{a,b}	0,26 ± 0,01 ^a	0,17 ± 0,01 ^{a,b,c}	1,86 ± 0,09 ^{a,b}	0,48 ± 0,00 ^{a,b}
ASS2	0,16 ± 0,01 ^b	0,24 ± 0,01 ^a	0,16 ± 0,01 ^{a,b,c}	1,85 ± 0,09 ^{a,b}	0,51 ± 0,03 ^{a,b}
ASS3	0,17 ± 0,01 ^b	0,26 ± 0,00 ^a	0,11 ± 0,00 ^c	1,69 ± 0,12 ^b	0,48 ± 0,03 ^{a,b}
Relative weight organs (g)					
	Heart	Lung	Spleen	Liver	Kidneys
NC	0,006 ± 0,0003 ^a	0,007 ± 0,0002 ^{a,b}	0,004 ± 0,0003 ^{a,b}	0,057 ± 0,0009 ^{a,b}	0,014 ± 0,0008 ^{a,b}
PC	0,006 ± 0,0003 ^a	0,007 ± 0,0005 ^{a,b}	0,004 ± 0,0001 ^{a,b}	0,051 ± 0,0006 ^a	0,013 ± 0,0009 ^{a,b}
D1	0,005 ± 0,0002 ^{a,b}	0,006 ± 0,0004 ^b	0,005 ± 0,0003 ^{a,b}	0,056 ± 0,0014 ^{a,b}	0,013 ± 0,0002 ^{a,b}
D2	0,005 ± 0,0002 ^{a,b}	0,007 ± 0,0004 ^{a,b}	0,005 ± 0,0003 ^{a,b}	0,051 ± 0,0009 ^a	0,012 ± 0,0004 ^b
D3	0,006 ± 0,0003 ^{a,b}	0,007 ± 0,0003 ^{a,b}	0,007 ± 0,0008 ^c	0,064 ± 0,0035 ^b	0,015 ± 0,0006 ^a
ASS1	0,006 ± 0,0002 ^a	0,007 ± 0,0003 ^{a,b}	0,004 ± 0,0004 ^{a,b}	0,050 ± 0,0016 ^a	0,013 ± 0,0001 ^{a,b}
ASS2	0,004 ± 0,0001 ^b	0,006 ± 0,0003 ^{a,b}	0,004 ± 0,0003 ^{a,b}	0,052 ± 0,0042 ^a	0,014 ± 0,0004 ^{a,b}
ASS3	0,005 ± 0,0003 ^{a,b}	0,008 ± 0,0002 ^a	0,003 ± 0,0002 ^b	0,052 ± 0,0025 ^a	0,015 ± 0,0006 ^a

Biometric parameters of mice treated with saline (DMSO 1%), cisplatin (6 mg/kg), different doses of compound RC1 (D1, D2 and D3) and different doses of RC1 associated with cisplatin (6 mg/kg) were used. The results are presented in Mean ± SEM. Different letters indicate statistically significant differences ($p \leq 0.05$; ANOVA/Tukey Kramer).

Table 4

Mean ± standard error, frequency of damaged cells, distribution between damage classes and score related to the comet assay.

Experimental group	Damaged cells ¹	Damaged class				Score ¹
		0	1	2	3	
NC	3.60 ± 0.50 ^a	96.40 ± 0.50	3.60 ± 0.50	0.00 ± 0.00	0.00 ± 0.00	3.60 ± 0.51 ^a
PC	81.60 ± 5.16 ^b	18.40 ± 5.16	70.20 ± 4.07	9 ± 1.48	2.40 ± 0.50	95.4 ± 6.98 ^b
D1	19.40 ± 2.04 ^c	80.60 ± 2.04	15.20 ± 1.02	3.60 ± 0.81	0.60 ± 0.40	24.2 ± 3.54 ^c
D2	22.40 ± 0.51 ^c	77.60 ± 0.51	18.60 ± 0.50	2.60 ± 0.24	1.20 ± 0.37	27.4 ± 1.12 ^c
D3	23.80 ± 1.50 ^c	76.20 ± 1.50	19.00 ± 1.05	3.60 ± 0.60	1.20 ± 0.37	29.8 ± 2.63 ^c
ASS1	76.40 ± 2.06 ^b	23.60 ± 2.06	68.60 ± 1.69	5.80 ± 1.24	2.00 ± 0.45	86.2 ± 3.61 ^b
ASS2	78.60 ± 2.04 ^b	21.40 ± 2.04	70.80 ± 1.31	6.00 ± 0.94	1.80 ± 0.37	88.2 ± 3.34 ^b
ASS3	86.40 ± 1.29 ^b	13.60 ± 1.29	75.60 ± 1.50	7.00 ± 1.40	3.80 ± 0.59	101.0 ± 2.92 ^b

Frequency of cells with genomic damage, distribution between classes and score of the comet assay performed with peripheral blood of mice treated with saline (DMSO 1%), cisplatin (6 mg/kg) different doses of compound RC1 (D1, D2 and D3) and different doses of RC1 associated with cisplatin (6 mg/kg). The results are presented in Mean ± EPM. Different letters indicate statistically significant differences ($p \leq 0.05$; ANOVA/Tukey Kramer).

the chemotherapeutic by increasing the frequency of micronuclei in the ASS2 and ASS3 groups within 48 h and of all associated groups within 72 h. This effect may be due to the competitiveness of the RC1 compound and cisplatin, since cisplatin is transported by copper receptors (Ishida et al., 2002). According to Ciarimboli (2014) several carriers are described for cisplatin, such as the copper-1 carrier (Ctr1), the copper-2 carrier (Ctr2), the ATP7A and ATP7B type P copper transport ATPases, the organic cation transporter-2 (OCT2) and the multidrug and toxin

extrusion transporter 1 (MATE1). The transporters OCTs and MATE1 are highly expressed in the liver and kidneys (Ciarimboli, 2008; Pabla et al., 2009), which justifies the increased time of cisplatin metabolism in the liver and kidneys for later elimination of the organism. Thus, there is an increase in cisplatin circulation time which would explain the increase in micronuclei frequency in the last evaluation times (48 and 72 h) since this compound is a direct acting genotoxic agent (Wang and Lippard, 2005).

Table 5

Frequency of micronuclei in the peripheral blood of mice treated with RC1 compound.

Experimental group	Mean ± EPM		
	24H	48H	72H
NC	3,20 ± 0,66 ^a	4,20 ± 0,80 ^a	3,80 ± 0,58 ^a
PC	79,20 ± 4,46 ^b	73,00 ± 1,00 ^b	69,80 ± 1,39 ^b
D1	3,80 ± 0,73 ^a	3,80 ± 0,58 ^a	4,40 ± 0,60 ^a
D2	3,40 ± 0,81 ^a	5,40 ± 0,51 ^a	4,60 ± 0,51 ^a
D3	5,20 ± 0,73 ^a	7,40 ± 1,08 ^a	5,20 ± 0,66 ^a
ASS1	73,60 ± 2,90 ^b	76,60 ± 0,93 ^{b,c}	80,00 ± 0,70 ^c
ASS2	79,60 ± 5,24 ^b	78,60 ± 0,93 ^c	79,00 ± 0,71 ^c
ASS3	84,40 ± 3,72 ^b	79,00 ± 1,43 ^c	79,60 ± 0,75 ^c

Frequency of micronucleus in peripheral blood in mice treated with saline (DMSO 1%), cisplatin (6 mg/kg), different doses of the RC1 compound (D1, D2 and D3) and different doses of RC1 compound associated with cisplatin (6 mg/kg). The results are presented in Mean ± SEM. Different letters indicate statistically significant differences ($p \leq 0.05$; ANOVA/Tukey Kramer).

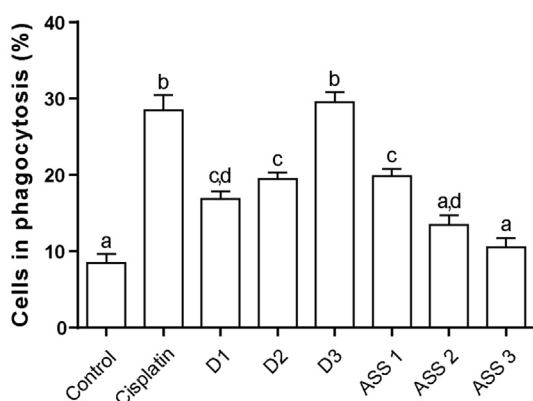


Fig. 6. Analysis of splenic phagocytosis in Swiss mice treated with RC1 compound.

Percentage of cells with phagocytic characteristics in DMSO, cisplatin (positive control) the RC1 compound at three different doses (D1, D2 and D3) and the three doses of RC1 compound associated with dose of cisplatin. Different letters indicate statistically significant differences ($p \leq 0.05$; ANOVA/Tukey Kramer).

The results presented in this study indicate that the RC1 compound possesses therapeutic potential, as it presented toxicity to 4 T1 murine mammary adenocarcinoma cells. The toxicity was triggered by DNA damage, which induced cell cycle arrest in G1, that was mediated by ATM and p21 expression, with subsequent cell death by mitochondrial apoptosis, which occurred due to increased expression of BAX and Caspase-7, and decrease in BCL-2 gene expression. Notably, in *in vivo*, the compound was less genotoxic than cisplatin, did not increase the frequency of micronuclei, thus DNA damage was not permanent, and at the doses tested there were no changes in biometric parameters.

Conflict of interest

The authors declare that there is no conflict of interest in the present study.

References

Acilan, C., Cevattemre, B., Adiguzel, Z., Karakas, D., Ulukaya, E., Ribeiro, N., Correia, I., Pessoa, J.C., 2017. Synthesis, biological characterization and evaluation of molecular mechanisms of novel copper complexes as anticancer agents. *Biochim. Biophys. Acta* 1861, 218–234. <https://doi.org/10.1016/j.bbagen.2016.10.014>.

Amarante-Mendes, G.P., Green, D.R., 1999. The regulation of apoptotic cell death. *Brazilian J. Med. Biol. Res. = Rev. Bras. Pesqui. Médicas e Biológicas/Soc. Bras. Biofísica* 32, 1053–1061. <https://doi.org/10.1590/S0100-879X1999000900001>.

ANVISA, 2013. Guia para a condução de estudos não clínicos de toxicologia e segurança

farmacológica necessários ao desenvolvimento de medicamentos. Versão 2, 1–48.

Bazo, A.P., Rodrigues, M.A.M., Sforcin, J.M., De Camargo, J.L.V., Ribeiro, L.R., Salvadori, D.M.F., 2002. Protective action of propolis on the rat colon carcinogenesis. *Teratog. Carcinog. Mutagen.* 22, 183–194. <https://doi.org/10.1002/tcm.10011>.

Berno, C.R., Rós, B., Dda Silveira, I.O.M.F., Coelho, H.R., Antonioli, A.C.M.B., Beatriz, A., Dde Lima, D.P., Monreal, A.C.D., Sousa, F.G., Dda Silva Gomes, R., Oliveira, R.J., 2016. 4-Aminoantipyrine reduces toxic and genotoxic effects of doxorubicin, cisplatin, and cyclophosphamide in male mice. *Mutat. Res. - Genet. Toxicol. Environ. Mutagen.* 805, 19–24. <https://doi.org/10.1016/j.mrgentox.2016.05.009>.

Bertoli, C., Skotheim, J.M., De Bruin, R.A.M., 2013. Control of cell cycle transcription during G1 and S phases. *Nat. Rev. Mol. Cell Biol.* <https://doi.org/10.1038/nrm3629>.

Bhat, G.A., Maqbool, R., Dar, A.A., Ul Hussain, M., Murugavel, R., 2017. Selective formation of discrete versus polymeric copper organophosphates: DNA cleavage and cytotoxic activity. *Dalt. Trans.* 46, 13409–13420. <https://doi.org/10.1039/C7DT02763J>.

Biazi, B.I., D'Epiro, G.F.R., Zanetti, T.A., de Oliveira, M.T., Ribeiro, L.R., Mantovani, M.S., 2017. Risk assessment via metabolism and cell growth inhibition in a HepG2/C3A cell line upon treatment with Arpadol and its active component Harpagoside. *Phyther. Res.* 31, 387–394. <https://doi.org/10.1002/ptr.5757>.

Carvalho, P.C., Santos, E.A., Schneider, B.U.C., Matuo, R., Pesarini, J.R., Cunha-Laura, A.L., Monreal, A.C.D., Lima, D.P., Antonioli, A.C.M.B., Oliveira, R.J., 2015. Diaryl sulfide analogs of combretastatin A-4: Toxicogenetic, immunomodulatory and apoptotic evaluations and prospects for use as a new chemotherapeutic drug. *Environ. Toxicol. Pharmacol.* 40, 715–721. <https://doi.org/10.1016/j.etap.2015.08.028>.

Ciarimboli, G., 2008. Organic cation transporters. *Xenobiotica.* <https://doi.org/10.1080/00498250701882482>.

Ciarimboli, G., 2014. Membrane transporters as mediators of cisplatin side-effects. In: *Anticancer Research*, pp. 547–550.

Dallavalle, F., Gaccioli, F., Franchi-Gazzola, R., Lanfranchi, M., Marchiò, L., Pellinghelli, M.A., Tegoni, M., 2002. Synthesis, molecular structure, solution equilibrium, and antiproliferative activity of thioxotriazoline and thioxotriazole complexes of copper (II) and palladium(II). *J. Inorg. Biochem.* 92, 95–104. [https://doi.org/10.1016/S0162-0134\(02\)00545-7](https://doi.org/10.1016/S0162-0134(02)00545-7).

Dasari, S., Bernard Tchounwou, P., 2014. Cisplatin in cancer therapy: molecular mechanisms of action. *Eur. J. Pharmacol.* <https://doi.org/10.1016/j.ejphar.2014.07.025>.

de Araújo, F.H.S., de Figueiredo, D.R., Auharek, S.A., Pesarini, J.R., Meza, A., Gomes, R., Monreal, A.C.D., Antonioli-Silva, A.C.M.B., Dde Lima, D.P., Kassuya, C.A.L., Beatriz, A., Oliveira, R.J., 2017. In vivo chemotherapeutic insight of a novel isocoumarin (3-hexyl-5,7-dimethoxy-isochromen-1-one): genotoxicity, cell death induction, leukometry and phagocytic evaluation. *Genet. Mol. Biol.* 40, 665–675. <https://doi.org/10.1590/1678-4685-gmb-2016-0316>.

De David, N., De Oliveira Mauro, M., Gonçalves, C.A., Pesarini, J.R., Strapasson, R.L.B., Kassuya, C.A.L., Stefanello, M.É.A., Cunha-Laura, A.L., Monreal, A.C.D., Oliveira, R.J., 2014. *Gochnatia polymorpha* ssp. *floccosa*: bioprospecting of an anti-inflammatory phytotherapy for use during pregnancy. *J. Ethnopharmacol.* 154, 370–379. <https://doi.org/10.1016/j.jep.2014.04.005>.

Domracheva, I., Kanepe-Lapsa, I., Jackevica, L., Vasiljeva, J., Arsenyan, P., 2017. Selenopheno quinolones and coumarins promote cancer cell apoptosis by ROS depletion and caspase-7 activation. *Life Sci.* 186, 92–101. <https://doi.org/10.1016/j.lfs.2017.08.011>.

European Commission, 2006. European Medicines Agency. pp. 1–12. <https://doi.org/10.1136/bmj.333.7574.873-a>.

Facchin, G., Veiga, N., Kramer, M.G., Batista, A.A., Várnagy, K., Farkas, E., Moreno, V., Torre, M.H., 2016. Experimental and theoretical studies of copper complexes with isomeric dipeptides as novel candidates against breast cancer. *J. Inorg. Biochem.* 162, 52–61. <https://doi.org/10.1016/j.jinorgbio.2016.06.005>.

Fan, L., Tian, M., Liu, Y., Deng, Y., Liao, Z., Xu, J., 2017. Salicylate dot Phenanthroline copper (II) complex induces apoptosis in triple-negative breast cancer cells. *Oncotarget* 8, 29823–29832. <https://doi.org/10.18632/oncotarget.16161>.

Ferlay, J., Soerjomataram, I., Dikshit, R., Eser, S., Mathers, C., Rebelo, M., Parkin, D.M., Forman, D., Bray, F., 2015. Cancer incidence and mortality worldwide: sources, methods and major patterns in GLOBOCAN 2012. *Int. J. Cancer* 136, E359–E386. <https://doi.org/10.1002/ijc.29210>.

Gao, E.J., Lin, L., Zhang, Y., Wang, R.S., Zhu, M.C., Liu, S.H., Sun, T.D., Jiao, W., Andrey, V.Z., 2011. Synthesis, characterization, and study on HeLa cells activity of a dinuclear complex [Cu4(phen)4(H2O) 2](pyri)3H2O. *Eur. J. Med. Chem.* 46, 2546–2554. <https://doi.org/10.1016/j.ejmech.2011.03.044>.

Gogvadze, V., Orrenius, S., 2006. Mitochondrial regulation of apoptotic cell death. *Chem. Biol. Interact.* 163, 4–14. <https://doi.org/10.1016/j.cbi.2006.04.010>.

Gouda, A.M., El-Ghamry, H.A., Bawazeer, T.M., Farghaly, T.A., Abdalla, A.N., Aslam, A., 2018. Antitumor activity of pyrrolizines and their Cu(II) complexes: design, synthesis and cytotoxic screening with potential apoptosis-inducing activity. *Eur. J. Med. Chem.* <https://doi.org/10.1016/j.ejmech.2018.01.009>.

Hayashi, M., Morita, T., Kodama, Y.K., Sofuni, T., Ishidate, M.J., 1990. The micronucleus assay with mouse peripheral blood reticulocytes using acridine orange-coated slides. *Mutat. Res. Toxicol.* 278, 127–130. [https://doi.org/10.1016/0165-1218\(92\)90222-L](https://doi.org/10.1016/0165-1218(92)90222-L).

Hoff Brait, D.R., Mattos Vaz, M.S., da Silva Arrigo, J., Borges De Carvalho, L.N., Souza De Araújo, F.H., Vani, J.M., da Silva Mota, J., Cardoso, C.A.L., Oliveira, R.J., Negrão, F.J., Kassuya, C.A.L., Arena, A.C., 2015. Toxicological analysis and anti-inflammatory effects of essential oil from Piper vicosanum leaves. *Regul. Toxicol. Pharmacol.* 73, 699–705. <https://doi.org/10.1016/j.yrtph.2015.10.028>.

Ishida, S., Lee, J., Thiele, D.J., Herskowitz, I., 2002. Uptake of the anticancer drug cisplatin mediated by the copper transporter Ctr1 in yeast and mammals. *Proc. Natl. Acad. Sci.* 99, 14298–14302. <https://doi.org/10.1073/pnas.162491399>.

- Ishii, P.L., Prado, C.K., Mauro, M., Carreira, C.M., Mantovani, M.S., Ribeiro, L.R., Dichi, J.B., Oliveira, R.J., 2011. Evaluation of Agaricus blazei in vivo for antigenotoxic, anticarcinogenic, phagocytic and immunomodulatory activities. *Regul. Toxicol. Pharmacol.* 59, 412–422. <https://doi.org/10.1016/j.yrtph.2011.01.004>.
- Ishikawa, R.B., Leitão, M.M., Kassuya, R.M., Macorini, L.F., Moreira, F.M.F., Cardoso, C.A.L., Coelho, R.G., Pott, A., Gelfuso, G.M., Croda, J., Oliveira, R.J., Kassuya, C.A.L., 2017. Anti-inflammatory, antimycobacterial and genotoxic evaluation of *Dolichocarpus dentatus*. *J. Ethnopharmacol.* 204, 18–25. <https://doi.org/10.1016/j.jep.2017.04.004>.
- Jha, A., Mukherjee, C., Prasad, A.K., Parmar, V.S., Vadaparti, M., Das, U., De Clercq, E., Balzarini, J., Stables, J.P., Shrivastav, A., Sharma, R.K., Dimmock, J.R., 2010. Derivatives of aryl amines containing the cytotoxic 1,4-dioxo-2-butenyl pharmacophore. *Bioorganic Med. Chem. Lett.* 20, 1510–1515. <https://doi.org/10.1016/j.bmcl.2010.01.098>.
- Kobayashi, H., Sugiyama, C., Morikawa, Y., Hayashi, M., Sofuni, T., 1995. A comparison between manual microscopic analysis and computerized image analysis in the single cell gel electrophoresis assay. *MMS Commun.* 3, 103–115.
- Koňariková, K., Perdikaris, G.A., Gbelcová, H., Andrezálová, L., Švéda, M., Ruml, T., Laubertová, L., Režnáková, S., Žitňanová, I., 2016. Autophagy in MCF-7 cancer cells induced by copper complexes. *Pharmacol. Reports* 68, 1221–1224. <https://doi.org/10.1016/j.pharep.2016.07.011>.
- Kosih, A., Parthiban, C., Elango, K.P., 2017. Synthesis, characterization and DNA binding/cleavage, protein binding and cytotoxicity studies of Cu(II), Ni(II), Cu(II) and Zn(II) complexes of aminonaphthoquinone. *J. Photochem. Photobiol. B Biol.* 168, 165–174. <https://doi.org/10.1016/j.jphotobiol.2017.02.010>.
- Lakomska, I., Hoffmann, K., Wojtczak, A., Sitkowski, J., Maj, E., Wietrzyk, J., 2014. Cytotoxic malonate platinum(II) complexes with 1,2,4-triazolo[1,5-a]pyrimidine derivatives: structural characterization and mechanism of the suppression of tumor cell growth. *J. Inorg. Biochem.* 141, 188–197. <https://doi.org/10.1016/j.jinorgbio.2014.08.005>.
- LakshmiPraba, J., Arunachalam, S., Riyasdeen, A., Dhivya, R., Vignesh, S., Akbarsha, M.A., James, R.A., 2013. DNA/RNA binding and anticancer/antimicrobial activities of polymer-copper(II) complexes. *Spectrochim. Acta* 109, 23–31. <https://doi.org/10.1016/j.saa.2013.02.020>.
- LakshmiPraba, J., Arunachalam, S., Riyasdeen, A., Dhivya, R., Akbarsha, M.A., 2015. Polyethyleneimine anchored copper(II) complexes: synthesis, characterization, in vitro DNA binding studies and cytotoxicity studies. *J. Photochem. Photobiol. B Biol.* 142, 59–67. <https://doi.org/10.1016/j.jphotobiol.2014.11.005>.
- Lee, H.L., Er, H.M., Radhakrishnan, A.K., 2009. In vitro anti-proliferative and antioxidant activities of stem extracts of *pereskia bleo* (Kunth) DC (Cactaceae). *Malaysian J. Sci.* 28, 225–239.
- Liu, N., Huang, H., Dou, Q.P., Liu, J., 2015. Inhibition of 19S proteasome-associated deubiquitinases by metal-containing compounds. *Oncoscience* 2, 457–466. <https://doi.org/10.18632/oncoscience.167>.
- Luchini, A.C., Rodrigues-Orsi, P., Cestari, S.H., Seito, L.N., Witaicenis, A., Pellizzon, C.H., Di Stasi, L.C., 2008. Intestinal anti-inflammatory activity of coumarin and 4-hydroxycoumarin in the trinitrobenzenesulphonic acid model of rat colitis. *Biol. Pharm. Bull.* 31, 1343–1350. <https://doi.org/10.1248/bpb.31.1343>.
- Manikandamathavan, V.M., Thangaraj, M., Weyhermuller, T., Parameswari, R.P., Punitha, V., Murthy, N.N., Nair, B.U., 2017. Novel mononuclear Cu (II) terpyridine complexes: impact of fused ring thiophene and thiazole head groups towards DNA/BSA interaction, cleavage and antiproliferative activity on HepG2 and triple negative CAL-51 cell line. *Eur. J. Med. Chem.* 135, 434–446. <https://doi.org/10.1016/j.ejmech.2017.04.030>.
- Márquez-Jurado, S., Díaz-Colunga, J., das Neves, R.P., Martínez-Lorente, A., Almazán, F., Gantes, R., Iborra, F.J., 2018. Mitochondrial levels determine variability in cell death by modulating apoptotic gene expression. *Nat. Commun.* 9, 389. <https://doi.org/10.1038/s41467-017-02787-4>.
- Martins, M.J.B., Batista, A.M.A., Brito, Y.N.F., Soares, P.M.G., Martins, C., Ribeiro, R., Brito, G.A., Dde Freitas, M.R., 2017. Effect of remote ischemic preconditioning on systemic toxicity and ototoxicity induced by cisplatin in rats: role of TNF- α and nitric oxide. *Orl* 60125001, 336–346. <https://doi.org/10.1159/000485514>.
- Marzano, C., Pellei, M., Tisato, F., Santini, C., 2009. Copper complexes as anticancer agents. *Anti Cancer Agents Med. Chem.* 9, 185–211. <https://doi.org/10.2174/187152009787313837>.
- Massagué, J., 2004. G1 cell-cycle control and cancer. *Nature*. <https://doi.org/10.1038/nature03094>.
- Mitra, A.K., Agrahari, V., Mandal, A., Cholkar, K., Natarajan, C., Shah, S., Joseph, M., Trinh, H.M., Vaishya, R., Yang, X., Hao, Y., Khurana, V., Pal, D., 2015. Novel delivery approaches for cancer therapeutics. *J. Control. Release* 219, 248–268. <https://doi.org/10.1016/j.jconrel.2015.09.067>.
- Nash, P., Tang, X., Orlicky, S., Chen, Q., Gertler, F.B., Mendenhall, M.D., Sicheri, F., Pawson, T., Tyers, M., 2001. Multisite phosphorylation of a CDK inhibitor sets a threshold for the onset of DNA replication. *Nature* 414, 514–521. <https://doi.org/10.1038/35107009>.
- Navarro, S.D., Beatriz, A., Meza, A., Pesarini, J.R., Gomes, R.D.S., Karaziack, C.B., Cunha-Laura, A.L., Monreal, A.C.D., Romão, W., Lacerda Júnior, V., Mauro, M.D.O., Oliveira, R.J., 2014. A new synthetic resorcinolic lipid 3-Heptyl-3,4,6-trimethoxy-3H-isobenzofuran-1-one: evaluation of toxicology and ability to potentiate the mutagenic and apoptotic effects of cyclophosphamide. *Eur. J. Med. Chem.* 75, 132–142. <https://doi.org/10.1016/j.ejmech.2014.01.057>.
- Oliveira, R.J., Matuo, R., da Silva, A.F., Matiazzi, H.J., Mantovani, M.S., Ribeiro, L.R., 2007. Protective effect of ??-glucan extracted from *Saccharomyces cerevisiae*, against DNA damage and cytotoxicity in wild-type (k1) and repair-deficient (xrs5) CHO cells. *Toxicol. Vitr.* 21, 41–52. <https://doi.org/10.1016/j.tiv.2006.07.018>.
- Oliveira, R.J., Salles, M.J.S., da Silva, A.F., Kanno, T.Y.N., Lourenço, A.C., Freiria, G.A., Matiazzi, H.J., Ribeiro, L.R., Mantovani, M.S., 2009. Effects of the polysaccharide ??-glucan on clastogenicity and teratogenicity caused by acute exposure to cyclophosphamide in mice. *Regul. Toxicol. Pharmacol.* 53, 164–173. <https://doi.org/10.1016/j.yrtph.2008.12.007>.
- Oliveira, R.J., Mantovani, M.S., Da Silva, A.F., Pesarini, J.R., Mauro, M.O., Ribeiro, L.R., 2014. Compounds used to produce cloned animals are genotoxic and mutagenic in mammalian assays in vitro and in vivo. *Brazilian J. Med. Biol. Res.* 47, 287–298. <https://doi.org/10.1590/1414-431X20143301>.
- Ooi, H.K., Ma, L., 2013. Modeling heterogeneous responsiveness of intrinsic apoptosis pathway. *BMC Syst. Biol.* 7. <https://doi.org/10.1186/1752-0509-7-65>.
- Pabla, N., Murphy, R.F., Liu, K., Dong, Z., 2009. The copper transporter Ctr1 contributes to cisplatin uptake by renal tubular cells during cisplatin nephrotoxicity. *Am. J. Physiol. Physiol.* 296, F505–F511. <https://doi.org/10.1152/ajprenal.90545.2008>.
- Pesarini, J.R., Oliveira, R.J., Pessatto, L.R., Milan Brochado Antonioli-Silva, A.C., Felicidade, I., Nardi, N.B., Camassola, M., Mantovani, M.S., Ribeiro, L.R., 2017. Vitamin D: correlation with biochemical and body composition changes in a southern Brazilian population and induction of cytotoxicity in mesenchymal stem cells derived from human adipose tissue. *Biomed Pharmacother* 91, 861–871. <https://doi.org/10.1016/j.biopha.2017.05.013>.
- Pfaffl, M.W., Horgan, G.W., Dempfle, L., 2002. Relative expression software tool (REST) for group-wise comparison and statistical analysis of relative expression results in real-time PCR. *Nucleic Acids Res.* 30, e36. <https://doi.org/10.1093/nar/30.9.e36>.
- Pivetta, T., Isaia, F., Verani, G., Cannas, C., Serra, L., Castellano, C., Demartin, F., Pilla, F., Manca, M., Pani, A., 2012. Mixed-1,10-phenanthroline-cu(II) complexes: synthesis, cytotoxic activity versus hematological and solid tumor cells and complex formation equilibria with glutathione. *J. Inorg. Biochem.* 114, 28–37. <https://doi.org/10.1016/j.jinorgbio.2012.04.017>.
- Rodrigues, J., Abramjuk, C., Vázquez, L., Gamboa, N., Domínguez, J., Nitzsche, B., Höpfner, M., Georgieva, R., Bäumler, H., Stephan, C., Jung, K., Lein, M., Rabien, A., 2011. New 4-maleamic acid and 4-maleamide peptidyl chalcones as potential multitarget drugs for human prostate cancer. *Pharm. Res.* 28, 907–919. <https://doi.org/10.1007/s11095-010-0347-8>.
- Roos, W.P., Kaina, B., 2006. DNA damage-induced cell death by apoptosis. *Trends Mol. Med.* <https://doi.org/10.1016/j.molmed.2006.07.007>.
- Sangeetha, S., Murali, M., 2017. Non-covalent DNA binding, protein interaction, DNA cleavage and cytotoxicity of [Cu(II)quomol]Cl \cdot H $_2$ O. *Int. J. Biol. Macromol.* <https://doi.org/10.1016/j.ijbiomac.2017.10.131>.
- Savio, A.L.V., da Silva, G.N., de Camargo, E.A., Salvadori, D.M.F., 2014. Cell cycle kinetics, apoptosis rates, DNA damage and TP53 gene expression in bladder cancer cells treated with allyl isothiocyanate (mustard essential oil). *Mutat. Res. - Fundam. Mol. Mech. Mutagen.* 762, 40–46. <https://doi.org/10.1016/j.mrfmmm.2014.02.006>.
- Schneider, B.U.C., Meza, A., Beatriz, A., Pesarini, J.R., de Carvalho, P.C., de Oliveira Mauro, M., Karaziack, C.B., Cunha-Laura, A.L., Monreal, A.C.D., Matuo, R., de Lima, D.P., Oliveira, R.J., 2016. Cardanol: Toxicogenetic assessment and its effects when combined with cyclophosphamide. *Genet. Mol. Biol.* 39, 279–289. <https://doi.org/10.1590/1678-4685-GMB-2015-0170>.
- Schweich, L.D.C., Oliveira, E.J.T.D., Pesarini, J.R., Hermeto, L.C., Camassola, M., Nardi, N.B., Brochado, T.M.M., Antonioli-Silva, A.C.M.B., Oliveira, R.J., 2017. All-trans retinoic acid induces mitochondria-mediated apoptosis of human adipose-derived stem cells and affects the balance of the adipogenic differentiation. *Biomed Pharmacother* 96, 1267–1274. <https://doi.org/10.1016/j.biopha.2017.11.087>.
- Singh, N.P., McCoy, M.T., Tice, R.R., Schneider, E.L., 1988. A simple technique for quantitation of low levels of DNA damage in individual cells. *Exp. Cell Res.* 175, 184–191. [https://doi.org/10.1016/0014-4827\(88\)90265-0](https://doi.org/10.1016/0014-4827(88)90265-0).
- Stewart, B.W., Wild, C.P., 2014. *World cancer report 2014*. In: *World Heal Organ*, pp. 1–2.
- Thalamuthu, S., Annaraj, B., Vasudevan, S., Sengupta, S., Neelakantan, M.A., 2013. DNA binding, nuclease, and colon cancer cell inhibitory activity of a Cu(II) complex of a thiazolidine-4-carboxylic acid derivative. *J. Coord. Chem.* 66, 1805–1820. <https://doi.org/10.1080/00958972.2013.791393>.
- Tsimberidou, A.M., Braiteh, F., Stewart, D.J., Kurzrock, R., 2009. Ultimate fate of oncology drugs approved by the US food and drug administration without a randomized trial. *J. Clin. Oncol.* <https://doi.org/10.1200/JCO.2009.23.6018>.
- U.S. Department of Health and Human Services, FDA, CDER, CBER, 2012. *S2(R1) genotoxicity testing and data interpretation for pharmaceuticals intended for human use*. *Guid. Ind.* 2, 1–31.
- Ueda, T., Kohama, Y., Kuge, A., Kido, E., Sakurai, H., 2017. GADD45 family proteins suppress JNK signaling by targeting MKK7. *Arch. Biochem. Biophys.* 635, 1–7. <https://doi.org/10.1016/j.abb.2017.10.005>.
- Urru, S.A.M., Gallus, S., Bosetti, C., Moi, T., Medda, R., Sollai, E., Murgia, A., Sanges, F., Pira, G., Manca, A., Palmas, D., Floris, M., Asunis, A.M., Atzori, F., Carru, C., D'Incalci, M., Ghiani, M., Marras, V., Onnis, D., Santana, M.C., Sarobba, G., Valle, E., Canu, L., Cossu, S., Bulfone, A., Rocca, P.C., De Miglio, M.R., Orrù, S., 2018. Clinical and pathological factors influencing survival in a large cohort of triple-negative breast cancer patients. *BMC Cancer* 18. <https://doi.org/10.1186/s12885-017-3969-y>.
- Wang, D., Lippard, S.J., 2005. Cellular processing of platinum anticancer drugs. *Nat. Rev. Drug Discov.* <https://doi.org/10.1038/nrd1691>.
- GLOBOCAN, 2012. World Health Organization, Global Cancer Observatory - Online analysis prediction. Available at: http://globocan.iarc.fr/Pages/summary_table_site_sel.aspx, Accessed date: 4 January 2018.